2013

Creep and Shrinkage of High Performance Concrete, and Prediction of Long-Term Camber of Prestressed Bridge Girders

Wenjun He
Iowa State University

Creep and shrinkage of high performance concrete and prediction of the long-term camber of prestressed bridge girders

by

Wenjun He

A thesis submitted to the graduate faculty

in partial fulfillment of the requirements for the degree of

MASTER OF SCIENCE

Major: Civil Engineering (Structural Engineering)

Program of Study Committee:

Jon M. Rouse, Co-Major Professor

Sri Sritharan, Co-Major Professor

Kejin Wang

Michael R. Kessler

Iowa State University

Ames, Iowa

2013

TABLE OF CONTENTS

LIST OF FIGURES

LIST OF TABLES

ACKNOWLEDGEMENTS

I thank Dr. Jon Rouse and Dr. Sri Sritharan for allowing me to participate in this project, and for providing me with considerable guidance and assistance. I also appreciate for the help from Dr. Kejin Wang and Dr. Michael Kessler as my committee members.

I thank the Iowa Highway Research Board (IHRB) for funding this project. I thank James Nervig and Ebadollah Honarvar for the help of transportation of concrete specimens and field measurements. I am indebted to Owen Steffens and Douglas Wood for the help of the preparation of creep frames. I appreciate Mark Rasmusson, Jim Goodknight and John Wolf for the help of preparations of concrete specimens from three precast plants. I thank each professor for the guidance of courses, from whom I have learnt knowledge and professional attitude for Civil Engineering work. I also appreciate for the support from my parents and friends, and without their support I couldn't have finished my coursework and research.

ABSTRACT

The long-term camber of prestressed bridge girders is typically over-estimated by current Iowa Department of Transportation (IA DOT) methods at erection (typically 3 month after production of girders), especially for long-span bulb tee girders. This often leads to increased costs due to the haunch modifications in the field, and unnecessary delay of construction. Creep and shrinkage of concrete play an important role in the long-term camber of a prestressed bridge girder. The current models used to predict the creep and shrinkage yield large disparties with the actual behavior of concrete in prestressed girders cast using local materials in Iowa. In order to improve the accuracy of prediction of the camber of prestressed bridge girders, creep and shrinkage tests of concrete using local materials were performed. Seven mixes from three precast plants were investigated in this study, in which four of them were high performance concrete (HPC) that are currently used to cast prestressed bridge girders, and three of them were normal concrete (NC) that were utilized to produce prestressed bridge girders previously. Mineral admixtures including slag and fly ash are typically added into HPC. Half of the creep and shrinkage specimens were sealed with Sikagard 62 to minimize the evaporation of water, and the rest were unsealed. All creep and shrinkage specimens with 4 in. diameter and 8 in. height were monitored in an environmentally controlled chamber for one year. In addition, twenty-six prestressed bridge girders produced using HPC from three precast plants were monitored and the corresponding long-term camber was measured.

It was observed that due to the early age of loading and the use of slag and fly ash HPC had higher average creep coefficient and average shrinkage strain than NC for both sealed and unsealed specimens during 1 year. It was also found that sealed specimens represent the creep and shrinkage behavior of a full scale prestressed bridge girder much better than unsealed specimens, in agreement with some of the previous literature. It was also observed that the sealed creep coefficient and sealed shrinkage strain measured from the four HPC mixes were similar, and it was acceptable to use the average sealed creep coefficient and average sealed shrinkage strain of the four HPC mixes tested to predict long-term camber of prestressed bridge girders produced in Iowa.

Three simplified methods were applied to predict long-term camber of the prestressed bridge girders, including Tadros's Method (2011), Naaman's Method (2004) and an incremental method. Naamans' Method and the incremental method yielded similar results, and both methods yielded ±25% errors relative to measured camber of 26 prestressed bridge girders, but Tadros's Method yielded up to ±50% errors. The calculation of Naaman's Method was simpler than for the incremental method. Therefore, Naaman's Method was the recommended method to predict the long-term camber of prestressed bridge girders produced in Iowa.

CHAPTER 1 INTRODUCTION

1.1 Background

The issue of inaccuracy of camber prediction at erection of prestressed bridge girders is found not only by Iowa Department of Transportation (IA DOT), but by other DOTs, including Washington DOT (2007), North Carolina DOT (2011) and Minnesota DOT (2012). For the camber prediction at erection of prestressed bridge girders, the current tolerance by IA DOT is ±30%, and typically the actual situation is beyond this limit. It is found that the long-term camber of prestressed bridge girder at erection by using the current simple multipliers method by the IA DOT is typically over-estimated, especially for long span bulb tee girders that are frequently used in Iowa. The over-estimation of long-term camber at erection of girders typically results in field modifications of concrete haunches, leading to the increase of cost and increase of self-weight of the superstructure of the bridge. This over-estimation is possibly caused by different factors, including material properties and the current prediction method itself. IA DOT changed the concrete of prestressed bridge girders from normal concrete (NC) to high performance concrete (HPC) after 2006. In HPC slag and fly ash are utilized to replace a certain percent of Portland cement, which results in different material properties and further different camber behavior with NC. For the material properties of concrete, creep and shrinkage, modulus of elasticity and compressive strength for HPC and NC should be investigated and compared with the corresponding current models. For the current method of camber prediction at erection, only simple multipliers are used, and the accuracy of this method should be evaluated. Uncertainty of the duration between production and erection of girders leads to additional errors in camber prediction. After the clarification of causes of errors of camber prediction, a new simplified method should be proposed to predict long-term camber at erection with satisfactory accuracy.

1.2 Research Scopes

The goal of this study is to improve the accuracy of long-term camber prediction of prestressed bridge girders. In order to realize this goal, material properties of concrete using local materials are investigated, and underlying reasons of inaccuracy of long-term camber prediction of IA DOT's current method are also quantified. A simplified method of long-term camber prediction is then proposed.

1.3 Research Objectives

The objectives of this study are shown below:

- Monitor creep, shrinkage and development of elastic modulus and strength for 7 mixes, including 4 high performance concrete (HPC) mixes that are currently used to cast prestressed bridge girders, and 3 normal concrete (NC) mixes that were used to produce prestressed bridge girders previously.
- Identify practices and conditions that affect camber development in prestressed bridge girders
- Correlate the creep and shrinkage behavior between concrete specimens and a full size of prestressed bridge girder.
- Measure the long-term camber of 26 prestressed bridge girders that are cast by using HPC from three precast plants.
- Evaluate the current camber prediction method.
- Propose a simplified method to predict the long-term camber of prestressed bridge girders by using measured data of creep and shrinkage of HPC

1.4 Assumptions

Assumptions applicable for reinforced concrete structures are also applied in this study, and two additional assumptions are utilized in this study, including the following:

- In the creep and shrinkage test of concrete, elastic shortening, creep strain and shrinkage strain are additive;
- A prestressed bridge girder has the linear-elastic behavior of camber under the combined effect of prestressing forces and self-weight of the girder.

CHAPTER 2 BACKGROUND INFORMATION

2.1 Creep of Concrete

2.1.1 Introduction

Creep is the time-dependent increase of strain in the hardened concrete under sustained stress (ACI 209R, 1992). Creep is generally obtained by subtracting instantaneous strain after loading application and shrinkage strain in the non-loaded specimen, from the total measured strain with the change of time in a loaded specimen. Creep is classified into basic creep and drying creep. Basic creep occurs under conditions without moisture movement between the specimen and the environment. Drying creep is the additional creep due to the moisture movement between the specimen and the environment. Figure 2.1 shows the relation of deformation of concrete after loading application with time.

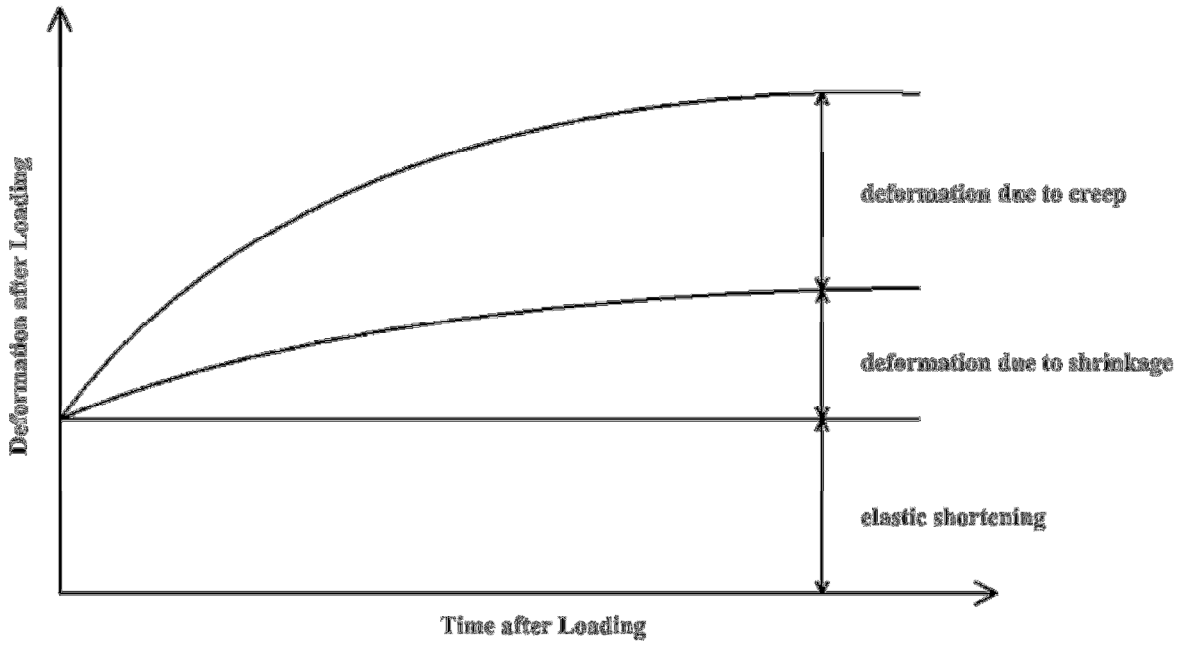

Figure 2.1. Relation of deformation after loading application versus time

2.1.2 Factors affecting creep of concrete

Creep in current study is on the creep behavior of concrete under compressive stress. Creep of concrete is influence by many factors, which are classified into intrinsic and extrinsic. Intrinsic factors consist of proportions and properties of materials in concrete. Extrinsic factors consist of size of concrete member, age of loading application, applied stress-strength ratio, curing conditions, ambient temperature and relative humidity surrounding concrete under load.

2.1.2.1 Aggregate

Aggregates play an important role in creep of concrete. Aggregates provide restraining effect on the creep (Neville A. M., 1970). Generally higher aggregate content results in lower creep. Neville (1970) proposed equations to indicate the relation between aggregate content and creep shown below:

$$log\frac{c_p}{c} = \alpha\, log\frac{1}{1-g} \qquad \text{(Eq 2-1)}$$

$$\alpha = \frac{3(1-\mu)}{1+\mu+2(1-2\mu_a)E/E_a} \qquad \text{(Eq 2-2)}$$

where:

c_p = creep of neat cement paste

c = creep of concrete

g = aggregate content

μ = Poisson's ratio of concrete

μ_a= Poisson's ratio of aggregate

E = modulus of elasticity of concrete

E_a = modulus of elasticity of aggregate

According to the study by Neville (1970), for concrete specimens loaded at 14 days with a stress-strength ratio of 0.5 stored in 90% relative humidity condition, a linear relationship was obtained between $log\frac{c_p}{c}$ and $log\frac{1}{1-g}$ after 28 days of loading for basic creep. The magnitude of α

was based on the age of initial loading and the change of modulus of elasticity of concrete with time after loading application. Similar observations were made by Polivka (1964) for both basic creep and drying creep of concrete.

Aggregate properties have a great influence on creep, including modulus of elasticity, porosity, roughness of surface, shape and size. Neville (1970) cited a study by Morlier, who investigated the creep of aggregates, and divided aggregates into three types, including elasto-brittle, visco-elastic and visco-plastic. Elasto-brittle aggregates consisted of magmaic, non-altered gneiss, hard limestone and quartzite, and this type of aggregates was typically used in concretes, and generally had small creep within 10% of elastic shortening deformation. Visco-elastic aggregates, such as calcareous minerals, shale, marl, porous limestone and granular gypsum, crept in a range of 12% to 40% of elastic shortening deformation. The first two types of aggregates had certain recoverable creep after the removal of the load. However, for visco-plastic aggregates such as chalk no reversible creep was observed.

Concretes made with different types of aggregates generally have different creep behavior. In the study by Davis (1931), six types of aggregates were used in concrete, including limestone, quartz, granite, gravel, basalt and sandstone. Concrete specimens were made with the same aggregate-cement ratio, water-cement ratio, the same applied stress and stored in the same condition. It was indicated that limestone concrete had the lowest creep, and sandstone concrete had the highest creep. Sandstone concrete crept as much as 2.5 times greater than limestone concrete. Kordina (1960) investigated the effect of eight types of aggregates on creep, and it was observed that concretes with different aggregates had different creep behavior, which confirmed the results from Davis. According to the study by Alexander (1996), the influence of 23 different aggregates on the properties of concrete was investigated, and they were divided into two series, including series 1 with 13 types of aggregates and series 2 with 10 types of aggregates. Series 1 and series 2 concretes, stored in water before loading and stored in air (23°C temperature and 60% relative humidity) after loading, were loaded approximately at the age of 600 days and 334 days respectively, because the change of mature concretes due to hydration of cement paste became mineral. It was found that creep coefficient of series 1 concretes varied from 1.29 to 2.97 after 11 months of loading, and that of series 2 concretes was in a range of 0.78 to 1.85 after 140 days of loading.

An explanation of aggregate type on creep of concrete provided by Neville (1970) was the modulus of elasticity of aggregate, and the higher modulus of elasticity of aggregate generally resulted in the higher restraining effect on cement paste, which caused lower creep. The study by Kordina (1960) and Alexander (1996) confirmed this explanation.

Porosity of aggregate has an influence on creep of concrete through elastic moduli of aggregate. In the study by Kordina (1960), the relation between absorption of eight types of aggregate and modulus of elasticity of aggregate was investigated. It was found that the higher absorption caused lower modulus of elasticity, which meant that higher porosity of aggregates resulted in lower elastic modulus of aggregate and higher creep of concrete.

The roughness of surface of aggregates also affects creep of concrete. The rougher the surface of aggregates, the better interface between aggregate and cement paste, and further the higher restraining effect of aggregate on cement paste, which results in lower creep.

Size of aggregate also has an effect on creep of concrete through aggregate content. Generally larger size of aggregates results in higher aggregate content and further causes lower creep. In the study by U.S. Army Engineers Laboratories (1958), sealed specimens were prepared by using two aggregate sizes including 1.5 inches and 6 inches. It was observed that concrete with 6 in. aggregate had 20% to 25% lower creep than concrete with 1.5 in. aggregate.

2.1.2.2 Cement

Cement paste is the base of creep phenomenon (Neville A. M., 1970), so cement has a great influence on creep of concrete. According to Neville (1970), it was observed that creep was inversely proportional to the rate of hardening of cement. It was logical that the higher rate of hardening of cement, the more hydrated cement and the more restraining effect on creep. Typically the concrete with rapid-hardening Portland (Type III) cement results in lower creep than the concrete with standard Portland (Type I) cement for both dry-stored and wet-stored conditions (Glanville W. H., 1939), which was due to the higher strength of Type III Portland cement concrete at the age of loading comparing with Type I cement concrete. For high-alumina cement, it was treated by Neville (1970) as a special case than other types of cement. According to the observations by Hummel (1959), rate of creep of concretes with type I and type III cement decreased with time almost down zero after 3 years. However, the creep of concrete made by

high alumina cement had the largely different behavior with the rest of two types of cement concretes. After 1 year of loading application, the rate of creep of high alumina cement concrete increased sharply. It was also found by Hummel that the strength of high-alumina cement concrete decreased considerably with time, and for instance, concrete specimens at 3 years only had 60% strength comparing with that at 90 days. This behavior was confirmed and explained by Neville (1958) (1963). The micro-structure of hydrated high-alumina cement pastes changed with time from hexagonal to cubic form, which resulted in an increase of porosity of the hydrated pastes. A considerable decrease of strength occurred, which resulted in considerable increase of creep.

2.1.2.3 Water to cementitious ratio

Typically creep increases with an increase of water to cementitious (w/c) ratio (Neville A. M., 1970). Lorman (1940) suggested that creep was approximately proportional to the square of the w/c ratio. This phenomenon was confirmed by Wagner and Hummel, whose results were cited by Neville (1970). From the study by Wagner, the effect of w/c ratio on creep was investigated, and specimens were prepared with constant cement paste content 20 percent by weight with w/c ratio ranging from 0.35 to 0.9. It was found that the higher w/c ratio, the higher ultimate specific creep. In another study by Hummel, all concretes had an aggregate-cement ratio of 5.4, and similar trend was found, and the ultimate specific creep with w/c ratio of 0.4 was approximately 10% higher than that with w/c ratio of 0.3.

2.1.2.4 Chemical admixtures

Chemical admixtures such as plasticizers and superplasticizers are commonly used in high performance concrete (HPC). The effect of chemical admixtures highly depends on chemical compositions and dosages. According to the study by Brooks (1989), admixtures added in HPC typically increased creep and drying shrinkage of concrete. In this study two types of plasticizers and three types of superplasticizers were investigated. It was indicated that generally plasticizers and superplasticizers increased creep of concrete comparing with concrete without any admixture. The mean increase of concrete creep due to admixtures was about 20%. In another study by Ngataki (1978), decrease of creep of concrete was observed by using superplasticizers.

2.1.2.5 Mineral admixtures

Mineral admixtures, including ground granulated blast furnace slag (GGBFS), fly ash and silica fume, are widely used as partial replacement of Portland cement in HPC. GGBFS is a glassy material with cementitious property formed when molten blast-furnace slag is rapidly cooled, such as by immersion in water, and slag mainly consists of silicates and aluminosilicates of calcium (ACI 233R, 2003). Fly ash is a by-product of coal combustion with both pozzolanic and cementitious properties (ACI 232.2R, 1996). Fly ash primarily consists of silicon dioxide, aluminum oxide and iron oxide. Silica fume is a by-product of the ferrosilicon industry consisting of very fine particles (4 to 8 x 10^{-6} in) with high pozzolanic property (ACI 234R, 2006), and silica fume consists primarily of non-crystalline silicon dioxide.

Neville (1975) investigated the effect of slag on properties of concrete. Concrete specimens, with three levels of replacement of Portland cement with slag including 0%, 30% and 50%, were loaded with the same stress after 28 days moist curing. It was indicated that slag decreased basic creep, and the higher level of slag replacement, the lower basic creep. It was also observed that slag resulted in slightly higher total creep under drying condition comparing with concrete without slag. Those behaviors of slag concrete were confirmed by Chern (1989). The effect of slag on creep highly depends on the age and strength of concrete at loading (Swamy, 1986). If slag concrete was loaded with the same stress at early ages such as 1-3 days, higher creep was observed under both dry and wet conditions. Reasonable explanation was that slag concrete developed strength more slowly comparing with concrete without slag, which resulted in higher stress-strength ratio at early age of loading and higher creep.

Fly ash is another type of mineral admixture commonly used in HPC. Fly ash is classified into Class F and Class C. Class F fly ash has pozzolanic properties but little or no cementitious properties, and Class C fly ash has pozzolanic properties and some autogenous cementitious properties. According to the studies by Ghosh (1981) and Lane (1982), when concrete with Class F fly ash and concrete without fly ash had similar strength at loading and similar applied stress, lower creep was observed for fly ash concrete due to higher rate of strength gain after loading application. Yuan and Cook (1983) investigated the effect of Class C fly ash on creep of concrete. There were four levels of replacement of Portland cement with fly ash, including 0%, 20%, 30% and 50%. It was indicated that 20% fly ash concrete had the

lowest creep during the first eight months of loading, and had comparable creep with 0% fly ash concrete after that until one year of loading. For 20%, 30% and 50% fly ash concrete, creep increased with an increase in the level of replacement.

In HPC silica fume is also used to partially replace Portland cement. Silica fume within certain percent decreases creep of concrete. In the study by Khatri and Sirivivatnanon (1995), significant decrease in creep was observed in the concrete with 10% silica fume comparing with concrete without silica fume. This behavior was due to the great increase of strength of the concrete with 10% silica fume at early days. According to the studies by Saucier (1984) and Buil (1985), it was indicated that concrete with both 15% and 33% silica fume had comparable creep with concrete without silica fume.

2.1.2.6 Stress-strength ratio at loading

According to a wide range of investigations (Neville A. M., 1970), creep is proportional to the applied stress and inversely proportional to the strength at the time of application of load. Although some other researches indicated higher upper limit of stress-strength ratio to 0.75 or 0.80, generally the upper limit was approximately 0.60. In the study by Jones and Richart (1936), the measured creep of concrete specimens was proportional with stress-strength ratio up to 0.6, and beyond this limit creep increased more quickly than the increase of applied stress. Similar behavior of concrete was observed by Gvozdev (1966) for concrete specimens with different stress-strength ratio and different initial application of load. According to the study by L'Hermite and Mamilla (1968), the linear relation was obtained for concrete stored in water initially loaded at 7 days, 35 days, 70 days, 1 year and 5.5 years. In the study by Haranki (2009), linear limit was 0.5 for HPC after the loading of 91 days. The linear limit for creep in compression is 40% of concrete compressive strength in ASTM C512 (2002).

2.1.2.7 Age at loading

The same concrete loaded at different ages undergoes a different growth in strength, so for the constant applied stress, creep depends on the age at loading. The strength of the younger concrete is lower, and the creep is higher, and the older concrete has the opposite characteristics. From the study by Yashin (1959), it was found that when the strength gain of concrete was smaller the creep was higher. Another study by Poivka (1964) confirmed this behavior, and for the same concrete, 18% higher creep was obtained for the concrete loaded at 1 day than 3 days

after the loading of 28 days. Loading age effect on creep of concrete also observed by Bryant (1987) for both unsealed and sealed specimens, and the earlier loading the higher creep. In the study by Khan (1997), the effect of age of loading on creep for normal concrete, medium concrete and high-strength concrete was investigated. It was found that the creep of high-strength concrete was more sensitive to the early age of loading than that of normal and medium concrete.

The extent of loading age of concrete also depends on the storage condition of concrete. In the study by Davis (1934), sustained stress was applied on all specimens during 80 days, and it was found that water-stored concrete specimens loaded at 7 days, 28 days and 3 months had the ratio of creep deformations at 3:2:1, but for dry-stored concrete specimens the effect of the age of loading was considerably smaller, and the creep of concrete loaded at 28 days was only 10% to 20% higher than that of concrete loaded at 3 months. Possible reason was that after 28 days of drying, the strength gain of concrete was very small. Davis also found that the earlier loaded concrete had higher rate of creep than later loaded concrete. Glanville (1933) found the similar behavior, and also that the rate of creep after one month was independent of the age at loading.

2.1.2.8 Size effect

It is important for the shape and size of specimens to make a transition from the results obtained in laboratory to actual full-size concrete members under drying condition. Neville (1970) summarized several investigations and found that the measured creep decreased with an increase in the size of the concrete specimens, but when the specimen thickness was greater than 3 ft. (90 cm) the size effect became negligible. Generally the influence of size on creep under drying condition is great during the initial period (first several weeks) after the application of load, but after that the rate of creep is comparable for all specimens with different sizes. In the study by Weil cited by Neville (1970), size effect of specimens with different diameters ranging from 3.9 in. (10 cm) to 23.6 in. (60 cm) on creep of concrete under drying condition was investigated. It was found that during the first two months after initial load application larger size of specimens resulted in lower creep and lower rate of creep, but after two months all specimens had similar rate of creep up to three years. L'Hermite (1968) observed the similar behavior. In this study specimens with 7 and 20 cm thickness were loaded at the age of 7 days, it was found that after three months all specimens had similar rate of creep up to three years. Size

effect on creep of concrete under drying condition was also observed by Bryant (1987), and it was found that increase of effective thickness of concrete member resulted in decrease of creep of concrete.

The loss of water from specimens to the ambient environment is an explanation of the effect of size on creep, which is correct for unsealed specimens, but not applicable for sealed specimens without moisture movement. According to study by Hansen and Mattock (1966), size effect was absent for sealed specimens, which indicated that basic creep was independent of size and shape. ACI Committee 209R (2008) confirmed this conclusion.

2.1.2.9 Curing conditions

Curing condition has a great effect on creep of concrete. Low-pressure steam curing is frequently used for the construction of prestressed concrete with the consideration of efficiency and economy. Generally low-pressure steam curing results in lower creep of concrete than moist curing, which is due to the accelerated hydration of cement causing higher strength of concrete at the age of loading (Neville A. M., 1970). According to the study by ACI Committee 517 (1963), the effect of two curing conditions was investigated, including steam curing at 150 °F (66 °F) for 13 hours and moist curing at 75°F (24 °F) for 5 or 6 days. It was observed that steam-cured concrete had lower specific creep by 30 to 50% comparing with moist-cured concrete loaded at the same stress-strength level. This behavior was confirmed by Hanson (1964), from which it was additionally indicated that type III Portland cement resulted in lower creep of concrete at the same steam curing condition comparing with type I Portland cement. According to the study by Townsend (2003), the effect of 1-day steam curing and 7-day moist curing on creep and shrinkage of HPC stored in an environmental-controlled chamber with 50% relative humidity was investigated. HPC contained 40% replacement of Portland cement with slag with 0.3 w/c ratio. It was found that steam-cured concrete had 5% lower creep strain at the storage of 1 week than moist-cured concrete but had 19% higher creep strain at the storage of 14 weeks. It was indicated that steam curing decreased initial creep strain of HPC, but increased it afterwards. It was additionally found that steam-cured concrete had similar creep coefficient with moist-cured concrete during 1 week, but higher creep coefficient afterwards, up to about 30% higher after the storage of 14 weeks.

2.1.2.10 Relative humidity

Relative humidity is an important extrinsic factor affecting creep of concrete. Typically higher relative humidity during loading application results in lower creep due to the decrease of drying effect of concrete (Neville A. M., 1970). In the study by Troxell (1958), 4 by 14 in. cylindrical specimens were prepared and after 28-day moist-curing loaded at relative humidity of 50%, 70% and 100%. It was observed that the creep of concrete specimens at 50% relative humidity was 2 to 3 times higher than that of concretes at a relative humidity of 100% after 25 years. Concrete at 70% relative humidity had the moderate creep. Concrete at 50% relative humidity had the highest rate of creep during the first 2 years, and the rate of creep decreased with an increase in relative humidity. However, after 2 years, concretes with three levels of relative humidity had comparable rate of creep. L'Hermite (1968) found the similar behavior of concrete specimens at the relative humidity of 50%, 75% and 100%. The effect of change of relative humidity on creep decreased with an increase in the size of concrete specimens, which was recognized by Troxell (1958) and confirmed by Keeton (1960).

The actual structures usually are under alternating humidity, which has an influence on creep of concrete. In the study by L'Hermite (1968), the difference of deformations of concrete specimens between laboratory and open air was observed. 8 by 8 by 24 in. concrete specimens were prepared and constant stress was applied. Half specimens were placed in the laboratory with constant 50% relative humidity, and the rest were located in the open air with humidity ranging from 60% to 90%. During 600 days of loading it was indicated that specimens in the laboratory had lower total deformation under load but higher deformation without load than specimens in the open air. If the additive theory was used to calculate creep by subtracting the unloaded deformation from total deformation, it was found that the creep of specimens in the laboratory was lower than those specimens stored in the open air. In another study by Muller and Pristl (1993) slightly lower total strain was observed for concretes stored at 65% relative humidity condition comparing with concretes stored at relative humidity ranging from 40 to 90%. Glucklich (1968) gave a possible explanation of the increase in creep due to the sudden wetting and drying. Sudden wetting induced the crack on the surface of solid with the absorption of water, and the crack resulted in reduced surface tension of the solid. This reduction led to the re-propagation of stable cracks, which further increased creep. Sudden drying induced not only the

cracks due to the moisture gradient but also the reduction of the effective cross-section of concrete, which resulted in higher creep.

2.1.2.11 Temperature under load

Temperature under load is another extrinsic factor affecting creep. Generally the higher temperature results in higher creep during the certain temperature range (Neville A. M., 1970). This behavior was confirmed by Hannant (1967). In this study it was observed that the specific creep of sealed specimens had the linear relationship with temperature ranging from 81 to 176°F (27 to 80°C) with duration of loading of 733 days. Nasser and Neville (1965) took another study to investigate the influence of temperature on creep of concrete. All specimens were submerged into the water all the time, and they were loaded at the age of 14 days. After 15 months under load linear behavior was observed between creep and temperature at the stress-strength ratio 0.35 for the temperature in the range of 115 to 205°F (46 to 96°C). According to the study by Brooks (1991), the effect of change of temperature within a certain range on basic creep of normal concrete and slag concrete was insignificant. Concrete specimens with three levels of replacement of Portland cement with slag were prepared, including 0%, 50% and 70%. After the comparison of specimens stored at constant temperature (40°C) and increasing and decreasing temperature within a certain range (40-65°C for normal concrete, 40-61°C for 50% slag concrete and 40-53°C for 70% slag concrete), it was found that the effect of change of temperature on basic creep of concrete in compression was negligible.

2.1.3 Prediction of creep of concrete

For the prediction of creep of concrete without actual measurements of local material mixtures, the following five models are commonly used, including AASHTO LRFD 2010, ACI 209R-90, ACI 209R Modified by Huo, CEB-FIP 90 and Bazant B3. CEB-FIP 90 also provides the relation between temperature and maturity of concrete. Therefore, if concrete is steam-cured, the maturity of concrete after steam-curing could be calculated, and the adjusted age of concrete could be used in creep and shrinkage models.

2.1.3.1 AASHTO LRFD (2010)

Equations provided by AASHTO LRFD 2010 Specification are applicable for concrete strength up to 15.0 ksi. The expression for the creep coefficient is given as:

$$\Phi(t,t_i) = 1.9 \cdot k_{vs} \cdot k_{hc} \cdot k_f \cdot k_{td} \cdot t_i^{-0.118} \quad \text{(Eq 2-3)}$$

in which:

t = maturity of concrete (day), defined as the age of concrete between time of loading for creep calculations, or end of curing for shrinkage calculations, and time being considered for analysis of creep or shrinkage effect

t_i = age of concrete when load is initially applied (day)

k_{vs} = factor for the effect of the volume-to-surface ratio of the component

$$k_{vs} = 1.45 - 0.13(V/S) \geq 1.0 \quad \text{(Eq 2-4)}$$

or for the detailed equation is

$$k_{vs} = \left[\frac{\frac{t}{26e^{0.0142(V/S)}+t}}{\frac{t}{45+t}}\right]\left[\frac{1.80+1.77e^{-0.0213(V/S)}}{2.587}\right] \quad \text{(Eq 2-5)}$$

V/S is volume to surface ratio, and maximum is 6 in.

k_{hc} = humidity factor for creep

$$k_{hc} = 1.56 - 0.008H \quad \text{(Eq 2-6)}$$

H is relative humidity of ambient condition in percent

k_f = factor for the effect of concrete strength

$$k_f = \frac{35}{7+f'_{ci}} \quad \text{(Eq 2-7)}$$

f'_{ci} = specified compressive strength of concrete at time of prestressing for pretensioned members and at time of initial loading for nonprestressed member

k_{td} = time development factor

$$k_{td} = \frac{t}{61 - 0.58 f'_{ci} + t} \qquad \text{(Eq 2-8)}$$

2.1.3.2 ACI 209R (1992)

The expression for creep coefficient at the standard condition is given as:

$$v_t = \frac{t^{0.60}}{10 + t^{0.60}} v_u \qquad \text{(Eq 2-9)}$$

This equation is applicable for both 1-3 days steam cured concrete and 7-dat moist-cured concrete.

Where:

t = days after loading

v_t = creep coefficient after t days of loading

v_u = ultimate creep coefficient, and the average value suggested $v_u = 2.35\ \gamma_c$

γ_c = correction factors for conditions other than the standard concrete composition, which is defined as:

$$\gamma_c = \gamma_{la} \cdot \gamma_\lambda \cdot \gamma_{vs} \cdot \gamma_s \cdot \gamma_\rho \cdot \gamma_\alpha \qquad \text{(Eq 2-10)}$$

in which:

γ_{la} = correction factor for loading age, which is defined as

$\gamma_{la} = 1.25 t^{-0.118}$ for loading ages later than 7 days for moist cured concrete (Eq 2-11)

$\gamma_{la} = 1.13 t^{-0.094}$ for loading ages later than 1-3 days for steam cured concrete (Eq 2-12)

γ_λ = correction factor for ambient relative humidity, which is defined as

$\gamma_\lambda = 1.27 - 0.0067\lambda$, for $\lambda > 40$, where λ is relative humidity in percent (Eq 2-13)

γ_{vs} = correction factor for average thickness of member or volume-to-surface ratio. When average thickness of member is other than 6 in. (150 mm) or volume-to-surface ratio is other 1.5 in. (38 mm), two methods are offered

(a) Average thickness method

For average thickness of member less than 6 in. (150 mm), the factors are given in Table 2.5.5.1 in ACI 209R-92. For average thickness of members greater than 6 in. (150 mm) and up to about 12 to 15 in (300 to 380 mm), equations are given:

$\gamma_{vs} = 1.14 - 0.023h$ during the first year after loading (Eq 2-14)

$\gamma_{vs} = 1.10 - 0.017h$ for ultimate values (Eq 2-15)

Where h is the average thickness of the member in inches

(b) Volume-surface ratio method

For members with volume-to-surface area other than 1.5 in. (38 mm), the equations are given:

$\gamma_{vs} = \frac{2}{3}[1+1.13e^{-0.54(\frac{v}{s})}]$ where v/s is the volume-surface ration in inches (Eq 2-16)

γ_s = correction factor for slump, and equations are given as:

$\gamma_s = 0.82 + 0.067s$ where s is the observed slump in inches (Eq 2-17)

γ_ρ = correction factor for fine aggregate percentage, which is defined as:

$\gamma_\rho = 0.88 + 0.0024\rho$ (Eq 2-18)

where ρ is the ratio of the fine aggregate to total aggregate by weight expressed as percentage

γ_α = correction factor for air content, which is defined as

$\gamma_\alpha = 0.46 + 0.09\alpha \geq 1.0$ where α is the air content in percent (Eq 2-19)

2.1.3.3 ACI-Modified by Huo (2001)

This model is the same as ACI 209-90, and additional modification factors for compressive strength are taken into account:

$v_t = \frac{t^{0.60}}{K_C + t^{0.60}} v_u$ $(K_C = 12 - 0.50f'_c)$ (Eq 2-20)

$\gamma_{st,c}$ = correction factor for compressive strength of concrete

$\gamma_{st,c} = 1.18 - 0.045f'c$ (Eq 2-21)

f'_c = 28-day compressive strength in ksi

2.1.3.4 CEB-FIP (1990)

The expression for creep coefficient is given:

$$\varphi(t, t_0) = \varphi_0 \cdot \beta_c(t - t_0) \quad \text{(Eq 2-22)}$$

where

t = age of concrete (days) at the moment considered

t_0 = age of concrete at loading (days)

φ_0 = notional creep coefficient

β_c = coefficient to describe the development of creep with time after loading

The expression for notional creep coefficient is given:

$$\varphi_0 = \varphi_{RH} \cdot \beta(f_{cm}) \cdot \beta(t_0) \quad \text{(Eq 2-23)}$$

where

φ_{RH} = coefficient for relative humidity and the dimension of member, and the expression is given:

$$\varphi_{RH} = 1 + \frac{1 - RH/RH_0}{0.46 \cdot (h/h_0)^{1/3}} \quad \text{(Eq 2-24)}$$

where:

RH = relative humidity of the ambient environment in percent (%)

RH_0 = 100%

h = notational size of member (mm), and the expression is $h = 2A_c/u$, where A_c is the area of cross section, and u is the perimeter of the member in constant with the atmosphere

h_0 = 100 mm

$$\beta(f_{cm}) = \frac{5.3}{(f_{cm}/f_{cmo})^{0.5}} \quad \text{(Eq 2-25)}$$

where

f_{cm} = the mean compressive strength of concrete at the age of 28 days (MPa)

f_{cmo} = 10 MPa

$$\beta(t_0) = \frac{1}{0.1 + (t_0/t_1)^{0.2}} \quad \text{(Eq 2-26)}$$

where t_1 = 1 day

The expression for the development of creep with time is given:

$$\beta_c(t - t_0) = \left[\frac{(t-t_0)/t_1}{\beta_H + (t - t_0)/t_1}\right]^{0.3} \quad \text{(Eq 2-27)}$$

with

$$\beta_H = 150 \cdot \{1 + 1.2(\frac{RH}{RH_0})^{18}\} \cdot \frac{h}{h_0} + 250 \leq 1500 \quad \text{(Eq 2-28)}$$

where: t_1 = 1 day, RH_0 = 100%, and h_0 = 100 mm

If concrete undergoes elevated or reduced temperature, the maturity of concrete could be calculated by using the following equation:

$$t_T = \sum_{i=1}^{n} \Delta t_i exp[13.65 - \frac{4000}{273 + T(\Delta t_i)/T_0}] \quad \text{(Eq 2-29)}$$

where:

t_T is the maturity of concrete which can be used in creep and shrinkage models

Δt_i = number of days where a temperature T prevails

$T(\Delta t_i)$ = temperature (°C) during the time of period Δt_i

T_0 = 1°C

2.1.3.5 Bazant B3 (2000)

The compliance function for loaded specimens is expressed as:

$$J(t, t') = q_1 + C_0(t, t') + C_d(t, t', t_0) \quad \text{(Eq 2-30)}$$

where

q_1 = instantaneous strain due to unit stress

$$q_1 = 10^6/E_{ci} \text{ or } (0.6 \times 10^6)/E_{c28} \quad \text{(Eq 2-31)}$$

$$E_{ci} = 57000\sqrt{f'_{ci}} \quad (f'_{ci} \text{ is compressive strength at the age of loading, psi}) \quad \text{(Eq 2-32)}$$

$$E_{c28} = 57000\sqrt{f'_{c28}} \quad (f'_{c28} \text{ is 28-day compressive strength, psi}) \quad \text{(Eq 2-33)}$$

$C_0(t, t')$ = compliance function for basic creep (in/in/psi)

$$C_0(t, t') = q_2 Q(t, t') + q_3 ln[1 + (t - t')^n] + q_4 ln(t/t') \quad \text{(Eq 2-34)}$$

t = age of concrete after casting (days)

t' = age of concrete at loading (days)

t_0 = age of concrete at the beginning of shrinkage (days)

$$q_2 = 451.4c^{0.5}(f'_{c28})^{-0.9} \quad (c \text{ is cement content in pcf}) \quad \text{(Eq 2-35)}$$

$$Q(t, t') = Q_f(t')[1 + (\frac{Q_f(t')}{Z(t,t')})^{\gamma(t')}]^{1/\gamma(t')} \quad \text{(Eq 2-36)}$$

$$Q_f(t') = [0.086(t')^{2/9} + 1.21(t')^{4/9}]^{-1} \quad \text{(Eq 2-37)}$$

$$Z(t, t') = (t')^{-m} \ln(1 + (t - t')^n) \qquad (m=0.5, n=0.1) \quad \text{(Eq 2-38)}$$

$$\gamma(t') = 1.7(t')^{0.12} + 8 \quad \text{(Eq 2-39)}$$

$C_d(t, t', t_0)$ = additional compliance function due to simultaneous drying (in/in/psi)

$$C_d(t, t', t_0) = q_5[exp\{-8H(t)\} - exp\{-8H(t')\}]^{1/2} \quad \text{(Eq 2-40)}$$

$$q_5 = 7.57 \times 10^5 (f'_{c28})^{-1} ABS(\varepsilon_{sh\infty})^{-0.6} \quad \text{(Eq 2-41)}$$

$$\varepsilon_{sh\infty} = \alpha_1\alpha_2[26\omega^{2.1}(f'_{c28})^{-0.28} + 270] \quad (\omega \text{ is water content in pcf}) \qquad \text{(Eq 2-42)}$$

$$\alpha_1 = \begin{cases} 1.0 \text{ for type I cement} \\ 0.85 \text{ for type II cement} \\ 1.1 \text{ for type III cement} \end{cases}$$

and

$$\alpha_2 = \begin{cases} 0.75 \text{ for steam} - \text{curing} \\ 1.2 \text{ for sealed or normal curing in air with inital protection against drying} \\ 1.0 \text{ for curing in water or at 100\% relative humidity} \end{cases}$$

$$H(t) = 1 - (1- h)S(t) \qquad \text{(h is relative humidity)} \qquad \text{(Eq 2-43)}$$

$$S(t) = tanh[(t - t_0)/\tau_{sh}]^{1/2} \qquad \text{(Eq 2-44)}$$

$$\tau_{sh} = K_t(K_sD)^2 \qquad \text{(Eq 2-45)}$$

$$D = 2v/s \qquad \text{(Eq 2-46)}$$

$$K_t = 190.8(t_0)^{-0.08}\,(f'_{c28})^{-0.25} \qquad \text{(Eq 2-47)}$$

K_s = 1.00 for infinite slab

= 1.15 for infinite cylinder

= 1.25 for infinite square prism

= 1.30 for sphere

= 1.55 for cube

= 1.00 for undefined member

$$H(t') = 1 - (1- h)S(t') \qquad \text{(h is relative humidity)} \qquad \text{(Eq 2-48)}$$

$$S(t') = tanh[(t' - t_0)/\tau_{sh}]^{1/2} \qquad \text{(Eq 2-49)}$$

Creep strain should be calculated as:

$$\varepsilon_{cr} = [C_0(t, t') + C_d(t, t', t_0)]\sigma \qquad (\sigma \text{ is the applied stress, psi}) \qquad \text{(Eq 2-50)}$$

Creep coefficient should be expressed as:

$$\varphi(t, t') = \frac{\varepsilon_{cr}}{q_1 \sigma} \quad \text{(Eq 2-51)}$$

Total strain may be expressed as:

$$\varepsilon_{total} = J(t, t')\,\sigma + \varepsilon_{sh} \quad \text{(Eq 2-52)}$$

where ε_{sh}= shrinkage strain in section 2.2.3.5

2.1.3.6 Comparison of five models

The considered parameters in each model and corresponding ranges are shown in Table 2.1.

Table 2.1. Comparison of Five Models for Prediction of Creep of Concrete

Considered Parameters	AASHTO LRFD 2010	ACI 209R-92	ACI-Modified by Huo	CEB-FIP 90	Bazant B3
f_{cm28}, psi	up to 15,000	-	up to 12360	2900 to 13,000	2500 to 10,000
Aggregate to cement ratio, *a/c*	-	-	-	-	2.5 to 13.5
Water to cementitous ratio, *w/c*	-	-	-	-	0.35 to 0.85
Cement content, pound per cubic yard	-	Considered	Considered	-	270 to 1215
Relative humidity, %	35 to 100	40 to 100	40 to 100	40 to 100	40 to 100
Type of cement	I, II, III	I or III	I, II, III	I, II, III	I, II, III
Age of steam curing before loading	1 to 3 days	1 to 3 days	1 to 3 days	-	-
Age of moist curing before loading	≥ 1 day	≥ 1 day	≥ 1 day	≤ 14 days	≥ 1 day
Age of loading	≥ 1 day	≥ 1 day	≥ 1 day	≥ 1 day	≥ 1 day
Fine aggregate content in total aggregate, %	-	Considered	Considered	-	-
Air content	-	Considered	Considered	-	-
Slump	-	Considered	Considered	-	-
Size effect	Considered	Considered	Considered	Considered	Considered

2.2 Shrinkage of Concrete

2.2.1 Introduction

Shrinkage is the decrease in volume of hardened concrete with time. Shrinkage of hardened concrete is divided into drying shrinkage, autogenous shrinkage and carbonation shrinkage (ACI 209R, 1992). Drying shrinkage is caused by the moisture loss in the concrete. Autogenous shrinkage (or basic shrinkage or chemical shrinkage) is due to the hydration of cement. Autogenous shrinkage typically is negligible in concrete with a higher water to cement (w/c) ratio, but it becomes an issue for concrete with a lower w/c ratio such as high performance concrete (Nishiyama, 2009). Carbonation shrinkage results from the carbonation of cement hydration products in the presence of carbon dioxide. Bazant (2000) found that in good concrete carbonation occurs only in the surface layer with the thickness of several millimeters, so the carbonation shrinkage is negligible. This was confirmed by Persson (1998) and Malhotra (2000). For high performance concrete used for prestressed bridge girders, carbonation shrinkage is negligible comparing with drying shrinkage and autogenous shrinkage.

2.2.2 Factors affecting shrinkage of concrete

Shrinkage of concrete is influenced by intrinsic and extrinsic factors similar with creep. Intrinsic factors contain the proportions and properties of mixtures. Extrinsic factors consist of size of concrete, age of concrete exposure to the ambient condition, curing conditions, ambient temperature and relative humidity after exposure.

2.2.2.1 Aggregate

Aggregate has a significant effect on shrinkage of concrete. Aggregate provides the restraining effect of shrinkage (Neville A. M., 1981), and the more aggregate the higher restraining effect and the lower shrinkage. Pickett (1956) proposed an equation to describe the effect of aggregate content on shrinkage of concrete:

$$\text{Shrinkage ratio} = \frac{S_c}{S_p} = (1 - a)^n \qquad \text{(Eq 2-53)}$$

where:

S_c = shrinkage of concrete

S_p = shrinkage of neat paste

a = percent aggregate content by volume

n = experimental exponent, and typically between 1.2 to 1.7 (L' Hermite R. G., 1968)

In this study, six levels of percent aggregate content by volume were used with a range from 0% to 62%. It was found that shrinkage decreased with an increase in aggregate content, and data fit the equation above when n = 1.7.

The effect of aggregate type on shrinkage of concrete under drying condition was investigated by Alexander (1996). In this study, two groups of concretes with 23 different types of aggregates were prepared, including shrinkage only specimens exposure to the air at 28 days and shrinkage specimens for creep exposure at the same age with creep specimens (600 days for series 1, 334 days for series 2). It was observed that shrinkage in the shrinkage only test was in a range of 86 to 463 microstrain at 28 days, and 247 to 841 microstrain at 6 months. It was also found that shrinkage for creep test varied from 83 to 561 microstrain at 28 days and from 236 to 826 microstrain for series 1 at 325 days, and from 140 to 459 microstrain for series 2 at the age of 140 days. It was additionally indicated that shrinkage for creep test had lower magnitude than shrinkage only test, because unloaded concretes for creep test had longer curing duration.

Modulus of elasticity of aggregate also has a great effect on shrinkage of concrete, and the higher modulus of elasticity of aggregate, the higher restraining effect on shrinkage and the lower shrinkage (Neville A. M., 1981). Hobbs (1974) also proposed equations to illustrate the effect of properties of aggregate including aggregate content and modulus of elasticity on the ratio of shrinkage of concrete and shrinkage of cement paste. Other properties of aggregate such as size and grading are indirect factors, and they affect shrinkage through aggregate content (Neville A. M., 1981).

2.2.2.2 Cement

Cement type and fineness have a slightly influence on shrinkage of concrete (Neville A. M., 1981). According to the studies by Swayze (1960), the finer cement typically resulted in higher shrinkage of cement pastes, but not necessarily caused higher shrinkage of concrete.

Similar conclusion was also made by Bennett (1970). Typically rapid-hardening (Type III) Portland cement and other mineral admixtures such as slag and fly ash resulted in higher autogenous shrinkage of concrete (Khayat, 2009).

2.2.2.3 Water to cemtitious ratio

Water to cementitious (w/c) ratio is another factor influencing both drying shrinkage and autogenous shrinkage. Higher w/c ratio typically causes higher drying shrinkage, which is due to the reduction of the effective volume of restraining aggregate caused by higher water content (Neville A. M., 1981). In the study by ODman (1968), the effect of w/c ratio on shrinkage of concrete was investigated, and it was found that shrinkage of concrete increased with an increase of w/c ratio in drying condition. Similar behaviors were observed by Soraka (1979).

Water to cementitious ratio has the opposite effect on autogenous shrinkage, and autogenous shrinkage becomes a concern with lower w/c ratio such as HPC. According to the study by Miyazawa (1997), it was observed that total shrinkage of cement paste almost kept constant with w/c ratio from 0.3 to 0.6, but increased significantly with w/c ratio of 0.2 due to the great increase of autogenous shrinkage. Autogenous shrinkage of cement paste was smaller than 100 microstrain when w/c ratio was 0.5 or greater at 90 days, and it increased with a decrease of w/c ratio from 0.5 to 0.2. Autogenous shrinkage of cement paste at 90 days was about half of total shrinkage with a w/c ratio of 0.3, and it became about three quarters with w/c ratio of 0.2. Those behaviors were consistent with observations by Tazawa (1997) and Persson (1998). Although the extent of effect of autogenous shrinkage of cement paste on autogenous shrinkage of concrete highly depends on properties of aggregate, typically higher autogenous shrinkage of cement paste means higher autogenous shrinkage of concrete. The relation between shrinkage of cement paste and shrinkage of concrete were proposed by Pickett (1956) and Hobbs (1974).

2.2.2.4 Chemical admixtures

Chemical admixtures are widely used in HPC, and the effect on shrinkage of concrete highly depends on the chemical compositions and dosages. According to the study by Keene (1960), it was found that air-entrainment agent had no effect on the shrinkage of concrete under drying condition. This was confirmed by Kosmatka (2008). In the study by Brooks (1989), seven sets of data on drying shrinkage of concrete were summarized, and it was indicated that plasticizers and superplasticiziers typically increased drying shrinkage of concrete by 20%.

However, some other investigators had the opposite conclusion, and decreased shrinkage of concrete was observed due to the use of high-range water reducing agents (Nagataki, 1978).

2.2.2.5 Mineral admixtures

Slag, fly ash and silica fume are three types of partial replacement materials of Portland cement used in HPC. They also influence the behavior of shrinkage of concrete.

Slag has an effect on shrinkage of concrete. In the study by Tazawa (1989), there were three levels of replacement of Portland cement with slag, including 0%, 35% and 55%. It was observed that slag decreased shrinkage of concrete under drying condition after 28 days of storage, and the higher slag content the lower shrinkage of concrete. It was additionally found that the extent of effect of slag on shrinkage under drying condition also depended on the curing duration, and the longer curing time the lower effect of slag on shrinkage of concrete. Another study by Sakai (1992), the effect of four levels of replacement of Portland cement with slag including 50%, 60%, 70% and 80% in concrete was investigated. It was indicated that shrinkage of concrete under drying condition increased with an increase of slag content from 50% to 60%, then decreased with an increase of slag content from 70% and 80%. Similar behavior of shrinkage of concrete with high slag content was also observed by Brooks (1992). According to a later study by Tazawa (1997), the effect of slag content in the range of 0%, 25%, 50% and 70% and three levels of fineness of slag particles on autogenous shrinkage was investigated. It was indicated that slag with lowest fineness decreased autegenous shrinkage of cement paste slightly with an increase of slag content from 0% to 70%, but for slags with higher fineness autogenous shrinkage increased significantly with an increase of slag content. It was found that cement paste with 70% slag content and the highest fineness resulted in the highest autogenous shrinkage. It was additionally found that cement paste and concrete had the similar trend of autogenous shrinkage for the effect of slag. Similar behavior of autogenous of slag concrete was observed by Lim (2000). In the study by Saric-Coric (2003), it was found that autogenous shrinkage of cement paste increased with an increase of slag content. Both studies by Lim and Saric-Coric confirmed Tazawa's observations.

Generally partial replacement of Portland cement with fly ash has no significant influence on shrinkage of concrete under a given drying condition (ACI 232.2R, 1996), but affects autogenous shrinkage. According to the study by Naik (2007), the effect of Class C fly ash of 0%

and 30% replacement of Portland cement on shrinkage of concrete was investigated. It was observed that fly ash decreased early age autogenous shrinkage of concrete and increased it at later ages. Fly ash concrete only had 64% autogenous shrinkage at 7 days comparing with concrete without fly ash, but was 164% at 56 days. Fly ash increased shrinkage of concrete slightly under drying condition. Class F fly ash used in HPC with 20% replacement of Portland cement increased autogenous shrinkage (Khayat, 2009).

Silica fume is typically used in HPC. According to the study by Mazloom (2004), four levels of replacement of Portland cement with silica fume were used, including 0%, 6%, 10% and 15%. It was observed that total shrinkage of HPC with fixed w/c ratio of 0.35 under drying condition decreased slightly with an increase of silica fume, but autogenous shrinkage of HPC measured from sealed specimens increased with an increase of replacement level of silica fume. It was found that autgenous shrinkage of concrete increased from 37% to 58% of total shrinkage with an increase of silica fume from 0% to 15% at the age of 587 days. Calculated drying shrinkage of concrete decreased with an increase of silica fume content. Similar behaviors were also found previously by Roy (1993) and Tazawa (1993) with silica fume content below 10%. When replacement level up to 20%, it was indicated that shrinkage of concrete increased slightly (ACI 234R, 2006).

2.2.2.6 Size effect

Size of a specimen has a significant effect on shrinkage of concrete under drying condition. In the study by Carlson (1937), mass concrete was stored in the air with 50% relative humidity. It was observed that drying thickness was about 3 inches from the surface after one month, and about 9 inches after one year and about 24 inches after ten years, which indicated the size effect on drying process of concrete. Hansen (1966) reported that volume to surface (v/s) ratio was a reasonable indicator of size effect on drying shrinkage, and it was observed that higher v/s ratio typically resulted in lower drying shrinkage during 1200 days. It was additionally indicated that the effect of shape of concrete members on drying shrinkage is small when specimens had similar v/s ratios. It was also found that concrete stored in water had very small shrinkage comparing with concrete stored in the air with 50% relative humidity, which indicated size effect on autogenous shrinkage of concrete was not significant. In the study by Bryant (1987), thickness of a concrete member was used to account for the size effect on

shrinkage, and it was found that the shrinkage under drying condition decreased with an increase of thickness of concrete members. It was also indicated that the shrinkage of sealed specimens were much smaller than unsealed specimens, which confirmed the observations by Hansen (1966).

2.2.2.7 Curing conditions

Curing condition is an extrinsic factor affecting shrinkage of concrete. Steam curing is widely used for HPC of prestressed members. In the study by Townsend (2003), it was observed that steam-cured concrete had 45% higher shrinkage than moist-cured concrete at storage of 1 week under drying condition, but after 14 weeks this value became 11%. It was indicated that steam curing increased initial shrinkage of concrete significantly, and decreased the rate of shrinkage at later ages. According to the study by Haranki (2009), it was found that concretes with 14-day moist-curing had smaller shrinkage under drying condition comparing with concretes with 7-day moist-curing, which was due to the higher maturity of concrete after 14-day moist curing.

2.2.2.8 Relative humidity

Relative humidity of storage has a great influence on shrinkage under drying condition. Concrete swells in the water or in the air with 100% relative humidity, and shrinks when the relative humidity is below 94% (Neville A. M., 1981). In the study by Troxell (1958), concrete specimens were stored in three conditions of relative humidity, including 50%, 70% and 100% (in water). It was observed that the concrete in water swelled with time with relatively small strain, and shrinkage increased with a decrease of relative humidity for concretes from 50% and 70% conditions. Concrete stored at the condition of 50% relative humidity had 30% higher shrinkage at 1 year and 45% higher shrinkage at 25 years comparing with concrete stored at the condition of 70% relative humidity. Similar conclusion was made by Bissonnette (1999).

2.2.3 Prediction of shrinkage of concrete

For the prediction of shrinkage of concrete without actual measurements of local material mixtures, the following five models are typically used, including AASHTO LRFD 2010, ACI 209R-90, ACI 209R Modified by Huo, CEB-FIP 90 and Bazant B3.

2.2.3.1 AASHTO LRFD (2010)

The expression for the shrinkage strain is given as:

$$\varepsilon_{sh} = k_{vs} \cdot k_{hs} \cdot k_f \cdot k_{td} \, (0.48) \times 10^{-3} \qquad \text{(Eq 2-54)}$$

In this equation, the ultimate shrinkage strain is taken as 0.00048 in. /in.

in which:

$$k_{vs} = 1.45 - 0.13(V/S) \geq 1.0 \qquad \text{(Eq 2-55)}$$

or the detailed equation is:

$$k_{vs} = \left[\frac{t}{\frac{26 \cdot e^{0.0142\left(\frac{V}{S}\right)} + t}{\frac{t}{45+t}}} \right] \left[\frac{1064 - 3.7\left(\frac{V}{S}\right)}{923} \right] \quad \text{(maximum } V/S \text{ is 6 in.)} \qquad \text{(Eq 2-56)}$$

k_{hs} = humidity factor for shrinkage

$$k_{hs} = 2.00 - 0.014H \qquad \text{(Eq 2-57)}$$

2.2.3.2 ACI 209R (1992)

The expression for shrinkage strain at the standard condition is given as:

$(\varepsilon_{sh})_t = \frac{t}{35+t} (\varepsilon_{sh})_u$ shrinkage after 7 days for moist cured concrete (Eq 2-58)

$(\varepsilon_{sh})_t = \frac{t}{55+t} (\varepsilon_{sh})_u$ shrinkage after 1-3 days for steam cured concrete (Eq 2-59)

where:

t = days after the end of the initial wet curing

$(\varepsilon_{sh})_t$ = shrinkage strain after t days

$(\varepsilon_{sh})_u$ = ultimate shrinkage strain, and the average value suggested for

$$(\varepsilon_{sh})_u = 780\gamma_{sh} \times 10^{-3} \text{ in./in., (mm./mm.)}$$

γ_{sh} = correction factors for conditions other than the standard concrete composition,

which is defined as:

$$\gamma_{sh} = \gamma_\lambda \cdot \gamma_{vs} \cdot \gamma_s \cdot \gamma_\rho \cdot \gamma_c \cdot \gamma_\alpha \quad \text{(Eq 2-60)}$$

in which:

γ_λ = correction factor for ambient relative humidity, which is defined as

$\gamma_\lambda = 1.40 - 0.0102\lambda$, for $40 \leq \lambda \leq 80$, where λ is relative humidity in percent (Eq 2-61)

$\gamma_\lambda = 3.00 - 0.030\lambda$, for $80 < \lambda \leq 100$, where λ is relative humidity in percent (Eq 2-62)

γ_{vs} = correction factor for average thickness of member or volume-to-surface ratio. When average thickness of member is other than 6 in. (150 mm) or volume-to-surface ratio is other 1.5 in. (38 mm), two methods are offered

(a) Average thickness method

For average thickness of member less than 6 in. (150 mm), the factors are given in Table 2.5.5.1 in ACI 209R-92. For average thickness of members greater than 6 in. (150 mm) and up to about 12 to 15 in (300 to 380 mm), equations are given:

$\gamma_{vs} = 1.23 - 0.038h$ during the first year after loading (Eq 2-63)

$\gamma_{vs} = 1.17 - 0.029h$ for ultimate values (Eq 2-64)

Where h is the average thickness of the member in inches

(b) Volume-surface ratio method

For members with volume-to-surface area other than 1.5 in. (38 mm), the equations are given:

$\gamma_{vs} = 1.2e^{-0.12(\frac{v}{s})}$ where v/s is the volume-surface ration in inches (Eq 2-65)

γ_s = correction factor for slump, and equations are given as:

$\gamma_s = 0.89 + 0.041s$ where s is the observed slump in inches (Eq 2-66)

γ_ρ = correction factor for fine aggregate percentage, which is defined as:

$\gamma_\rho = 0.30 + 0.014\rho$ where $\rho \leq 50$ percent (Eq 2-67)

$\gamma_\rho = 0.90 + 0.002\rho$ where $\rho > 50$ percent (Eq 2-68)

where ρ is the ratio of the fine aggregate to total aggregate by weight expressed as percentage

γ_c = correction factor for cement content, which is defined as

$$\gamma_c = 0.75 + 0.00036c \quad \text{where c is the cement content in lb/yd}^3 \qquad \text{(Eq 2-69)}$$

γ_α = correction factor for air content, which is defined as

$$\gamma_\alpha = 0.95 + 0.008\alpha \quad \text{where } \alpha \text{ is the air content in percent} \qquad \text{(Eq 2-70)}$$

2.2.3.3 ACI-Modified by Huo (2001)

$$v_t = \frac{t}{K_S + t}(\varepsilon_{sh})_u \quad (K_S = 45 - 2.5f'_c) \qquad \text{(Eq 2-71)}$$

$\gamma_{st,s}$ = correction factor for compressive strength of concrete

$$\gamma_{st,s} = 1.20 - 0.05f'c \qquad \text{(Eq 2-72)}$$

f'_c = 28-day compressive strength in ksi

2.2.3.4 CEB-FIP (1990)

The expression for the shrinkage strain in compression is given:

$$\varepsilon_{cs}(t, t_s) = \varepsilon_{cso} \cdot \beta_s(t - t_s) \qquad \text{(Eq 2-73)}$$

where

ε_{cso} = the notional shrinkage coefficient

β_s = the coefficient to describe the development of shrinkage with time

t = the age of concrete (days)

t_s = the age of concrete (days) at the beginning of shrinkage

The notional shrinkage coefficient is given:

$$\varepsilon_{cso} = \varepsilon_s(f_{cm}) \cdot \beta_{RH} \qquad \text{(Eq 2-74)}$$

within

$$\varepsilon_s(f_{cm}) = [160 + 10 \cdot \beta_{sc}(9 - f_{cm}/f_{cmo})] \cdot 10^{-6} \qquad \text{(Eq 2-75)}$$

where:

f_{cm} is the mean compressive strength of concrete at the age of 28 days (MPa)

f_{cmo} = 10 MPa

β_{sc} is the coefficient which depends on the type of cement: β_{sc} = 4 for slowly hardening cements SL, β_{sc} = 5 for normal or rapid hardening cements N and R, and β_{sc} = 8 for rapid hardening high strength cements RS

$\beta_{RH} = -1.55 \cdot \beta_{sRH}$ for $40\% \leq RH \leq 99\%$ (Eq 2-76)

$\beta_{RH} = +0.25$ for $RH \geq 99\%$ (Eq 2-77)

where $\beta_{sRH} = 1 - (\frac{RH}{RH_0})^3$ (Eq 2-78)

with

RH is the relative humidity of the ambient atmosphere (%)

RH_0 = 100%

The development of shrinkage with time is given by

$$\beta_s(t - t_s) = [\frac{(t - t_s)/t_1}{350 \cdot (h/h_0)^2 + (t - t_s)/t_1}]^{0.5}$$ (Eq 2-79)

where

h = notational size of member (mm), and the expression is $h = 2A_c/u$, where A_c is the area of cross section, and u is the perimeter of the member in constant with the atmosphere

h_0 = 100 mm

t_1 = 1 day

2.2.3.5 Bazant B3 Model (2000)

The shrinkage strain is expressed as:

$\varepsilon_{sh}\,(t,\,t') = \varepsilon_{sh\infty}\,K_h\,S(t)$ (Eq 2-80)

where $\varepsilon_{sh\infty}$ could be calculated by using Eq 2-45 and *S(t)* could be calculated by using Eq 2-47, and

$$K_h = \begin{cases} 1 - h^3 \text{ for } h < 0.98 \\ -0.2 \text{ for } h = 1 \\ \text{use linear interpolation for } 0.98 < h < 1 \end{cases}$$

2.3 Modulus of Elasticity of Concrete

2.3.1 Introduction

Modulus of elasticity is an important property of hardened concrete. Concrete is a composite material, including aggregate and cement paste. Modulus of elasticity of concrete highly depends on properties and proportions of mixture materials. ASTM Standard C469 provides the method to measure static modulus of elasticity of concrete in compression. Elastic modulus of concrete has a significant effect on behavior of pretressed bridge girders, such as camber. In the following sections, factors affecting modulus of elasticity of concrete and four prediction models are presented.

2.3.2 Factors affecting modulus of elasticity of concrete

Modulus of elasticity of concrete is greatly influenced by the material properties and mineral admixtures, and the effect of other factors is not significant.

2.3.2.1 Material properties

Concrete is a composite of aggregate and cement paste, and it is typically a composite soft material due to higher modulus of elasticity of aggregate than cement paste (Neville A. M., 1970). Neville (1970) cited two equations for elastic moduli of composite shown below:

$E = (1-g)\,E_m + gE_p$ (composite hard material when $E_m > E_p$) (Eq 2-81)

$E = \left(\frac{1-g}{E_m} + \frac{g}{E_p}\right)^{-1}$ (composite soft material when $E_m < E_p$) (Eq 2-82)

Where:

E is modulus of elasticity of the composite material; E_m is modulus of elasticity of the matrix phase; E_p is modulus of elasticity of the particle phase; g = fractional volume of the particles.

Aggregate plays an important role in the modulus of elasticity of concrete. Typically higher aggregate content and higher modulus of elasticity of aggregate result in higher elastic

moduli of concrete. Those conclusions were confirmed by Hirsch (1962) and Hansen (1965), and also empirical equations were proposed.

The relations of stress and strain for aggregate, cement paste and concrete are shown in Figure 2.1 (Neville A. M., 1981). A reasonable explanation for the curved shape of concrete was given by Neville (1981). The rate of increase of induced strain at the interface of aggregate and cement paste was much higher than the rate of applied stress development beyond a certain range. Further explanation of the effect of bond of aggregate and cement paste on elastic modulus of concrete was also provided by Neville (1997). The difference of modulus of elasticity between aggregate and cement paste plays an important role in modulus of elasticity of concrete. In HPC the difference of modulus of elasticity between aggregate and cement paste was smaller than normal concrete, which resulted in better bond of aggregate and cement and higher modulus of elasticity of concrete. In HPC the linear part in a stress & strain curve as high as 85% of ultimate strength or even higher was observed.

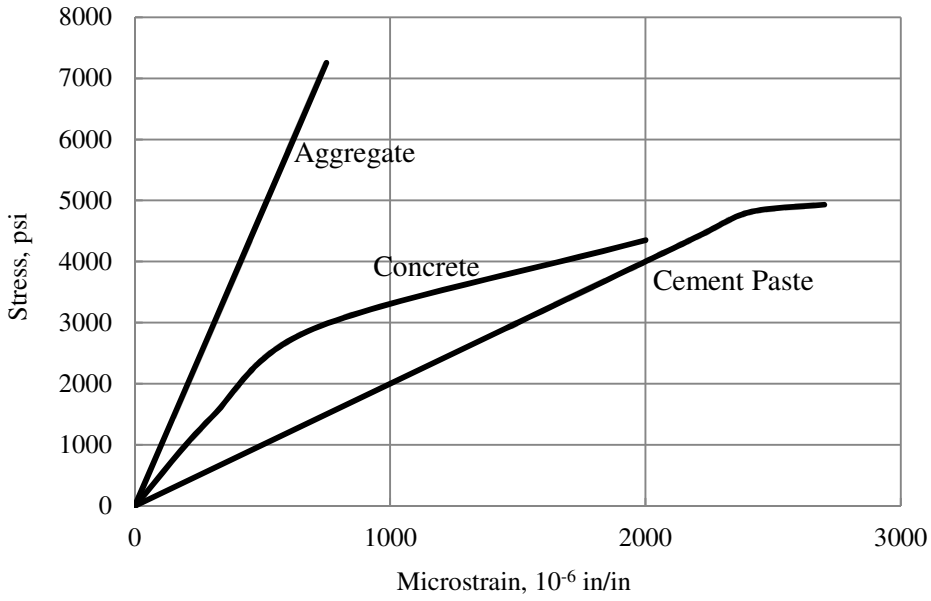

Figure 2.2. Stress-strain relations for aggregate, cement paste and concrete

2.3.2.2 Mineral admixtures

Mineral admixtures are typically added in HPC as partial replacement materials of Portland cement. The influence of slag on modulus of elasticity of concrete is small (ACI 233R, 2003). In the study by Brooks (1992), the effect of 0%, 30%, 50% and 70% slag replacement of

Portland cement on the property of concrete was investigated. No significant influence of slag on elastic moduli was observed. It was indicated that dry-stored slag concrete had higher elastic moduli at early ages, but lower at later ages comparing with concrete without slag, and the opposite trend was found for water-stored concrete. Fly ash has also slightly influence on modulus of elasticity of concrete, including Class F fly ash (Lane, 1982) and Class C fly ash (Yildirim, 2011). Silica fume increases elastic moduli of concrete within certain content. According to the study by Alfes (1992), it was indicated that 10% silica fume as the replacement of Portland cement increased elastic moduli of concrete by 12% at 28 days, but 20% silica fume increased it by 7% at 28 days comparing with concrete without silica fume. In the study by Mazloom (2004), effect of four levels of replacement of Portland cement with silica fume including 0%, 6%, 10% and 15% on modulus of elasticity of concrete was investigated. It was found that elastic moduli increased within 10% at 7 days and 28 days with an increase of silica fume content.

2.3.3 Prediction of elastic modulus of elasticity of concrete

Typically the relation between modulus of elasticity of concrete and corresponding compressive strength is provided, which is not due to a direct relation between elastic moduli and compressive strength, but because of the convenience of measurement of compressive strength. The following four models are commonly used for the prediction of modulus of elasticity when the actual measurements are not available.

2.3.3.1 AASHTO LRFD (2010)

In the absence of measured data, the modulus of elasticity, E_c, for concretes with unit densities between 90 and 155 pcf and specified compressive strengths up to 15.0 ksi may be taken as:

$$E_c = 33\, K_1\, w_c^{1.5}\, \sqrt{f_c'} \qquad \text{(Eq 2-83)}$$

Where:

E_c = elastic modulus of elasticity of concrete (psi)

K_1 = correction factor for source of aggregate to be taken as 1.0 unless determined by physical test, and as approved by the authority of jurisdiction

w_c = unit density of concrete (lb/ft^3)

f_c' = specified compressive strength of concrete (psi)

2.3.3.2 ACI 363R (1992)

According to the study by Martinez (1982), it was found that the expression of Eq 2-83 overestimated the modulus of elasticity for high performance concretes with compressive strength between 6000 psi and 12000 psi. A correlation between the modulus of elasticity E_c and compressive strength f_c' for normal weight concretes was reported below:

$$E_c = (40{,}000\sqrt{f_c'} + 1.0 \times 10^6)\left(\frac{w_c}{145}\right)^{1.5} \qquad (3{,}000 \text{ psi} < f'_c < 12{,}000 \text{ psi}) \qquad \text{(Eq 2-84)}$$

where:

f'_c = specified compressive strength of concrete (psi)

w_c = the density of concrete (lb/ft^3)

2.3.3.3 CEB-FIP (1990)

Values of the modulus of elasticity for normal weight concrete can be estimated from the specified characteristic strength by using:

$$E_{ci} = E_{co}[(f_{ck} + \Delta f)/f_{cmo}]^{1/3} \qquad \text{(Eq 2-85)}$$

where

E_{ci} = the modulus of elasticity (MPa) at a concrete age of 28 days

$E_{co} = 2.15 \times 10^4$ MPa

f_{ck} = the characteristic strength (MPa) mentioned at Table 2.1.1 in CEB-FIP 1990

Δf = 8 MPa

f_{cmo} = 10 MPa

When the actual compressive strength of concrete at an age of 28 days f_{cm} is known, E_{ci} may be estimated from:

$$E_{ci} = E_{co}[f_{cm}/f_{cmo}]^{1/3} \qquad \text{(Eq 2-86)}$$

When only an elastic analysis of a concrete structure is carried out, a reduced modulus of elasticity E_c can be calculated in order to account for initial plastic strain shown below:

$$E_c = 0.85\ E_{ci} \qquad \text{(Eq 2-87)}$$

2.3.3.4 Tadros (2003)

The modulus of elasticity of high performance concrete can be expressed as:

$E_c = 33{,}000K_1K_2(0.140 + \frac{f_c'}{1000})^{1.5}\sqrt{f_c'}$ (E_c is in ksi, and f_c' is in ksi) (Eq 2-88)

Where:

K_1 = correction factor for local material variability, and $K_1 = 1.0$ for the average of all data obtained by Tadros (2003).

K_2 = correction factor based on the 90th percentile upper-bound and the 10th percentile lower-bound for all data, and for the average of all data $K_2 = 0.777$ (10th percentile) and $K_2 = 1.224$ (90th percentile).

2.4 Long-Term Camber of Prestressed Bridge Girders

Camber of a prestressed bridge girder is the elevation difference between the midspan and the end of the girder. Figure 2.3 shows the detail below. Typically elevation is measured from the top flange by using an accurate laser level.

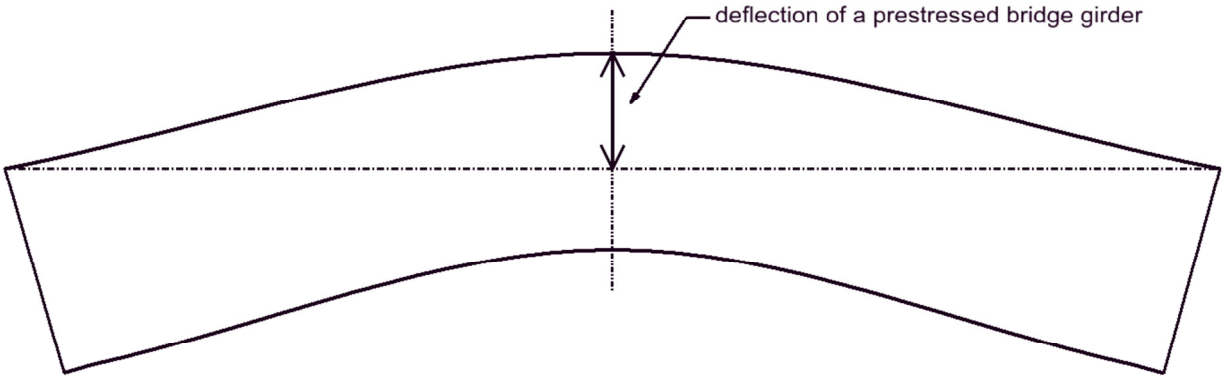

Figure 2.3. Camber of a prestressed bridge girder

2.4.1 Factors affecting long-term camber of prestressed bridge girders

2.4.1.1 Introduction

Long-term camber of a prstressed bridge girder is affected by camber at transfer, self-weight, creep, prestress forces and losses, and cross section properties.

2.4.1.2 Camber at transfer

For a prestressed bridge girder after strands are cut, instantaneous upward camber occurs. Instantaneous camber varies for different types of girders, and it is influenced by prestress forces, self-weight, modulus of elasticity of concrete and cross section of the girder.

2.4.1.3 Camber due to self-weight

Camber of a prestressed girder due to self-weight is significantly influenced by the length of an overhang. Overhang length is the distance from the end of girder to the center of the support.

If there is no overhang, the camber at midspan relative to the end of the girder due to self-weight can be calculated by using:

$$\Delta_{sw} = \frac{5w_{sw}L^4}{384E_{ce}I} \quad \text{(Eq 2-89)}$$

where:

w_{sw} = self-weight per unit length

L = length of a girder

I = moment of inertia of cross section

If there is an overhang, the camber at midspan respect to the end of the girder due to self-weight can be calculated:

$$\Delta_{sw} = \Delta_{overhang} + \Delta_{midspan} \quad \text{(Eq 2-90)}$$

$$\Delta_{overhang} = \frac{\omega_{sw}L_c}{24E_{ce}I}\left[3L_c^{\,2}\left(L_c + 2L_n\right) - L_n^{\,3}\right] \quad \text{(Eq 2-91)}$$

$$\Delta_{midspan} = \frac{\omega_{sw}L_n^2}{384E_{ce}I}\left[5L_n^{\,2} - 24L_c^{\,2}\right] \quad \text{(Eq 2-92)}$$

where:

$\Delta_{overhang}$ = the camber of the end of overhang relative to the support

$\Delta_{midspan}$ = the camber at the midspan relative to the support

L_c = length of overhang

L_n = distance between two supports

Time dependent camber of a prestressed bridge girder with overhang can be adjusted to the camber without overhang by using the Eq 2-90, 2-91 and 2-92.

2.4.1.4 Camber due to creep

After transfer for a prstressed girder, prestressing force and self-weight result in different stresses along the cross section of concrete of a girder, and the applied stress increases the upward camber. This additional camber is due to creep of concrete.

2.4.1.5 Prestress losses

2.4.1.5.1 Introduction

Pretress losses of prestressed bridge girders before deck is placed consist of short-term losses and long-term losses. Short-term losses are due to anchorage set at jacking, relaxation before transfer and elastic shortening at transfer. Long-term losses result from creep, shrinkage and relaxation after transfer. Prestress losses result in a decrease of camber of a girder. AASHTO LRFD (2010) provides refined estimations of time-dependent prestress losses:

$$\Delta f_p = \Delta f_{pA} + \Delta f_{pR1} + \Delta f_{pES} + \Delta f_{pC} + \Delta f_{pSH} + \Delta f_{pR2} \qquad \text{(Eq 2-93)}$$

2.4.1.5.2 Prestress loss due to anchorage set

Anchorage set loss is due to the movement of the strand prior to seating the anchorage gripping device. This is a major loss before transfer comparing with relaxation loss. The magnitude of this movement depends on the prestressing system used in precast factory, and AASHTO LRFD 2010 provides a common value of 0.375 inch. Anchorage set loss stress is expressed as:

$$\Delta f_{pA} = \frac{\Delta_{set}}{L_p} E_p \qquad \text{(Eq 2-94)}$$

Δ_{set} = anchorage set at jacking, which is provided by manufacturer of prestressing system, in

L_p = total length of prestressing strand, in

E_p = modulus of elasticity of strand (typical value is 28,500 ksi)

2.4.1.5.3 Prestress loss due to relaxation

When a strand is stressed, the magnitude of stress decreases with time, which is relaxation loss. Relaxation loss occurs not only between jacking and transfer, and also after transfer for a long-term.

Relaxation loss for stress-relieved strand from jacking to transfer:

$$\Delta f_{pR1} = \frac{log(24.0t)}{10.0}\left[\frac{f_{pi}}{f_{py}} - 0.55\right] f_{pi} \quad \text{(Eq 2-95)}$$

Relaxation loss for low-relaxation strand from jacking to transfer:

$$\Delta f_{pR1} = \frac{log(24.0t)}{40.0}\left[\frac{f_{pi}}{f_{py}} - 0.55\right] f_{pi} \quad \text{(Eq 2-96)}$$

where:

t = time between initial jacking and transfer (days)

f_{pi} = strand stress after jacking (ksi)

f_{py} = yield strength of strand (ksi)

$f_{py} = 0.85 f_{pu}$ for stress-relieved strand, and $f_{py} = 0.90 f_{pu}$ for low-relaxation strand

Relaxation loss for stress-relieved strand after transfer:

$$\Delta f_{pR2} = 20.0 - 0.4\Delta f_{pES} - 0.2\,(\Delta f_{pSR} + \Delta f_{pCR}) \quad \text{(Eq 2-97)}$$

Relaxation loss for low-relaxation strand after transfer:

$$\Delta f_{pR2} = 6.0 - 0.12\Delta f_{pES} - 0.06\,(\Delta f_{pSR} + \Delta f_{pCR}) \quad \text{(Eq 2-98)}$$

where:

Δf_{pES} is loss due to elastic shortening at transfer

Δf_{pSR} is loss due to shrinkage

Δf_{pCR} is loss due to creep.

According to the study by Tadros (2003), relaxation loss after transfer is between 1.8 to 3.0 ksi, which is relatively a small part of total prestressing losses.

2.4.1.5.4 Prestress loss due to elastic shortening

A direct solution method to calculate elastic shortening loss was proposed by Cole (2000). Equations are shown below:

$$\Delta f_{pES} = abs(f_{cgp}) \frac{E_P}{E_{ci}} \quad \text{(Eq 2-99)}$$

where:

$$f_{cgp} = -\frac{P_{at}}{A} - \frac{P_{at}\, e^2}{I} + \frac{M_g e}{I} \quad \text{(Eq 2-100)}$$

$$P_{at} = f_{pat} A_{ps} \quad \text{(Eq 2-101)}$$

$$f_{pat} = f_{pbt} - \Delta f_{pES} \quad \text{(Eq 2-102)}$$

where:

f_{cgp} = concrete stress at the level of the strands due to the weight of the girder and the prestressing force after transfer (ksi)

A = area of cross section (in^2)

I = moment of inertia of cross section (in^4)

A_{ps} = total area of strands (in^2)

e = eccentricity of strands with respect to centroid of girder (in)

M_g = moment due to the self-weight of the girder (kip-in)

E_{ci} = modulus of elasticity of concrete at transfer (ksi)

It is necessary to do iterations to obtain the appropriate Δf_{pES}, and for the initial assumption $f_{pat} = 0.9 f_{pbt}$.

2.4.1.5.5 Prestress loss due to creep

Prestress loss due to creep from transfer to deck placement is shown below:

$$\Delta f_{pCR} = \Delta f_{pES} \Phi_{bid} K_{id} \quad \text{(Eq 2-103)}$$

where:

$$K_{id} = \frac{1}{1 + \frac{E_p A_{ps}}{E_{ci} A}\left(1 + \frac{A e_{pg}^2}{I}\right)[1 + 0.7\Phi_{bif}]} \quad \text{(Eq 2-104)}$$

Φ_{bid} = specified creep coefficient of concrete

Φ_{bif} = ultimate creep coefficient of concrete

A_{ps} = total area of prestressing strands (in^2)

A = area of cross section (in^2)

I = moment of inertia of cross section (in^4)

e_{pg} = eccentricity of the strand with respect to the centroid of girder (in)

2.4.1.5.6 Prestress loss due to shrinkage

Prestress loss due to shrinkage from transfer and to deck placement shown below:

$$\Delta f_{pSH} = E_p \, \varepsilon_{bid} \, K_{id} \qquad \text{(Eq 2-105)}$$

where:

ε_{bid} = specified shrinkage strain (10^{-6} in/in)

2.4.1.6 Cross section properties

Cross section of a prestressed bridge girder has two types of properties, including gross section property and transformed section property. It is easier to calculate gross section property. Transformed section properties are dependent on the ratio of modulus of elasticity of strands and concrete, strand locations and strand quantities. Transformed section property is widely used for reinforced concrete. Short-term and long-term cambers of girders by using gross section and transformed section properties are compared in Section 5.8.4.

2.4.2 Calculation of long-term camber of prestressed bridge girders

2.4.2.1 Introduction

For a prestressed bridge girder, creep increases camber, and prestress losses decreases camber, and the combination of these two effects typically results in an increase of camber. Figure 2.4 shows the camber of prestressed girder after transfer. Moment area method, Tadros's Method, Naaman's Method and Incremental method are discussed in the following sections, which are used to calculated long-term camber of a pretressed bridge girder in this study.

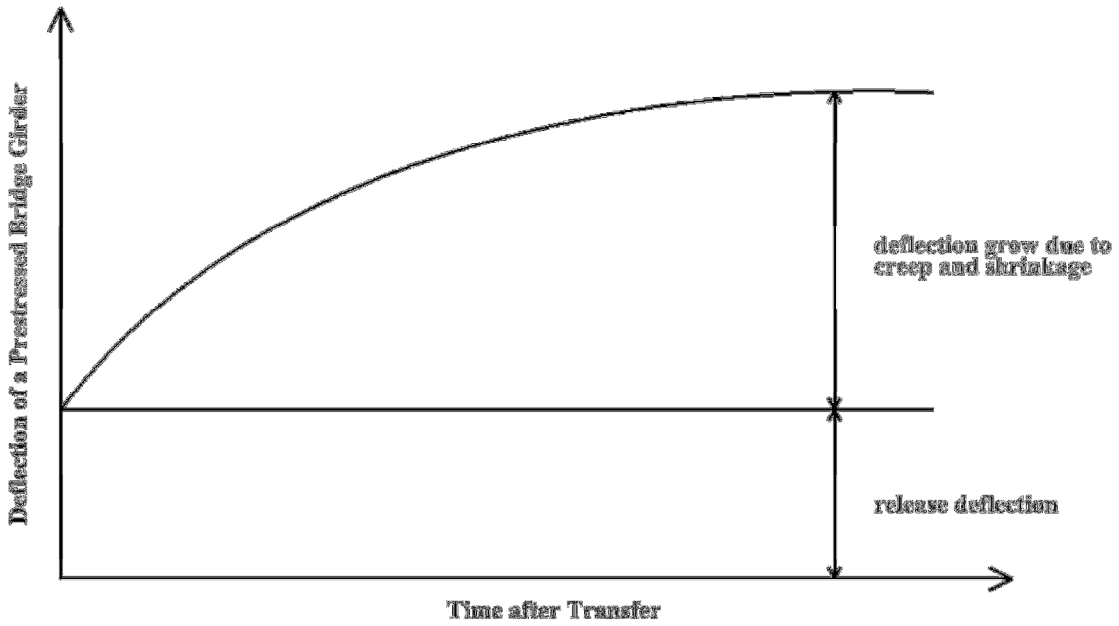

Figure 2.4. Camber of a prestressed bridge girder versus time after transfer

2.4.2.2 Moment area mothod

Second moment-area theorem (or camber theorem) is typically used to calculate the camber of beam members. The expression of camber at point j relative to point i is shown below:

$$\Delta_{j/i} = \int_{x_i}^{x_j} x(\frac{M}{EI})dx \qquad \text{(Eq 2-106)}$$

For prestressed girders, it is convenient to choose midspan as point i and end span as point j. Figure 2.5 below shows the typical strand layout of a prestressed girder, curvature diagram and deflected shape of a girder. Naaman's method and Incremental method are based on this theorem.

Transfer length of a prestressed girder is typically about 3 ft. (e.g. 60 times 0.6 in. diameter of strand) in this study according to AASHTO LRFD 2010. The effect of transfer length on camber of girder is very small mentioned in the study by Tadros (2011), and it can be neglected if necessary.

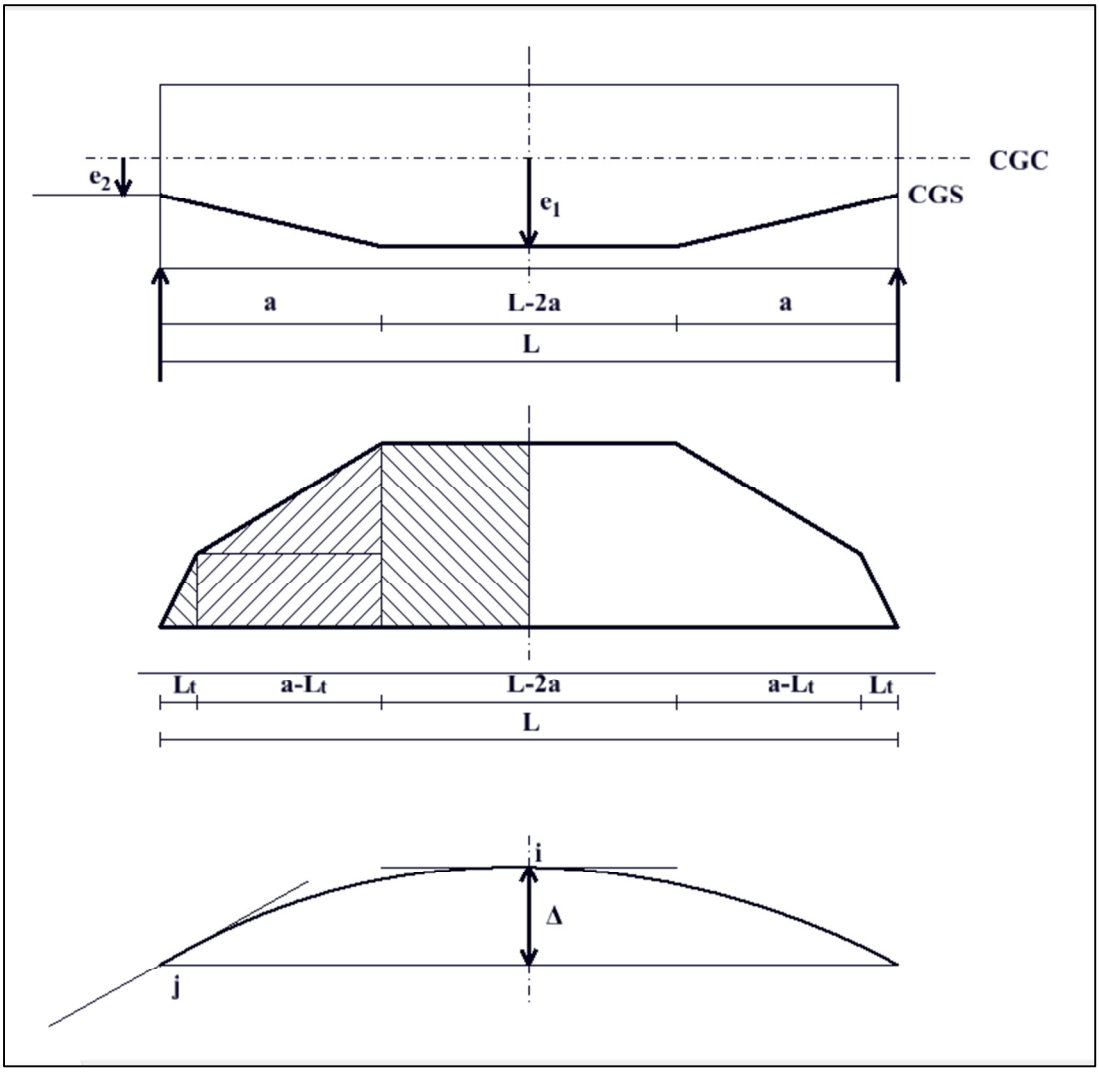

Figure 2.5. Moment area method for a prestressed bridge girder

2.4.2.3 Tadros's Method

Tadros (2011) provided a simplified method to calculate the long-term camber of prestressed bridge girders before the placement of deck, and expression is shown below:

$$\Delta_{long\text{-}term} = (1 + \Phi_{bid})\,\Delta_{release} - (1 + 0.7\Phi_{bid})\,\Delta_{loss} \qquad \text{(Eq 2-107)}$$

where:

$\Delta_{long\text{-}term}$ = long-term camber of a prestressed girder before the placement of deck (in)

$\Delta_{release}$ = release camber of a prestressed girder (in)

Δ_{loss} = camber loss due to prestress losses resulting from creep, shrinkage and relaxation between the time of transfer to the time of placement of deck (in)

$= \frac{\Delta f}{f} \Delta_{release}$

Where:

Δf = long-term prestress losses due to creep, shrinkage and relaxation (ksi)

f = prestress stress after transfer (ksi)

Φ_{bid} = specified creep coefficient of concrete

In this equation, 0.7 is an aging coefficient used to calculate the camber loss due to prestress losses, which is based on considerations of *v/s* ratio, relative humidity and loading age.

2.4.2.4 Naaman's Mothod

Naaman (2004) proposed another simplified method to calculate long-term camber of pretressed girders. Equivalent modulus is used for the calculation of camber shown as follows:

$$E_{ce}\,(t,\, t_A) = \frac{E_c(t)}{1+C_C(\tau)} \qquad \text{(Eq 2-108)}$$

where:

$E_c(t)$ = time-dependent modulus of elasticity of concrete

$= \sqrt{\frac{t}{b+ct}}\, Ec(28)$

Moist-curing: $b = \begin{cases} 4.0 \text{ for Type I cement} \\ 2.3 \text{ for Type III cement} \end{cases}$ and $c = \begin{cases} 0.85 \text{ for Type I cement} \\ 0.92 \text{ for Type III cement} \end{cases}$

Steam-curing: $b = \begin{cases} 1.0 \text{ for Type I cement} \\ 0.7 \text{ for Type III cement} \end{cases}$ and $c = \begin{cases} 0.95 \text{ for Type I cement} \\ 0.98 \text{ for Type III cement} \end{cases}$

$C_C(\tau)$ = specified creep coefficient of concrete

t = age of concrete (days)

t_A = age of concrete at transfer (days)

Long-term camber of a prestressed girder shown in Figure 2.5 can be calculated by using the following equations:

$$\Delta_{long\text{-}term} = \frac{FL^2}{8\,Ece\,(t,t_A)\,I}\,[e_1 + (e_2 - e_1)\frac{4a^2}{3L^2}] \qquad \text{(Eq 2-109)}$$

where:

F = prestressing force in strands; I = moment of inertia of cross section

or

$$\Delta_{long\text{-}term} = (\phi_1 - \phi_2)\,\frac{a^2}{6} - \phi_1\,\frac{L^2}{8} \qquad \text{(Eq 2-110)}$$

where:

ϕ_1 = curvature at the midspan of the girder due prestressing force and self-weight

$$\phi_1 = \frac{M_{ps1} + M_{sw1}}{Ece\,(t,t_A)\,I} \qquad \text{(Eq 2-111)}$$

where M_{ps1} is the moment due to prestressing force at midspan of a girder, and M_{sw1} is the moment due to self-weight at midspan

ϕ_2 = curvature at the end of the girder due prestressing force and self-weight

$$\phi_2 = \frac{M_{ps2} + M_{sw2}}{Ece\,(t,t_A)\,I} \qquad \text{(Eq 2-112)}$$

where M_{ps2} is the moment due to prestressing force at end of a girder, and M_{sw2} is the moment due to self-weight at end (for a simply supported girder, this value equals zero).

2.4.2.5 Incremental Method

For incremental method, a girder is divided into 1 in. sections, and properties of each section are analyzed, including cross section properties and applied moments and stresses.

Curvature of each section is calculated by using time-dependent equivalent modulus, and the camber of a girder is obtained by integrating curvature along half span of the girder:

$$\Delta_{long\text{-}term} = \int_0^{L/2} \frac{M_i}{Ece\ (t,t_A)\ I_i}\, dx \qquad \text{(Eq 2-113)}$$

where:

i = number of 1 in. section of half span of a prestressed girder

M_i = applied moment on the section of i due to prestress force and self-weight of a girder, in which time-dependent prestress losses are calculated section by section by using time-dependent cross section properties

$Ece\ (t, t_A)$ = equivalent modulus of concrete, which can be calculated by using Eq 2-108

I_i = moment of inertia on the section of i

2.4.3 Three previous studies of the prediction of the long-term camber of prestressed bridge girders

Three previous studies of the prediction of the long-term camber of prestressed bridge girders were reviewed and summarized in the following sections, including Washington Report (2007), North Carolina Report (2011) and Minnesota Report (2012).

2.4.3.1 Washington Report (2007)

This study indicated that in order to improve the accuracy of prediction of the long-term camber of prestressed bridge girders, properties of concrete of local materials should be taken, which were used to calibrate the camber, and also the time effect should be also taken into account to calculate camber of a girder by using time-step method. A computer program was developed to calculate long-term camber of prestressed girders, in which time-step method was used to calculate time-dependent camber with the consideration of time-dependent material properties including concrete and prestressing steel. Two adjustment factors were used to calibrate the calculated camber of a girder, including 1.15 for elastic modulus of AASHTO model and 1.4 for creep coefficient of AASHTO model. Refined method of prestress loss

calculations from AASHTO LRFD 2006 was recommended for the prediction of long-term camber of girders. Creep and shrinkage tests were taken by using local materials of concretes, but the unexpected elongation of some shrinkage specimens were observed, which could result in errors of calculation of creep strain and camber of the girder.

2.4.3.2 North Carolina Report (2011)

In this study in order to improve the accuracy of the prediction of the long-term camber of prestressed bridge girders, adjustment factors of concrete properties were recommended, including 1.25 for design compressive strength at release and 1.45 for design compressive strength at 28-day, and 0.85 for elastic modulus of AASHTO model, and also approximate method and refined method for the prediction of camber of girders were proposed. Simply multipliers from PCI were used as approximate method, and refined method of calculation of prestressed losses from AASHTO LRFD 2010 was used to calculate the camber of a girder at 28-day and 1-year as the refined method of camber calculation. Temperature gradient effect on the measurement of girders was recognized, and it was recommended to take the measurement of girder before dawn. It was also found that the transfer length of the prestressed girder had effect on the camber of the girder. Creep and shrinkage tests of concretes of local materials were not taken, and AASHTO LRFD 2010 creep and shrinkage model was used.

2.4.3.3 Minnesota Report (2012)

In this study in order to improve the accuracy of the prediction of the long-term camber of prestressed bridge girders, adjustments of concrete properties were used, including 1.15 for design release compressive strength and change of elastic modulus prediction from ACI 363 to AASHTO model. Additional prestress losses due to relaxation and thermal effect were considered for the calculation of camber of a girder. Creep and shrinkage tests of concretes of local materials were not taken, and ACI 209R 1992 creep and shrinkage model was selected for the calculation of prestressed losses and camber of the girders. Effect of relative humidity and temperature on creep and shrinkage were taken into account to calculate time-dependent camber of the girder. A computer program was used to predict time-dependent camber of a girder all the consideration of factors discussed above. Also simple multipliers were also proposed to predict long-term camber of a girder.

2.4.3.4 Comparison of three studies

According to the three studies, it was found that inaccuracy of prediction of concrete properties, including compressive strength, elastic modulus and creep and shrinkage was one important cause of errors of camber of a prestressed girder. In three studies, compressive strength and elastic modulus tests were taken, and adjustment factors of material properties were provided. Three studies also provided the prediction method of time dependent camber of the prestressed girder by using computer programs or time-dependent equations. For two studies simple multipliers were also proposed for the prediction of camber. Three studies indicated that AASHTO LRFD 2010 refined method for prestress losses provided a good prediction of the camber of girders. Creep and shrinkage tests were only taken in Washington DOT study.

CHAPTER 3 EXPERIMENTS

3.1 Introduction

Each procedure involved in this study was performed according to the appropriate ASTM specification. Materials and specimens of concrete are discussed in section 3.2. Compressive strength test, creep test and shrinkage test are presented in section 3.3, 3.4 and 3.5 respectively. Shrinkage of 4-ft. beam section and measurements of long-term cambers of the prestressed bridge girders are discussed in section 3.6 and 3.7.

3.2 Materials and Specimens

A total of 7 mixtures of concrete specimens were prepared by three precast plants. Four of seven were high performance concretes (HPC) currently used to cast prestressed bridge girders, and the rest of them were normal concretes (NC) used in girders in the past. In HPC slag and fly ash were added as partial replacement materials of Portland cement. NC concretes didn't contain those materials. 4 by 8 in. cylindrical concrete specimens were used in this study and all of them were cast by the quality control staffs of three precast plants. Specimens of HPC were made and stored in the mold along with steam-cured prestressed bridge girders, and NC specimens were cast and stored in the mold in the quality control room in precast plants. HPC 1 and NC 1 were prepared by precast plant A, and HPC 2, HPC 4 and NC 2 were cast by precast plant B, and HPC 3 and NC 3 were provided by precast plant C.

Typically prestressed bridge girders were released after 1-day steam curing, so specimens at the age of 1 day for both HPC and NC were transported from precast plants to the laboratory on campus during the early morning of the day of girder release. Sometimes girders were kept on the bed of fabrication during the weekend, and those girders were released at the age of 2 – 4 days.

Totally 14 cylindrical specimens for each mix were brought in the laboratory. 3 specimens were used for 1-day compressive strength test, 3 for 28-day compressive strength test, 4 for creep test, and 4 for shrinkage test. For the creep and shrinkage test, half specimens were sealed by using a type of coating material, and the rest were unsealed. All specimens were sulfur-capped (ASTM C617, 2009) for compressive strength test, creep and shrinkage tests. Photos of sealed and unsealed specimens are shown in Figure A.1 in Appendix A.

3.3 Compressive Strength Test

Compressive strength test was performed according to ASTM C39 (2004). For each mix, three sulfur-capped 4 by 8 in. cylindrical specimens were used for the compressive strength test at 1 day and 28 days, respectively. Three specimens for 28 days compressive strength test were stored in the same chamber of creep and shrinkage tests before the test. Photos of the compressive strength test are shown in Figure A. 2 in Appendix A.

3.4 Creep Test

3.4.1 Introduction

Creep test in compression was performed according to ASTM C 512 (2002). Creep frame, loading of creep test, storage of specimens, device and method of measurements are presented in the following sections.

3.4.2 Creep frame

Creep frame was designed and assembled in accordance with ASTM C512 (2002). Figure 3.1 shows the details of a creep frame. For each steel plate in the creep frame the locations of three holes for thread rods and the geometry center of the triangle of three holes

were carefully determined. Steel nuts were also carefully selected in order to minimize the relaxation of the frame after loading application.

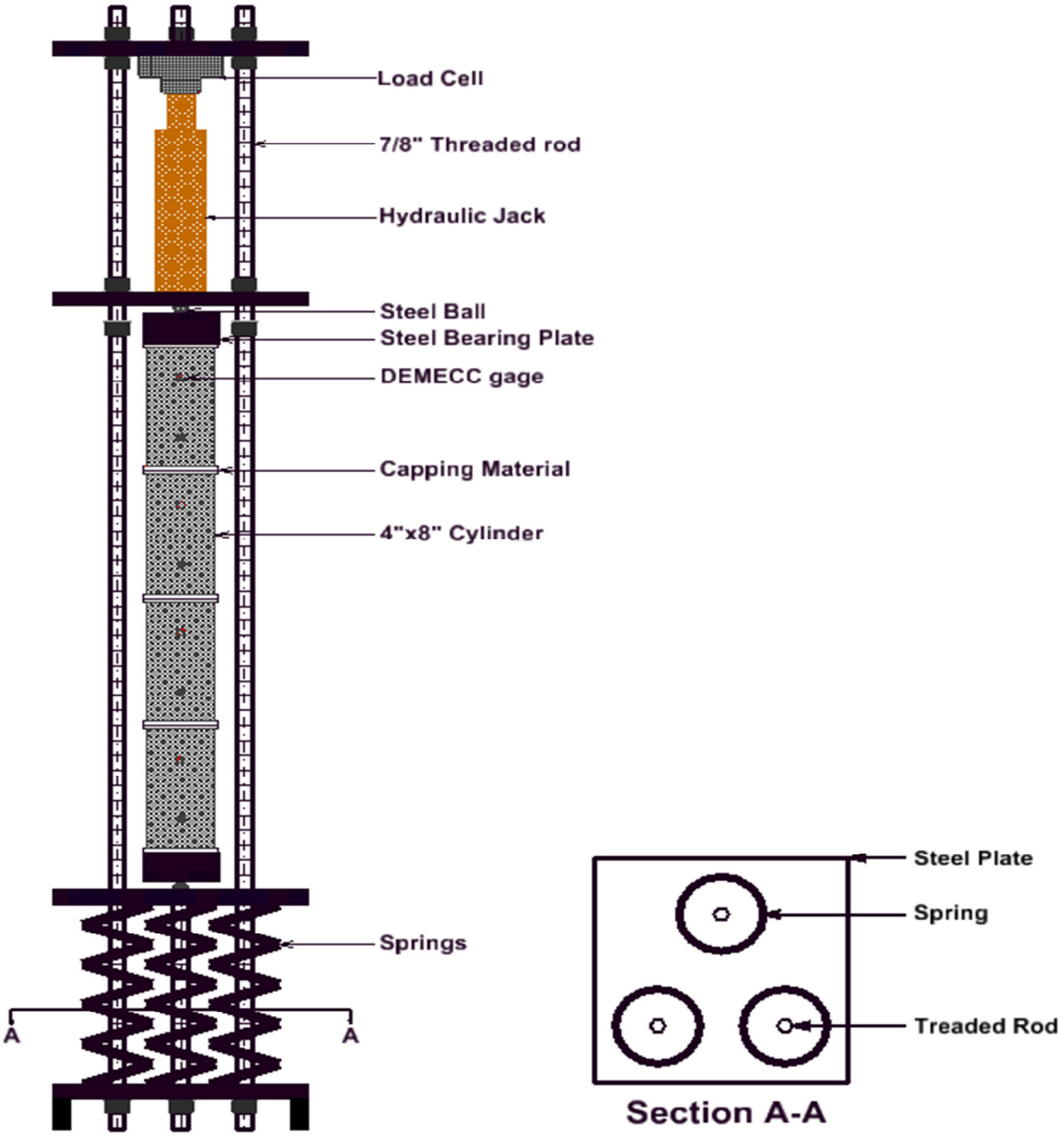

Figure 3.1. Details of a creep frame

3.4.3 Loading of creep test

Constant stress was applied in all creep frames, and the magnitude was 2125 psi. A load cell and a hydraulic jack were used to apply the load in the creep frame shown in Figure 3.1, and they were removed after loading application. In order to apply the load at the same location each time, a circle that fit the bottom shape of the hydraulic jack was drawn. Load was re-applied every time before measurements due to the relaxation of creep frame after loading application, and the tolerance of load variation was 2% according to ASTM C512 (2002).

3.4.4 Storage condition of specimens

Specimens for creep test, shrinkage test and 28-day compressive strength test were stored in an environmentally controlled chamber, in which the temperature was 73.4 ± 2.0 °F (23.0 ± 1.1 °C) and the relative humidity was 50 ± 4 %. For each mix four 4 by 8 in. cylindrical specimens were stacked in each creep frame and four specimens were placed on the wood shelf without loading. Photos of creep test and shrinkage test are shown in Figure A. 3 and Figure A. 4 in Appendix A.

3.4.5 Device and method of measurements

Demountable mechanical (DEMEC) strain gauge was used to measure the change of length between two vertical gage points with a length of 4 inches. The DEMEC gage had the precision of 0.00005 in. On each specimen three sides of vertical gage points were located. For each measurement, three instantaneous readings were obtained from each side of gage points, and the average was used as the reading of this side. If the difference of those three readings was greater than 0.00010 in, additional three measurements were taken and the average of total six readings was used as the reading of the two gage points. Photos of DEMEC gage and measurement are shown in Figure A. 5 in Appendix A.

Strain was the quotient of the change of length and the initial length between two gage points. Strain measured in loaded specimens in the creep frame was total strain, and strain measured in unloaded specimens was shrinkage strain. Sealed and unsealed creep strain could be calculated by subtracting sealed and unsealed shrinkage strain from total sealed and unsealed

strain with a change of time. Creep coefficient was the ratio of creep strain and instantaneous strain after loading application.

3.5 Shrinkage Test

Shrinkage specimens were unloaded specimens stored in the same chamber with loaded specimens. Shrinkage strain was measured in the unloaded specimens at the same time with total strain in the loaded specimens.

3.6 Shrinkage Behavior of 4-ft Beam Section

In order to correlate the shrinkage behavior of actual beam and specimens in the laboratory, a BTB beam section with a length of 4 feet was cast and stored in the yard of precast plant A. Strands in the beam section were debonded by using plastics and grease. DEMEC gauge and gage points were used to measure the strain of the beam section. Each group of two gage points was glued on the surface of the middle part of the beam section horizontally, and there were 6 groups of gage points along one side and 7 groups along the other side. Four temperature sensing thermistor probes attached with wires were located in the beam section when the beam section was cast. Three probes were laid at the bottom flange, web and top flange along the center of the cross section at the center of beam section, and the rest was placed near the end of the top flange. A handled thermistor thermometer was used to obtain the reading from the thermistor probes. Photo of this beam section is shown in Figure A. 6 in Appendix A.

Four 4 by 8 in. cylindrical specimens were also cast along with the beam section, and those specimens were transported to the laboratory for shrinkage tests at the same day of the release of the beam section. Two cylindrical specimens were sealed and the other two were unsealed.

3.7 Measurements of Long-Term Camber of Prestressed Girders

The long-term cambers of 26 prestressed bridge girders were monitored after the production at the precast plant until the bridge deck was placed. The camber of a prestressed bridge girder was the difference of elevation between the midspan and the two edges of the girder. The elevations were measured at the top flange of a girder by using an accurate laser level. For the measurement of each section three readings were taken along the width of the top flange, including two edges and middle of the top flange. The average of three readings was used as the effective elevation at that section, and elevation difference between the midspan and the average of two ends of the girder was the measured camber of a girder.

The measured camber changed with time. Before the girder was shipped to the construction site, it was stored in the yard of the precast plant. Typically wood supports were not located at the end of a girder, and there existed an overhang with a varying length from the center of the support to the end of a girder. The overhang length of a girder stored in the yard could be changed by the precast plant to adjust the camber of a girder. If the camber was smaller than the desired value, the length of overhang could be increased to increase the camber during a certain period. Overhang length could also be decreased to decrease the camber. Sometimes a certain weight could be applied at the top flange of a girder to decrease the camber quickly within a certain period. The overhang had an influence of the camber of a girder, which was discussed in 2.4.1.3. The length of an overhang was measured, and it was used to adjust the measured camber of a girder for comparison with the camber without an overhang.

CHAPTER 4 RESULTS

4.1 Introduction

This chapter discusses the results of tests and measurements. Compressive strength and modulus of elasticity are presented in Section 4.2 and Section 4.3. Measurements of creep and shrinkage tests are shown in Section 4.4. Results of long-term cambers of 26 prestressed girders are presented in Section 4.5.

4.2 Compressive Strength

For each mix 1-day and 28-day compressive strength were measured, and the results shown below are the average magnitude, standard deviation and maximum difference in percent of three measurements. Table 4.1 shows the results of the 1-day compressive strength test, and Table 4.2 summarizes the results of 28-day compressive strength test. Maximum difference of three specimens ranges from 4% to 11% for 1-day compressive strength test, and from 2% to 10% for 28-day compressive strength, which are less than the limit value of 14% according to ASTM C39 (2004). The results of compressive strength tests are acceptable.

Table 4.1. Results of 1-day compressive strength test

Mix I.D.	HPC 1	HPC 2	HPC 3	HPC 4	NC 1	NC 2	NC 3
Average 1-Day Strength, psi	6784	6247	5417	6640	8902	6547	9750
Standard Deviation, psi	182	116	132	91	89	55	123
Maximum Difference of Three Specimens	9%	8%	11%	6%	4%	4%	5%

Table 4.2. Results of 28-day compressive strength test

Mix I.D.	HPC 1	HPC 2	HPC 3	HPC 4	NC 1	NC 2	NC 3
Average 28-Day Strength, psi	8750	7938	6884	8212	10215	7545	11020
Standard Deviation, psi	86	35	161	106	58	132	227
Maximum Difference of Three Specimens	4%	2%	10%	6%	5%	7%	9%

4.3 Modulus of Elasticity

Elastic modulus of elasticity is the quotient of applied stress and elastic shortening measured in the creep test immediately before and after the loading application at 1-day. The average magnitude and standard deviation for each mix are summarized in Table 4.3 for sealed specimens and Table 4.4 for unsealed specimens.

Table 4.3. Results of modulus of elasticity for sealed specimens

Mix I.D.	HPC 1	HPC 2	HPC 3	HPC 4	NC 1	NC 2	NC 3
Modulus of Elasticity, ksi	4870	5596	5226	5629	5425	4399	4671
Standard Deviation, ksi	306	593	517	389	369	202	442

Table 4.4. Results of modulus of elasticity for unsealed specimens

Mix I.D.	HPC 1	HPC 2	HPC 3	HPC 4	NC 1	NC 2	NC 3
Modulus of Elasticity, ksi	3216	3105	4080	5129	5602	5027	4297
Standard Deviation, ksi	91	233	324	413	543	480	302

4.4 Creep and Shrinkage

Table 4.5 summarizes the stress-strength ratio of creep tests. It is found that stress-strength ratio has a range from 0.31 to 0.39 for four HPC mixes, and from 0.22 to 0.32 for three NC mixes. Stress-strength ratios are less than 0.40, which is the limit of linear theory provided by ASTM C512 (2002) mentioned previously. Detailed results of creep and shrinkage tests for seven mixes are shown from Table 4.9 to Table 4.16. In those tables, there are two "0" values for "Time after Loading", which stand for before and after loading application.

Table 4.5. Stress-strength ratio of creep tests

Mix I.D.	HPC 1	HPC 2	HPC 3	HPC 4	NC 1	NC 2	NC 3
Average 1-Day Strength, psi	6784	6247	5417	6640	8902	6547	9750
Applied Stress, psi	2125	2125	2125	2125	2125	2125	2125
Stress-strength Ratio	0.31	0.34	0.39	0.32	0.24	0.32	0.22

From Table 4.6 to Table 4.8, the results of creep and shrinkage tests are shown, including 3-month, 6-month and 1-year. According to those data, the following are observed:

- Unsealed total strain for each mix is higher than sealed total strain ranging from 6% to 52% at 3-month, from 5% to 53% at 6-month and from 0% to 63% at 1-year;
- Unsealed shrinkage strain for each mix is higher than sealed shrinkage strain with a range from 17% to 106%, from 17% to 120% and from 18% to 169%;
- Unsealed total strain of HPC 4 mix is higher than the rest of six mixes ranging from 3% to 43% at 3-month, and unsealed total strain of HPC 2 is higher than the rest of six mixes ranging from 2% to 45% at 6-month and ranging from 4% to 51% at 1-year. HPC 3 mix has the lowest unsealed total strain at 3-month, 6-month and 1-year;
- Sealed total strain of HPC 1 mix is higher than the rest of six mixes ranging from 19% to 29% at 3-month, from 19% to 28% at 6-month and from 6% to 19% at 1-year. NC 2 mix has the lowest sealed total strain at 3-month and 6-month, and NC 1 mix has the lowest sealed total strain at 1-year;
- Unsealed shrinkage strain of HPC 3 mix is higher than the rest of six mixes ranging from 14% to 59% at 3-month and from 12% to 41% at 6-month, and unsealed shrinkage strain

of HPC 1 is higher than the rest of six mixes in a range from 8% to 63% at 1-year. HPC 2 mix has the lowest unsealed shrinkage strain at 3-month, HPC 4 mix has the lowest unsealed shrinkage strain at 6-month and at 1-year;

- Sealed shrinkage strain of HPC 3 mix is higher than the rest of six mixes ranging from 40% to 101% at 3-month, from 12% to 117% at 6-month, and from 27% to 92% at 1-year. NC 2 mix has the lowest sealed shrinkage strain at 3-month and 6-month, and HPC 1 mix has the lowest sealed shrinkage strain at 1-year;
- HPC 2 mix has the highest unsealed and sealed creep coefficient during one year. HPC 2 mix has higher unsealed creep coefficient ranging from 13% to 163% and higher sealed creep coefficient ranging from 23% to 96% than the rest of six mixes at 3-month. HPC 2 mix has higher unsealed creep coefficient ranging from 20% to 165% and higher sealed creep coefficient ranging from 15% to 87% than the rest of six mixes at 6-month. HPC 2 mix has higher unsealed creep coefficient ranging from 35% to 154% and higher sealed creep coefficient ranging from 9% to 84% than the rest of six mixes at 1-year;
- Unsealed creep coefficient of NC 3 is lowest than the rest of six mixes at 3-month, and unsealed creep coefficient of HPC 3 is the lowest at 6-month and 1-year;
- Sealed creep coefficient of NC 3 is lowest than the rest of six mixes at 3-month, and unsealed creep coefficient of NC 1 is the lowest at 6-month and 1-year.

Table 4.6. Results of creep and shrinkage tests for seven mixes at 3-month

Mix I.D.	Unsealed Total Strain, 10^-6 in/in	Sealed Total Strain, 10^-6 in/in	Unsealed Shrinkage Strain, 10^-6 in/in	Sealed Shrinkage Strain, 10^-6 in/in	Unsealed Creep Coefficient	Sealed Creep Coefficient
HPC 1	1596	1292	353	171	0.62695	0.84151
HPC 2	1587	1054	254	185	0.88825	1.03454
HPC 3	1151	1088	404	344	0.37776	0.73522
HPC 4	1650	1086	306	229	0.78334	0.81871
NC 1	1196	1076	287	246	0.59498	0.55266
NC 2	1254	979	315	157	0.47820	0.58374
NC 3	1126	1005	278	204	0.33835	0.52824

Table 4.7. Results of creep and shrinkage tests for seven mixes at 6-month

Mix I.D.	Unsealed Total Strain, 10^-6 in/in	Sealed Total Strain, 10^-6 in/in	Unsealed Shrinkage Strain, 10^-6 in/in	Sealed Shrinkage Strain, 10^-6 in/in	Unsealed Creep Coefficient	Sealed Creep Coefficient
HPC 1	1698	1370	414	188	0.68093	0.94038
HPC 2	1756	1149	344	260	0.99976	1.08155
HPC 3	1212	1152	465	373	0.37749	0.81697
HPC 4	1716	1145	330	251	0.83552	0.88930
NC 1	1422	1178	391	333	0.80871	0.57925
NC 2	1345	1068	358	172	0.56235	0.71463
NC 3	1260	1190	375	277	0.40353	0.72637

Table 4.8. Results of creep and shrinkage tests for seven mixes at 1-year

Mix I.D.	Unsealed Total Strain, 10^-6 in/in	Sealed Total Strain, 10^-6 in/in	Unsealed Shrinkage Strain, 10^-6 in/in	Sealed Shrinkage Strain, 10^-6 in/in	Unsealed Creep Coefficient	Sealed Creep Coefficient
HPC 1	1942	1448	576	214	0.78800	1.02522
HPC 2	2027	1245	429	324	1.26346	1.15647
HPC 3	1345	1234	533	410	0.49840	0.92176
HPC 4	1820	1249	353	263	0.93464	1.06521
NC 1	1506	1217	443	344	0.86399	0.62822
NC 2	1507	1353	425	360	0.73004	0.88432
NC 3	1358	1360	375	285	0.54098	1.01115

Table 4.9. Results of creep and shrinkage test for HPC 1

Time after Loading, days	Unsealed Total Strain, 10^-6 in/in	Sta. Dev., 10^-6 in/in	Sealed Total Strain, 10^-6 in/in	Sta. Dev., 10^-6 in/in	Unsealed Shrinkage, 10^-6 in/in	Sta. Dev., 10^-6 in/in	Sealed Shrinkage, 10^-6 in/in	Sta. Dev., 10^-6 in/in	Unsealed Creep Coefficient	Sealed Creep Coefficient
0	0	0	0	0	0	0	0	0	0.00000	0.00000
0	764	66	609	46	0	0	0	0	0.00000	0.00000
1	898	53	744	51	98	8	31	23	0.04613	0.17186
2	1002	64	794	55	163	9	62	25	0.09829	0.20138
3	1031	50	824	68	166	7	59	21	0.13338	0.25699
7	1145	59	916	64	219	13	74	18	0.21138	0.38265
14	1268	95	1005	65	276	13	101	16	0.29875	0.48378
21	1323	97	1041	65	285	16	115	19	0.35857	0.52042
28	1379	101	1077	66	295	19	129	18	0.41839	0.55707
60	1543	117	1227	73	319	25	151	21	0.60306	0.76635
90	1596	117	1292	89	353	27	171	22	0.62695	0.84151
120	1631	119	1330	96	373	28	180	25	0.64573	0.88788
150	1663	120	1359	97	392	29	187	22	0.66325	0.92430
180	1698	122	1370	92	414	29	188	23	0.68093	0.94038
210	1737	126	1382	93	433	29	192	24	0.70615	0.95341
240	1760	128	1388	93	443	34	197	24	0.72343	0.95564
270	1786	129	1395	94	453	29	205	23	0.74416	0.95299
300	1867	129	1420	93	500	30	213	25	0.78917	0.98059
330	1905	130	1434	94	538	38	214	26	0.78859	1.00290
360	1942	132	1448	95	576	42	214	32	0.78800	1.02522
	Average	103	Average	78	Average	22	Average	21		

Table 4.10. Results of creep and shrinkage test for HPC 2

Time after Loading, days	Unsealed Total Strain, 10^-6 in/in	Sta. Dev., 10^-6 in/in	Sealed Total Strain, 10^-6 in/in	Sta. Dev., 10^-6 in/in	Unsealed Shrinkage, 10^-6 in/in	Sta. Dev., 10^-6 in/in	Sealed Shrinkage, 10^-6 in/in	Sta. Dev., 10^-6 in/in	Unsealed Creep Coefficient	Sealed Creep Coefficient
0	0	0	0	0	0	0	0	0	0.00000	0.00000
0	706	47	427	52	0	0	0	0	0.00000	0.00000
1	831	66	535	62	51	7	20	2	0.10519	0.20649
2	880	70	573	70	76	11	30	3	0.13924	0.27289
3	976	66	657	73	125	13	46	10	0.20651	0.42961
7	1092	68	712	72	132	17	50	8	0.36018	0.55016
14	1254	88	789	71	142	23	54	9	0.57533	0.71894
21	1365	108	842	71	150	29	61	10	0.72104	0.82920
28	1429	119	874	71	157	33	68	11	0.80130	0.88609
60	1530	123	985	82	216	38	131	10	0.86230	0.99837
90	1587	136	1054	76	254	37	185	10	0.88825	1.03454
120	1650	144	1092	74	287	37	216	12	0.93161	1.05018
150	1707	143	1127	69	319	39	245	12	0.96715	1.06514
180	1756	138	1149	65	344	40	260	13	0.99976	1.08155
210	1805	133	1166	65	366	40	269	13	1.03922	1.10117
240	1851	126	1186	66	383	40	279	14	1.07995	1.12276
270	1884	123	1203	65	396	40	290	14	1.10826	1.13770
300	1938	139	1213	69	404	45	302	25	1.17376	1.13435
330	1979	137	1231	70	418	45	313	26	1.21172	1.15021
360	2027	145	1245	72	429	48	324	36	1.26346	1.15647
	Average	111	Average	69	Average	31	Average	13		

Table 4.11. Results of creep and shrinkage test for HPC 3

Time after Loading, days	Unsealed Total Strain, 10^-6 in/in	Sta. Dev., 10^-6 in/in	Sealed Total Strain, 10^-6 in/in	Sta. Dev., 10^-6 in/in	Unsealed Shrinkage, 10^-6 in/in	Sta. Dev., 10^-6 in/in	Sealed Shrinkage, 10^-6 in/in	Sta. Dev., 10^-6 in/in	Unsealed Creep Coefficient	Sealed Creep Coefficient
0	0	0	0	0	0	0	0	0	0.00000	0.00000
0	542	44	429	38	0	0	0	0	0.00000	0.00000
1	687	60	533	36	105	9	36	6	0.07272	0.15996
2	852	82	657	38	147	7	73	12	0.30072	0.36042
3	873	79	685	38	164	11	90	16	0.30802	0.38626
7	997	62	856	47	265	10	195	15	0.35181	0.54134
14	1009	55	885	46	277	10	214	13	0.35113	0.56266
21	1026	50	925	44	295	10	242	12	0.35019	0.59250
28	1048	54	977	41	317	10	277	14	0.34897	0.63087
60	1088	63	1033	45	351	16	311	13	0.35959	0.68287
90	1151	85	1088	62	404	16	344	13	0.37776	0.73522
120	1165	83	1103	61	418	16	352	14	0.37773	0.75161
150	1192	80	1129	59	445	17	365	15	0.37764	0.78198
180	1212	80	1152	55	465	19	373	16	0.37749	0.81697
210	1226	79	1170	52	478	21	381	19	0.38106	0.84013
240	1247	78	1179	50	486	23	389	16	0.40511	0.84229
270	1274	87	1196	60	500	21	392	15	0.42800	0.87278
300	1296	90	1207	62	509	24	399	18	0.45176	0.88203
330	1321	102	1221	71	522	29	404	20	0.47493	0.90544
360	1345	112	1234	77	533	26	410	22	0.49840	0.92176
	Average	75	Average	52	Average	16	Average	14		

Table 4.12. Results of creep and shrinkage test for HPC 4

Time after Loading, days	Unsealed Total Strain, 10^-6 in/in	Sta. Dev., 10^-6 in/in	Sealed Total Strain, 10^-6 in/in	Sta. Dev., 10^-6 in/in	Unsealed Shrinkage, 10^-6 in/in	Sta. Dev., 10^-6 in/in	Sealed Shrinkage, 10^-6 in/in	Sta. Dev., 10^-6 in/in	Unsealed Creep Coefficient	Sealed Creep Coefficient
0	0	0	0	0	0	0	0	0	0.00000	0.00000
0	814	53	525	32	0	0	0	0	0.00000	0.00000
1	870	55	540	27	22	9	17	5	0.20137	0.21487
2	919	57	579	29	33	11	26	7	0.22125	0.24085
3	959	60	604	34	51	12	40	9	0.24892	0.26184
7	1145	77	719	60	133	14	103	14	0.37690	0.35891
14	1334	99	874	60	229	16	160	15	0.49110	0.54802
21	1459	108	959	67	286	35	212	19	0.57438	0.61062
28	1493	107	983	63	293	38	220	24	0.60676	0.63966
60	1581	109	1044	51	296	42	225	28	0.71138	0.74767
90	1650	120	1086	52	306	40	229	33	0.78334	0.81871
120	1683	128	1113	51	312	38	235	27	0.81742	0.86035
150	1701	131	1133	65	319	36	244	23	0.83024	0.87970
180	1716	143	1145	73	330	48	251	29	0.83552	0.88930
210	1732	151	1155	81	341	46	259	36	0.84156	0.89390
240	1750	158	1174	86	344	49	260	38	0.86018	0.92817
270	1768	162	1197	97	342	57	257	43	0.88508	0.97726
300	1785	164	1214	104	345	59	259	46	0.90160	1.00658
330	1802	167	1230	109	351	61	262	48	0.91603	1.03095
360	1820	172	1249	114	353	63	263	45	0.93464	1.06521
	Average	117	Average	66	Average	33	Average	25		

Table 4.13. Results of creep and shrinkage test for NC 1

Time after Loading, days	Unsealed Total Strain, 10^-6 in/in	Sta. Dev., 10^-6 in/in	Sealed Total Strain, 10^-6 in/in	Sta. Dev., 10^-6 in/in	Unsealed Shrinkage, 10^-6 in/in	Sta. Dev., 10^-6 in/in	Sealed Shrinkage, 10^-6 in/in	Sta. Dev., 10^-6 in/in	Unsealed Creep Coefficient	Sealed Creep Coefficient
0	0	0	0	0	0	0	0	0	0.00000	0.00000
0	570	91	515	68	0	0	0	0	0.00000	0.00000
1	604	92	538	69	25	7	19	6	0.06025	0.03997
2	665	113	596	109	40	9	30	8	0.09649	0.08978
3	714	126	654	117	68	11	59	13	0.13272	0.13959
7	845	137	797	123	150	18	130	15	0.21936	0.26657
14	901	189	869	142	185	23	161	16	0.25714	0.33955
21	928	212	890	153	193	27	167	18	0.28914	0.36494
28	944	206	903	162	199	31	171	24	0.30834	0.38016
60	1105	217	1025	172	253	39	216	27	0.49544	0.51619
90	1196	231	1076	182	287	37	246	28	0.59498	0.55266
120	1295	230	1114	200	328	38	278	29	0.69625	0.56393
150	1379	225	1150	193	369	41	312	32	0.77192	0.56711
180	1422	227	1178	197	391	42	333	37	0.80871	0.57925
210	1442	226	1190	189	397	49	338	39	0.83287	0.59197
240	1455	228	1195	210	406	50	339	34	0.83909	0.59922
270	1464	254	1197	208	417	59	338	36	0.83635	0.60374
300	1478	267	1204	194	426	69	340	43	0.84556	0.61190
330	1493	284	1212	186	434	69	343	48	0.85776	0.62097
360	1506	289	1217	203	443	67	344	47	0.86399	0.62822
	Average	202	Average	162	Average	36	Average	26		

Table 4.14. Results of creep and shrinkage test for NC 2

Time after Loading, days	Unsealed Total Strain, 10^-6 in/in	Sta. Dev., 10^-6 in/in	Sealed Total Strain, 10^-6 in/in	Sta. Dev., 10^-6 in/in	Unsealed Shrinkage, 10^-6 in/in	Sta. Dev., 10^-6 in/in	Sealed Shrinkage, 10^-6 in/in	Sta. Dev., 10^-6 in/in	Unsealed Creep Coefficient	Sealed Creep Coefficient
0	0	0	0	0	0	0	0	0	0.00000	0.00000
0	666	75	489	36	0	0	0	0	0.00000	0.00000
1	791	83	564	46	130	14	70	8	-0.00768	0.00779
2	841	94	604	49	161	16	73	11	0.02393	0.07495
3	940	110	685	53	225	20	77	14	0.08715	0.20926
7	984	117	727	56	236	22	91	17	0.14514	0.25892
14	1069	118	802	55	259	27	122	25	0.25188	0.33585
21	1108	124	835	66	271	28	139	30	0.30063	0.36312
28	1138	129	862	83	279	30	141	33	0.33857	0.40630
60	1214	131	936	89	299	34	150	40	0.43608	0.52148
90	1254	135	979	95	315	39	157	47	0.47820	0.58374
120	1280	135	1008	98	330	40	161	46	0.49850	0.62707
150	1321	119	1053	91	352	45	165	44	0.53189	0.70029
180	1345	123	1068	103	358	55	172	46	0.56235	0.71463
210	1381	129	1136	115	373	59	218	45	0.60038	0.75244
240	1411	135	1203	107	387	60	265	49	0.62798	0.78744
270	1437	149	1236	119	396	69	286	53	0.65742	0.80916
300	1465	152	1292	122	408	69	325	56	0.68564	0.83973
330	1492	158	1337	136	419	68	354	52	0.71447	0.86587
360	1507	164	1353	144	425	77	360	59	0.73004	0.88432
	Average	125	Average	88	Average	40	Average	35		

Table 4.15. Results of creep and shrinkage test for NC 3

Time after Loading, days	Unsealed Total Strain, 10^-6 in/in	Sta. Dev., 10^-6 in/in	Sealed Total Strain, 10^-6 in/in	Sta. Dev., 10^-6 in/in	Unsealed Shrinkage, 10^-6 in/in	Sta. Dev., 10^-6 in/in	Sealed Shrinkage, 10^-6 in/in	Sta. Dev., 10^-6 in/in	Unsealed Creep Coefficient	Sealed Creep Coefficient
0	0	0	0	0	0	0	0	0	0.00000	0.00000
0	655	75	499	28	0	0	0	0	0.00000	0.00000
1	677	77	545	32	14	9	9	5	0.01379	0.06562
2	694	84	578	39	28	11	18	8	0.01916	0.10648
3	711	91	610	43	42	14	27	11	0.02452	0.14733
7	753	98	667	46	67	19	48	15	0.05440	0.21115
14	839	108	753	55	104	25	88	21	0.14018	0.29153
21	876	117	777	69	126	24	99	22	0.16816	0.31410
28	1012	109	864	73	204	24	140	27	0.26889	0.39536
60	1084	123	946	79	252	28	180	37	0.31187	0.46723
90	1126	127	1005	84	278	29	204	41	0.33835	0.52824
120	1179	139	1074	89	315	32	233	43	0.36531	0.60072
150	1230	127	1145	96	353	34	261	47	0.38972	0.67654
180	1260	149	1190	99	375	29	277	43	0.40353	0.72637
210	1270	143	1203	117	383	31	281	42	0.40667	0.74236
240	1298	155	1252	103	387	38	282	45	0.44864	0.82635
270	1313	167	1283	114	383	34	280	48	0.48179	0.88451
300	1331	156	1311	135	391	49	283	51	0.49901	0.92715
330	1347	162	1341	149	392	52	283	46	0.52618	0.97949
360	1358	178	1360	157	395	61	285	53	0.54098	1.01115
	Average	126	Average	85	Average	27	Average	30		

4.5 Long-term Camber of Prestressed Bridge Girders

Measured cambers of 26 prestressed bridge girders with overhang and adjusted cambers without overhang are shown from Figure 4.1 to Figure 4.8, including 3 BTC 120 girders produced by plant A, 9 BTE 110 girders and 6 BTE 145 girders cast by precast plant B, and 8 BTD 135 girders made by plant C. The equivalent modulus is used to adjust the measured upward camber, which is discussed in Section 2.4.1.3. It is found that overhang increases upward camber with time, and the extent of the effect increases with an increase of the length of overhang. The cross section properties and material properties of four types of girders are shown in Appendix E, in which figures of cross sections of girders are obtained from *Beam Standards Issued by Iowa DOT* (2012).

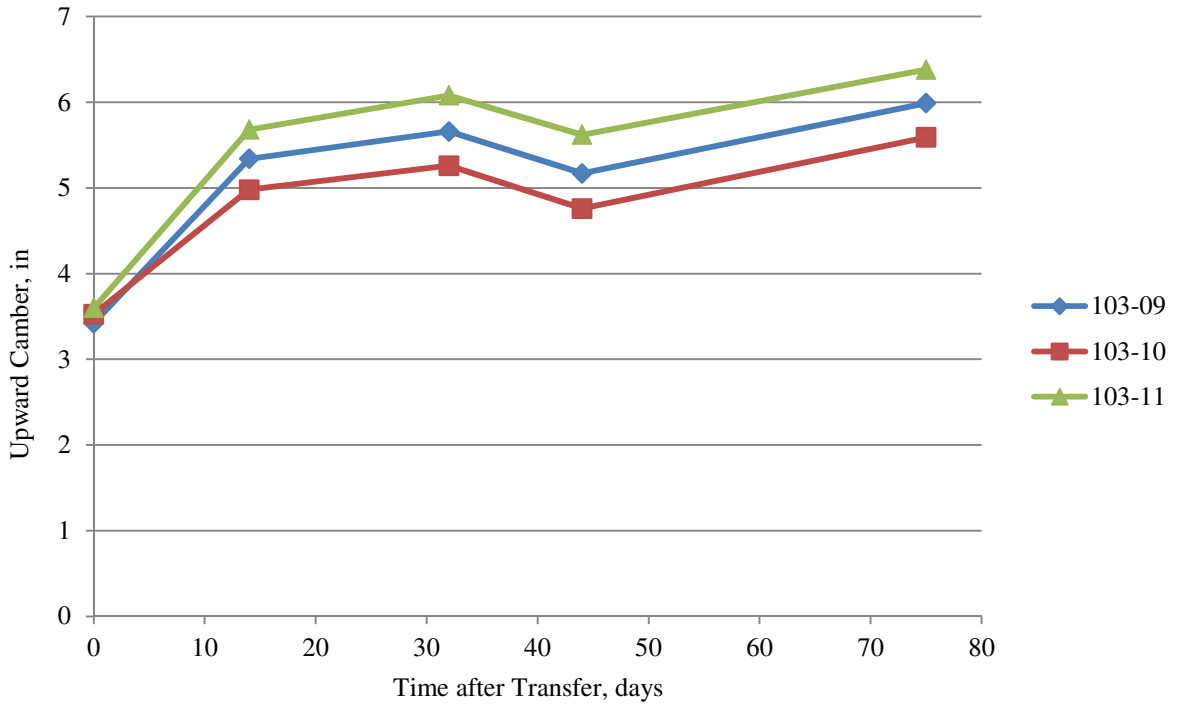

Figure 4.1. Measured upward camber of 3 BTC 120 prestressed bridge girders at plant A

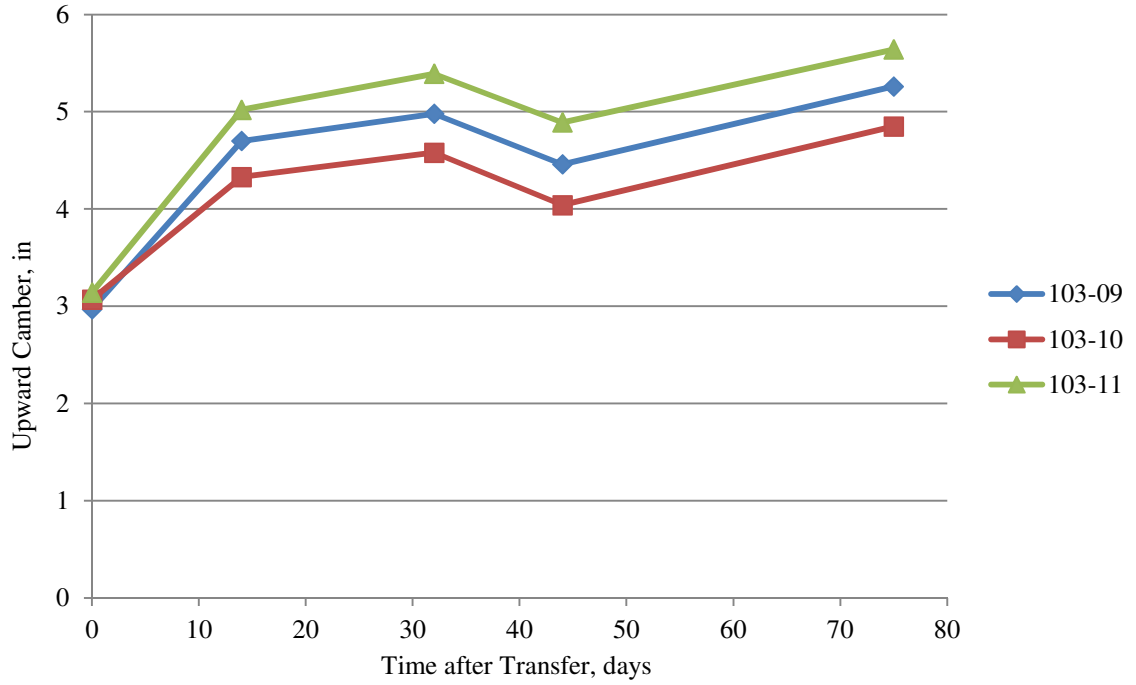

Figure 4.2. Adjusted upward camber of 3 BTC 120 prestressed bridge girders at plant A

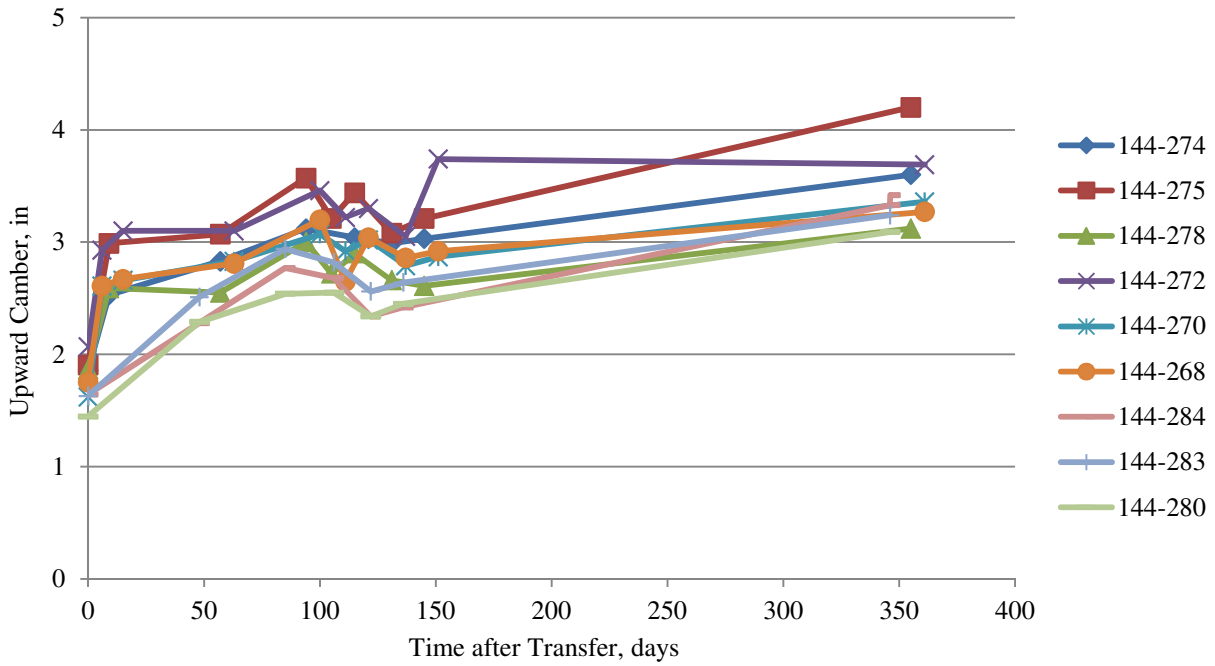

Figure 4.3 Measured upward camber of 9 BTE 110 prestressed bridge girders at plant B

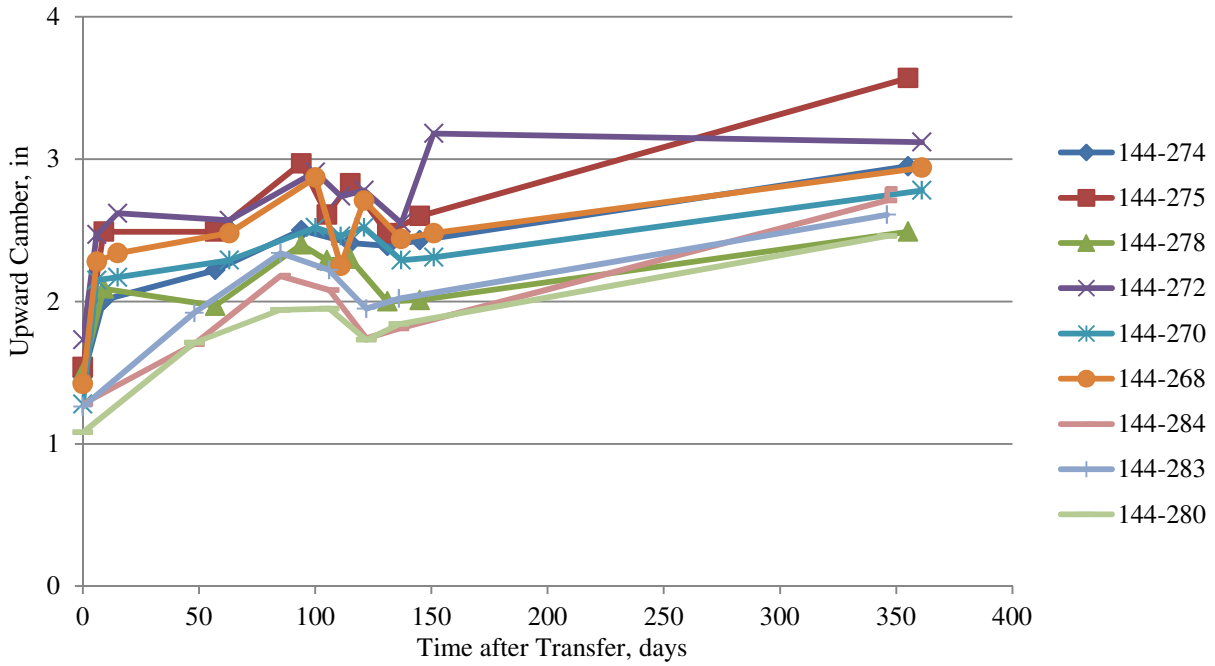

Figure 4. 4 Adjusted upward camber of 9 BTE 110 prestressed bridge girders at plant B

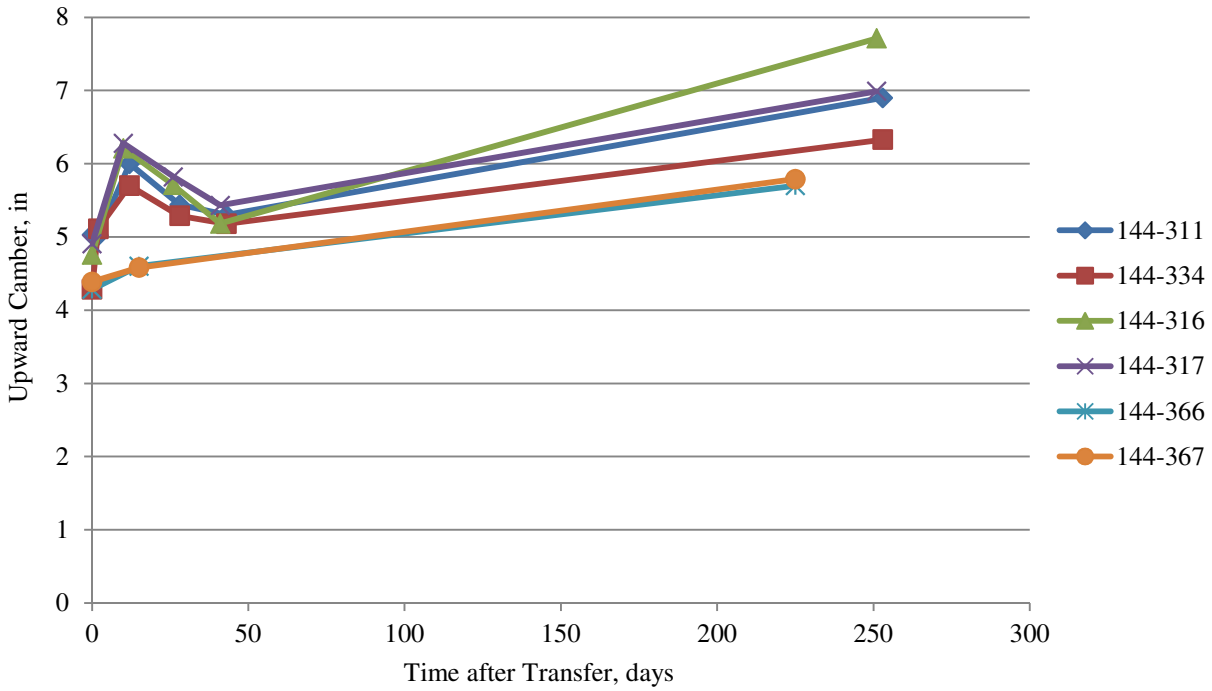

Figure 4. 5 Measured upward camber of 6 BTE 145 prestressed bridge girders at plant B

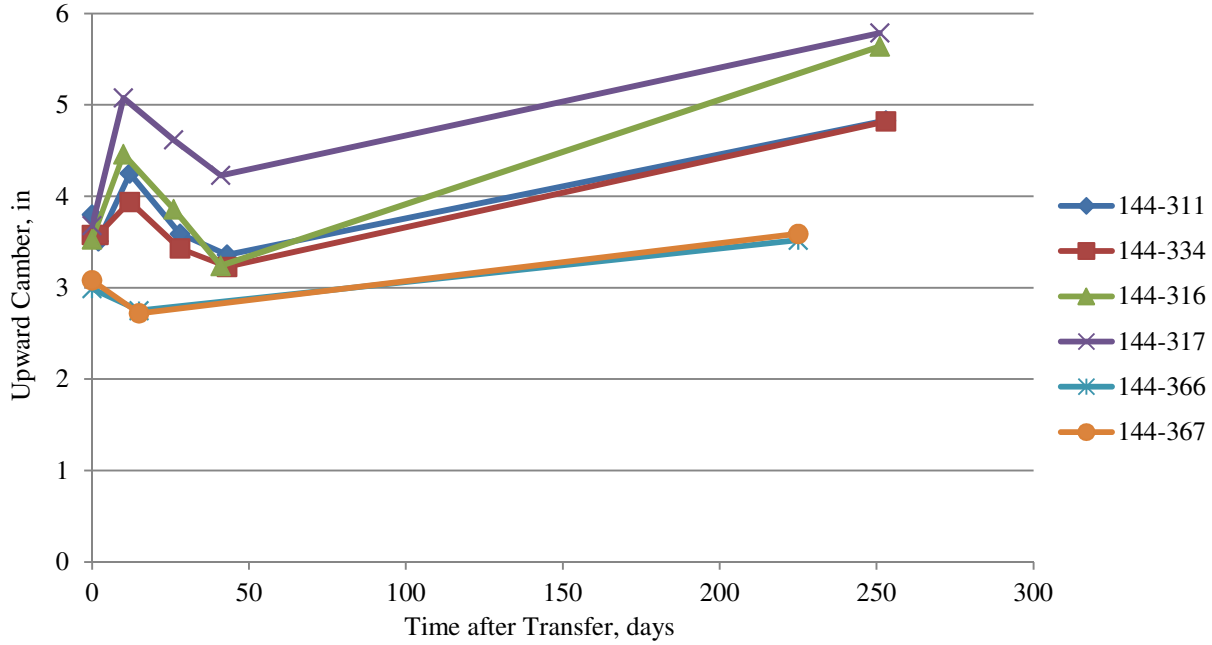

Figure 4. 6 Adjusted upward camber of 6 BTE 145 prestressed bridge girders at plant B

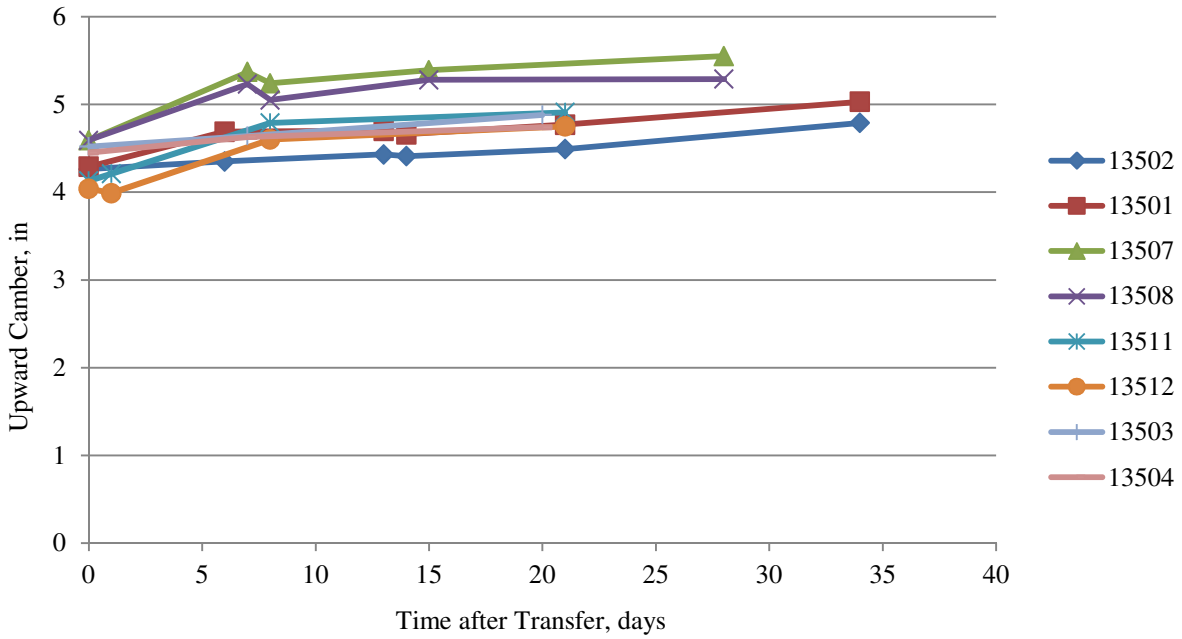

Figure 4.7. Measured upward camber of 8 BTD 135 prestressed bridge girders at plant C

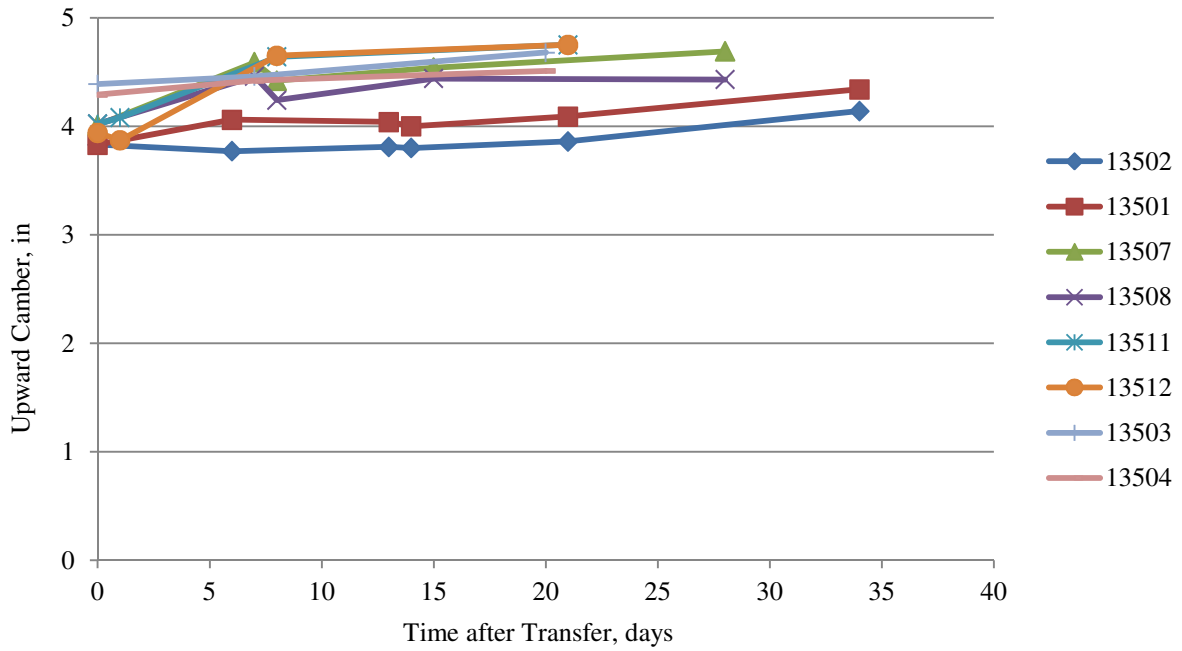

Figure 4.8. Adjusted upward camber of 8 BTD 135 prestressed bridge girders at plant C

CHAPTER 5 ANALYSIS AND DISCUSSION

5.1 Introduction

In this chapter, the analysis and discussion on compressive strength and modulus of elasticity are performed in the section 5.2 and 5.3. Comparison of measured results of creep and shrinkage tests and five models is presented in section 5.4. Equations of sealed creep coefficient and sealed shrinkage obtained according to the measured data are proposed in section 5.5. Section 5.6 discusses the prediction of long-term camber of prestressed girders.

5.2 Compressive Strength

Average compressive strength of four HPC mixes is 6272 psi at 1-day, 7946 psi at 28-day. Average compressive strength of three NC mixes is 8400 psi at 1-day, 9593 psi at 28-day. Average compressive strength of three NC mixes is higher 34% at 1-day and 21% at 28-day than that of four HPC mixes. The values of strength gain in percent from 1-day to 28-day for HPC and NC are shown in Table 5.1. It is observed that HPC has a higher rate of strength gain from 1-day to 28-day than NC, which is due to the effect of slag and fly ash in HPC. This result is consistent with previous studies, including Brooks (1992), Baalbaki (1992) and Wainwright (2000).

Table 5.1. Strength gain from 1-day to 28-day for HPC and NC

Mix I.D.	HPC 1	HPC 2	HPC 3	HPC 4	NC 1	NC 2	NC 3
Average 1-Day Strength, psi	6784	6247	5417	6640	8902	6547	9750
Average 28-Day Strength, psi	8750	7938	6884	8212	10215	7545	11020
Strength Gain from 1-Day to 28-Day	29%	27%	27%	24%	15%	15%	13%
Average Strength Gain from 1-Day to 28-Day	27%				14%		

5.3 Modulus of Elasticity

Comparison of modulus of elasticity of concrete at the age of loading between the measured values and four models is shown in Table 5.2. Table 5.3 and Table 5.4 summarize the percent difference of modulus of elasticity between measured values and four models for sealed specimens and unsealed specimens respectively. Measured values of modulus of elasticity versus compressive strength of HPC from five different research projects are summarized in Figure 5.1, including Haranki (2009), Schindler (2007), Townsend (2003), Wang (2013) and the current research.

It is found that for sealed specimens AASHTO and Tadros (2003) models have a good agreement with measured values, and ACI 363R model has the largest difference with measured values. It is observed that for unsealed specimens ACI 363R model has a good prediction, and CEB-FIP 90 model has the largest difference with measured data.

As discussed previously because sealed specimens represent the behavior of mass concrete such as bridge girders better than unsealed specimens, AASHTO model provides a good prediction of elastic modulus of sealed specimens. Tadros's model also has a good agreement with AASHTO model in a certain range of compressive strength from 5000 psi to 11000 psi, which was the range of observed release strength for different types of prestressed bridge girders.

In Figure 5.1, average density of all concrete mixtures is used for AASHTO model. It is observed that most data points are within or close with the boundary of ±20% AASHTO model, which means AASHTO model provides a good prediction of modulus of elasticity according to corresponding compressive strength of HPC. AASHTO model for modulus of elasticity is acceptable for the calculation of camber of prestressed bridge girders.

Table 5.2. Comparison of measured modulus of elasticity and four models (ksi)

Mix I.D.	Sealed	Unsealed	AASHTO	ACI 363R	CEB-FIP 90	Tadros
HPC 1	4870	3216	5114	4628	5215	4834
HPC 2	5596	3105	4422	4041	5074	4613
HPC 3	5226	4080	4334	4030	4838	4259
HPC 4	5629	5129	4733	4293	5178	4775
NC 1	5425	5602	5653	4964	5709	5657
NC 2	4399	5027	4867	4423	5154	4737
NC 3	4671	4297	5882	5118	5885	5971

Table 5.3. Difference in percent of modulus of elasticity between measured values and four models for sealed specimens

Mix I.D.	Sealed elastic modulus	AASHTO	ACI 363R	CEB-FIP 90	Tadros
HPC 1	0	5	-5	7	-1
HPC 2	0	-21	-28	-9	-18
HPC 3	0	-17	-23	-7	-19
HPC 4	0	-16	-24	-8	-15
NC 1	0	4	-8	5	4
NC 2	0	11	1	17	8
NC 3	0	26	10	26	28
Average	0	-1	-11	4	-2

Table 5.4. Difference in percent of modulus of elasticity between measured values and four models for unsealed specimens

Mix I.D.	Unsealed elastic modulus	AASHTO	ACI 363R	CEB-FIP 90	Tadros
HPC 1	0	59	44	62	50
HPC 2	0	42	30	63	49
HPC 3	0	6	-1	19	4
HPC 4	0	-8	-16	1	-7
NC 1	0	1	-11	2	1
NC 2	0	-3	-12	3	-6
NC 3	0	37	19	37	39
Average	0	19	7	27	19

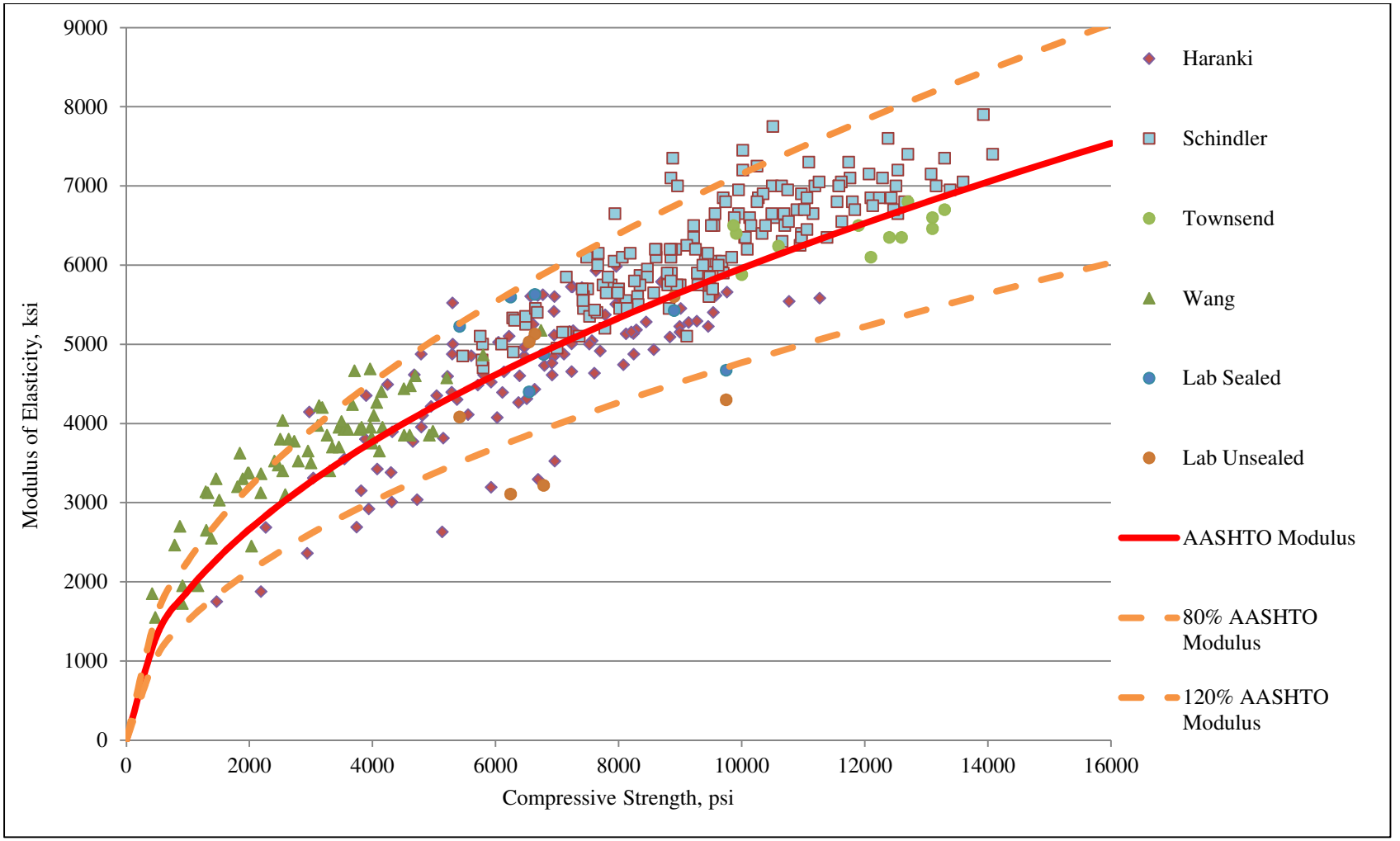

Figure 5.1. Comparison of modulus of elasticity between AASHTO model and measured values from five research projects

5.4 Summary of Creep and Shrinkage Tests

Three parts are presented in this section, including summary of seven mixes, relations between creep and shrinkage and material properties, and comparison of HPC and NC.

5.4.1 Summary of seven mixes

The properties of seven concrete mixes are summarized in Table 5.5, including w/c (water to cementitious) ratio, coarse aggregate content, a/c (aggregate to cementitious) ratio, slag replacement and fly ash replacement, and all values in this table are calculated by weight. It is observed that w/c ratio of seven mixes ranges from 0.300 to 0.380, and a/c ratio is in the range from 3.5 to 4.1, and slag replacement ranges from 0% to 25%, and fly ash replacement is in the range from 0% to 10%.

Table 5.5. Summary of seven concrete mixes

Mix I.D.	w/c ratio	Coarse Aggregate Content	a/c ratio	Slag Replacement	Fly Ash Replacement
HPC 1	0.335	41%	4.0	20%	0%
HPC 2	0.380	34%	4.1	25%	10%
HPC 3	0.300	33%	3.9	30%	0%
HPC 4	0.370	40%	3.5	25%	10%
NC 1	0.334	41%	3.9	0%	0%
NC 2	0.380	29%	4.0	0%	0%
NC 3	0.360	41%	4.0	0%	0%

5.4.2 Relations between results of creep and shrinkage tests and material properties

Relations between shrinkage strain and creep coefficient during one year and material properties are shown from Figure 5.2 to Figure 5.11. According to the observation below, It is observed that results of sealed creep coefficient and sealed shrinkage agree with previous research projects mentioned in Chapter 2 very well except for w/c ratio effect, and for unsealed creep coefficient and unsealed shrinkage some opposite trends are observed. The detailed observations are shown below:

- Shrinkage strain for both unsealed and sealed specimens decreases with an increase of w/c ratio, which is an opposite trend comparing with results from previous researches mentioned Section 2.2.2.3. The possible reason is that the range of w/c ratio for seven mixes is narrow, and other factors may also cause this opposite trend, including coarse aggregate content, a/c ratio, slag replacement and fly ash replacement;
- Creep coefficient for both unsealed and sealed specimens increases with an increase of w/c ratio, which is the similar trend with other studies discussed in Section 2.1.2.3;
- Both unsealed and sealed shrinkage strain decrease with an increase of coarse aggregate content, which is consistent with previous studies mentioned in Section 2.2.2.1;
- Unsealed creep coefficient is not affected significantly by coarse aggregate content, and it increases slightly with an increase of coarse aggregate content, which is not consistent with previous researches mentioned in Section 2.1.2.1. Unsealed creep coefficient is also affected by other factors, including w/c ratio, a/c ratio, slag replacement and fly ash replacement. Sealed creep coefficient decreases with an increase of coarse aggregate content, which is consistent with previous studies mentioned in Section 2.1.2.1;
- Unsealed shrinkage increases with an increase of a/c ratio, which is the opposite trend discussed in Section 2.2.2.1. The possible reason is that other factors also have an influence on the unsealed shrinkage, including w/c ratio, slag replacement and fly ash replacement. Sealed shrinkage decreases with an increase of a/c ratio, and this observation is consistent with previous researches mentioned in Section 2.2.2.1;
- Unsealed creep coefficient decreases with an increase of a/c ratio, which is consistent with previous studies discussed in Section 2.1.2.1. The influence of a/c ratio on sealed creep coefficient is small, which is possibly caused by other factors, including w/c ratio, slag replacement and fly ash replacement;
- Both unsealed and sealed shrinkage increase with an increase of slag replacement of Portland cement from 0% to 30%, and the effect of slag replacement is similar for both unsealed and sealed specimens. The similar trend is observed by other researchers mentioned in Section 2.2.2.5 for early age loaded slag concrete;
- Both unsealed and sealed creep coefficient increase with an increase of slag replacement of Portland cement from 0% to 30%, and the extent of the effect of slag replacement for sealed specimens is higher than that for unsealed specimens. Those observations are

consistent with previous studies discussed in Section 2.1.2.2 for early age loaded slag concrete;

- Class C Fly ash decreases shrinkage for both unsealed and sealed specimens, and the extent of decrease effect for unsealed specimens is slightly higher than that for sealed specimens, which is consistent with previous researches discussed in Section 2.2.2.5;
- Class C Fly ash increases both unsealed and sealed creep coefficient, and the extent of effect for unsealed specimens is slightly higher than that for sealed specimens. Those observations are consistent with previous studies mentioned in Section 2.1.2.5.

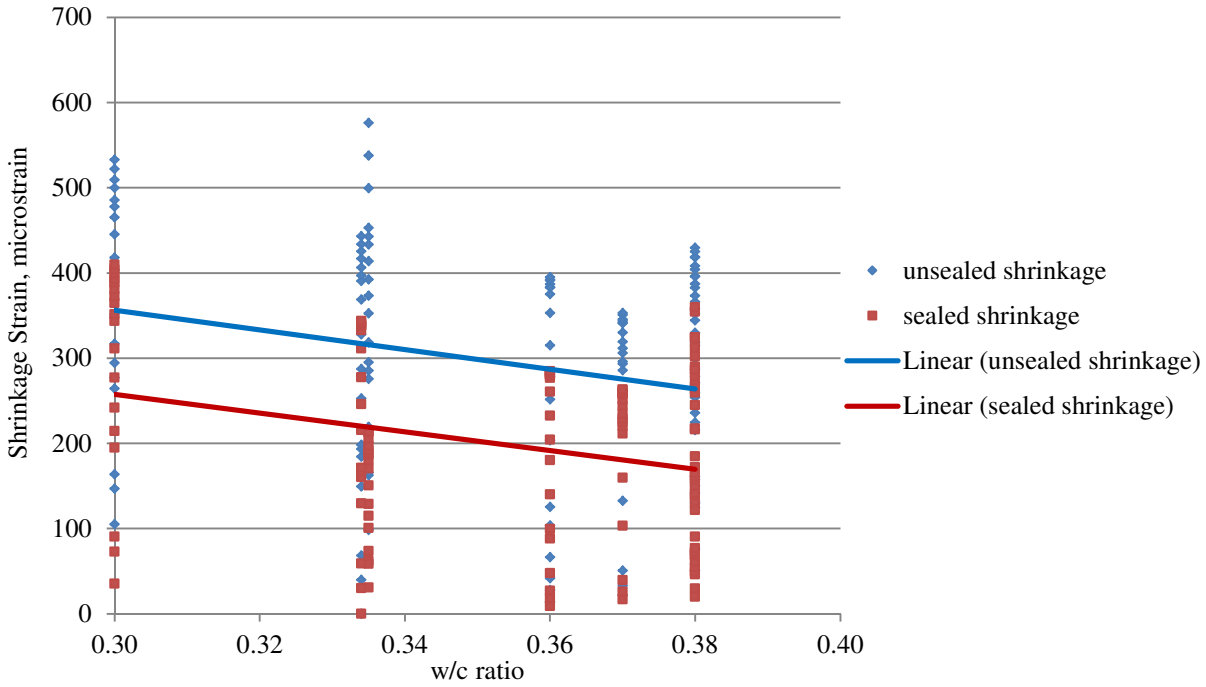

Figure 5.2. Relation between shrinkage and w/c ratio

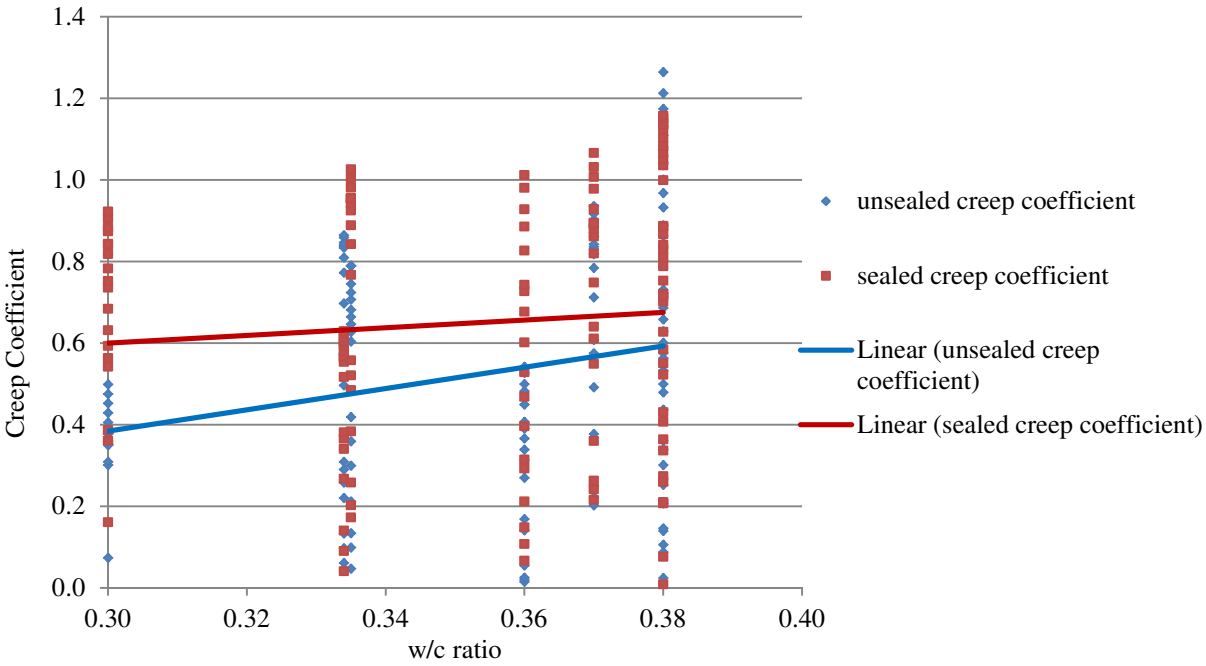

Figure 5.3. Relation between creep coefficient and w/c ratio

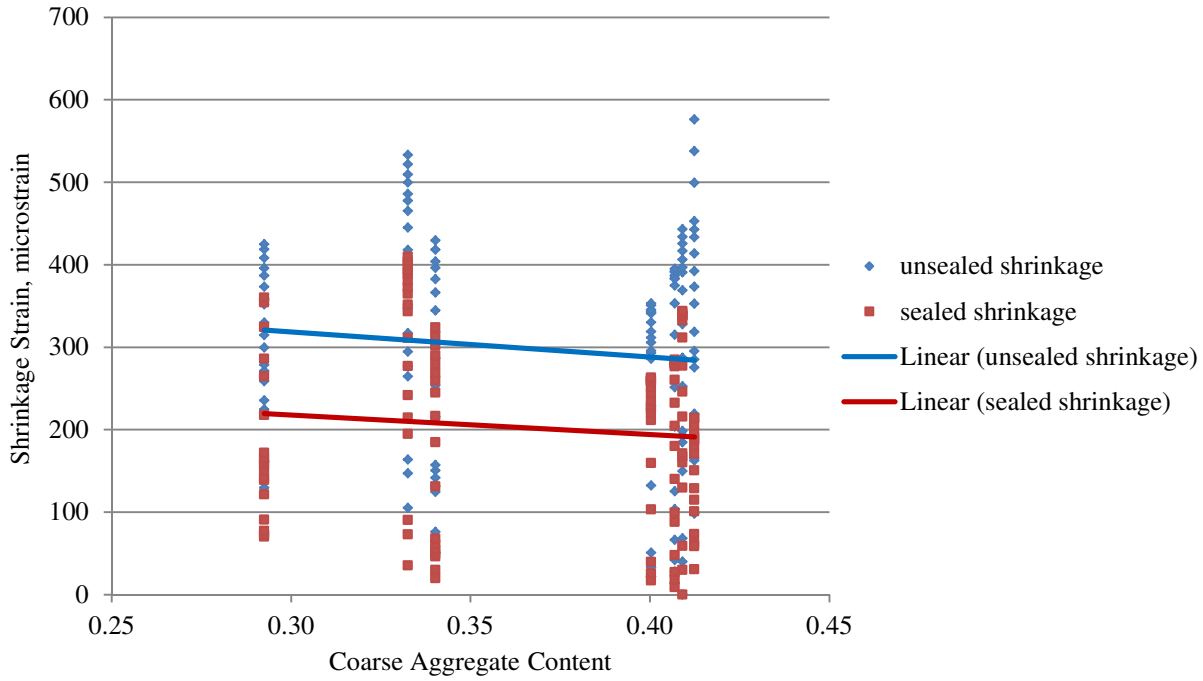

Figure 5.4. Relation between shrinkage and coarse aggregate content

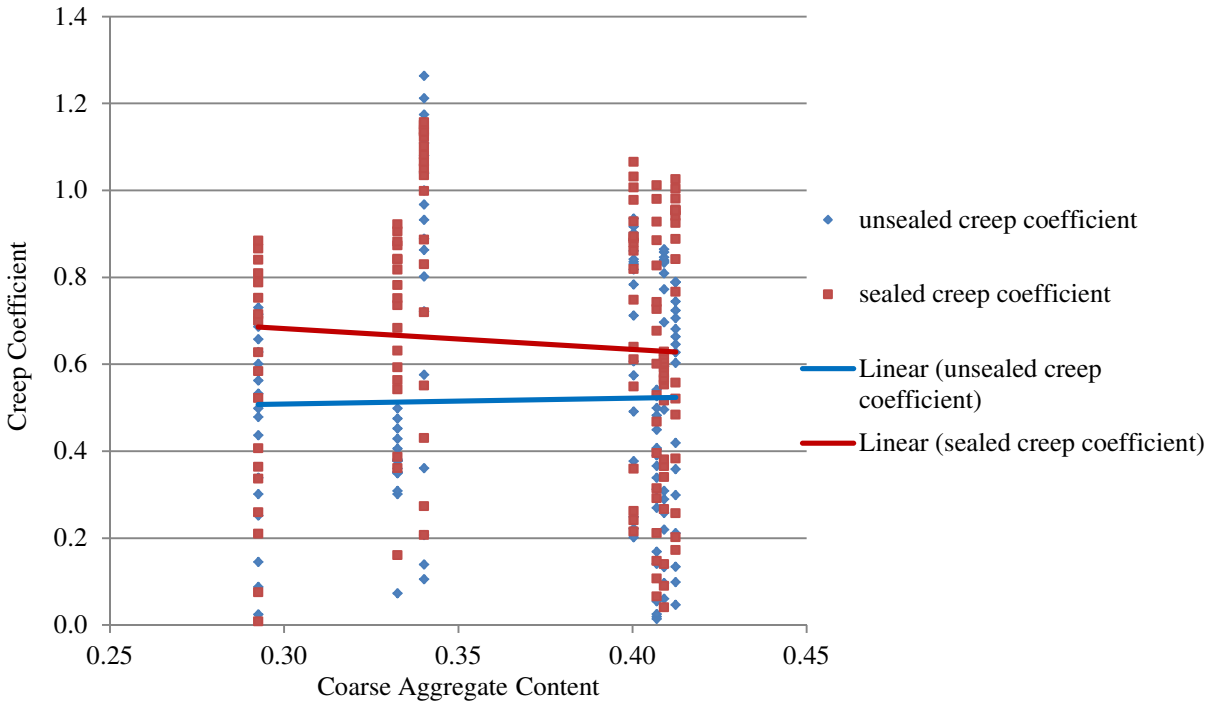

Figure 5.5. Relation between creep coefficient and coarse aggregate content

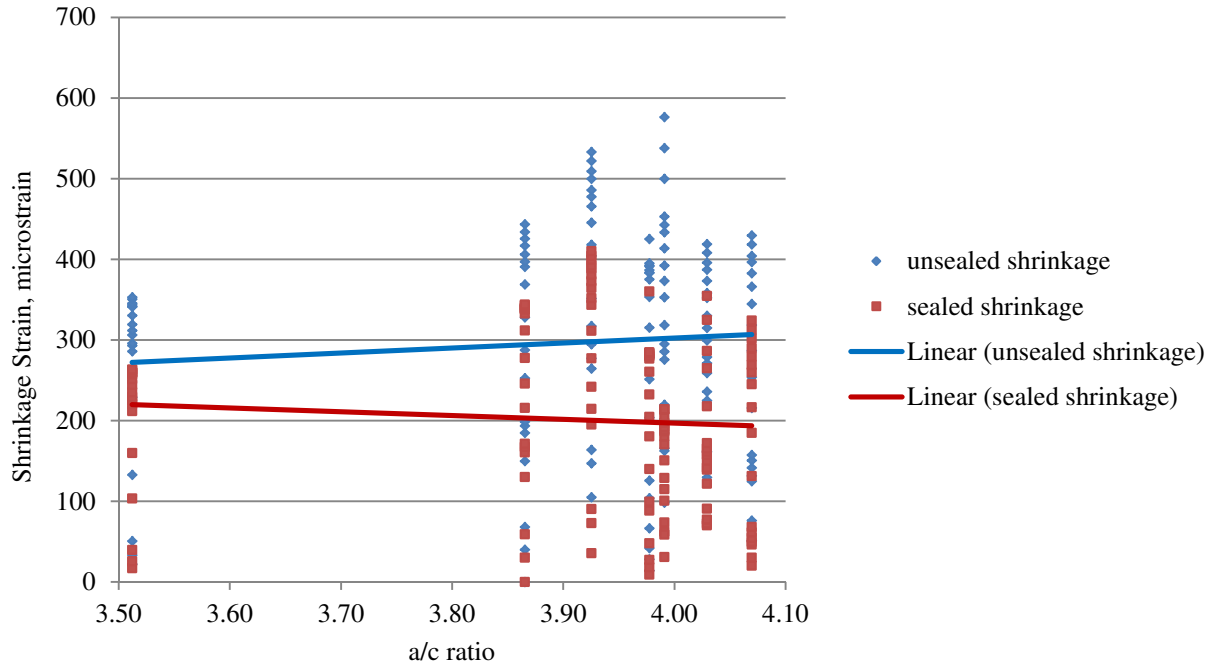

Figure 5.6. Relation between shrinkage and a/c ratio

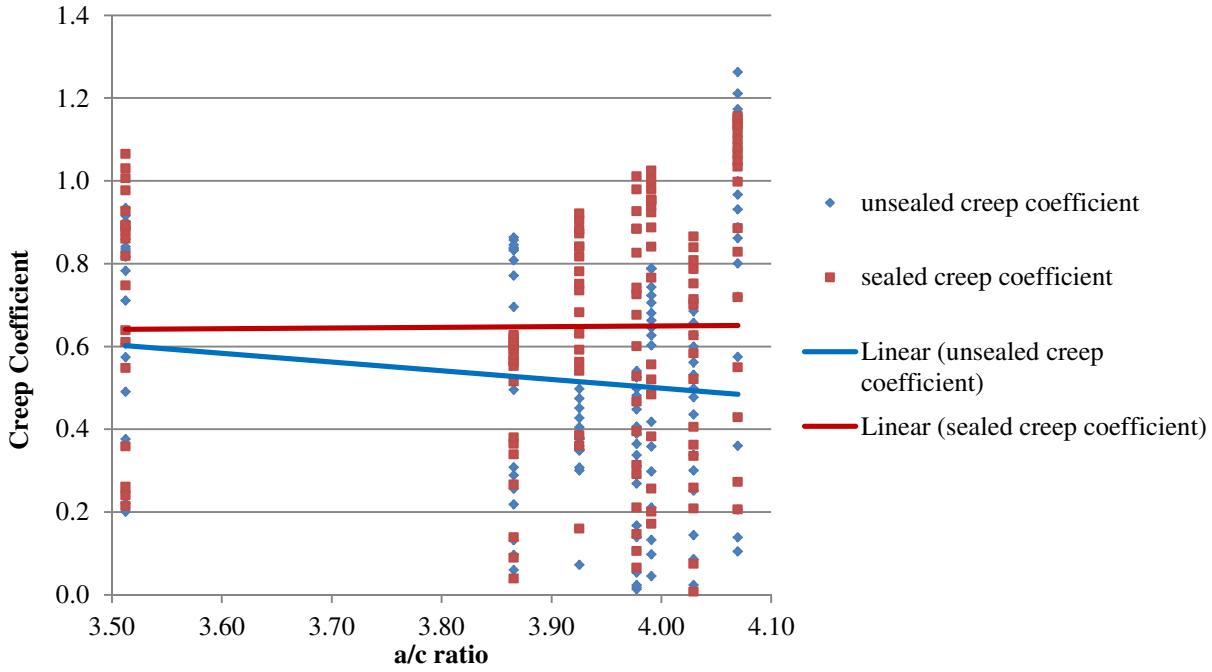

Figure 5.7. Relation between creep coefficient and a/c ratio

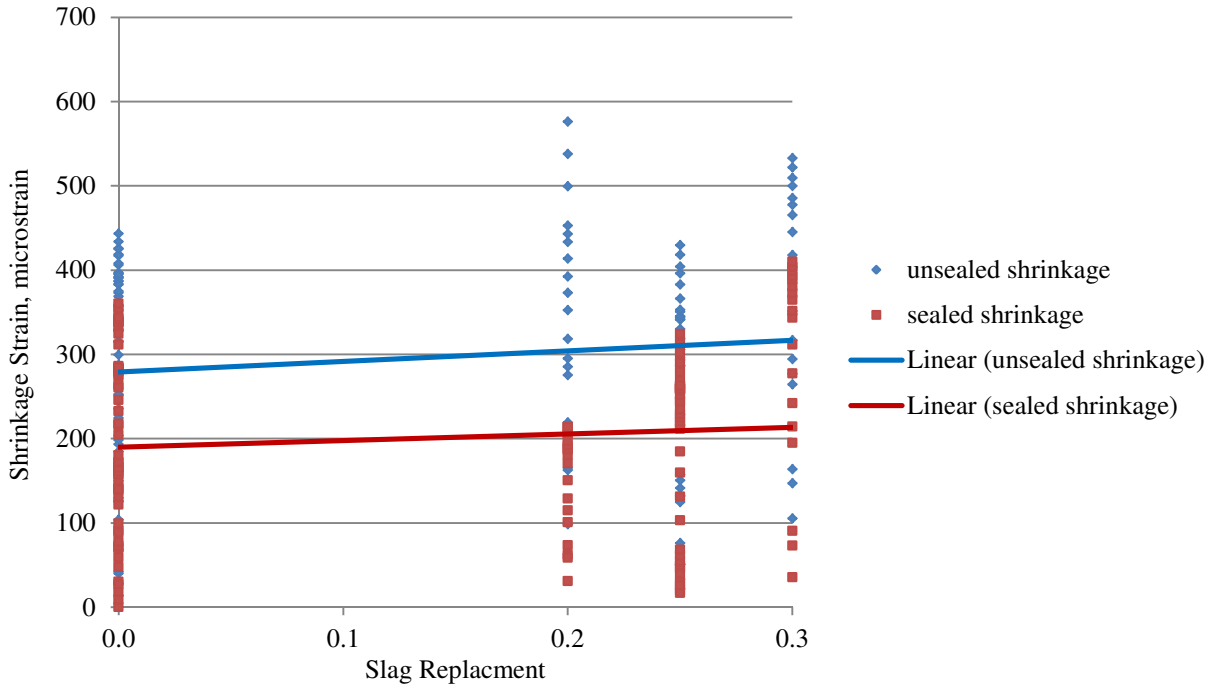

Figure 5.8. Relation between shrinkage and slag replacement

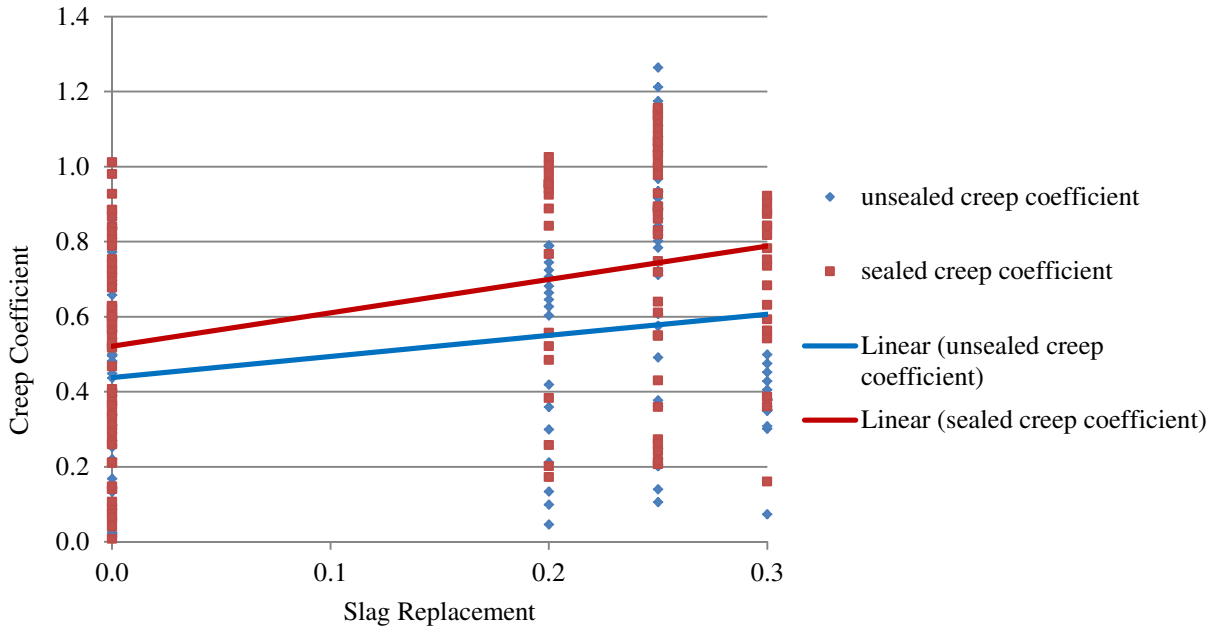

Figure 5.9. Relation between creep coefficient and slag replacement

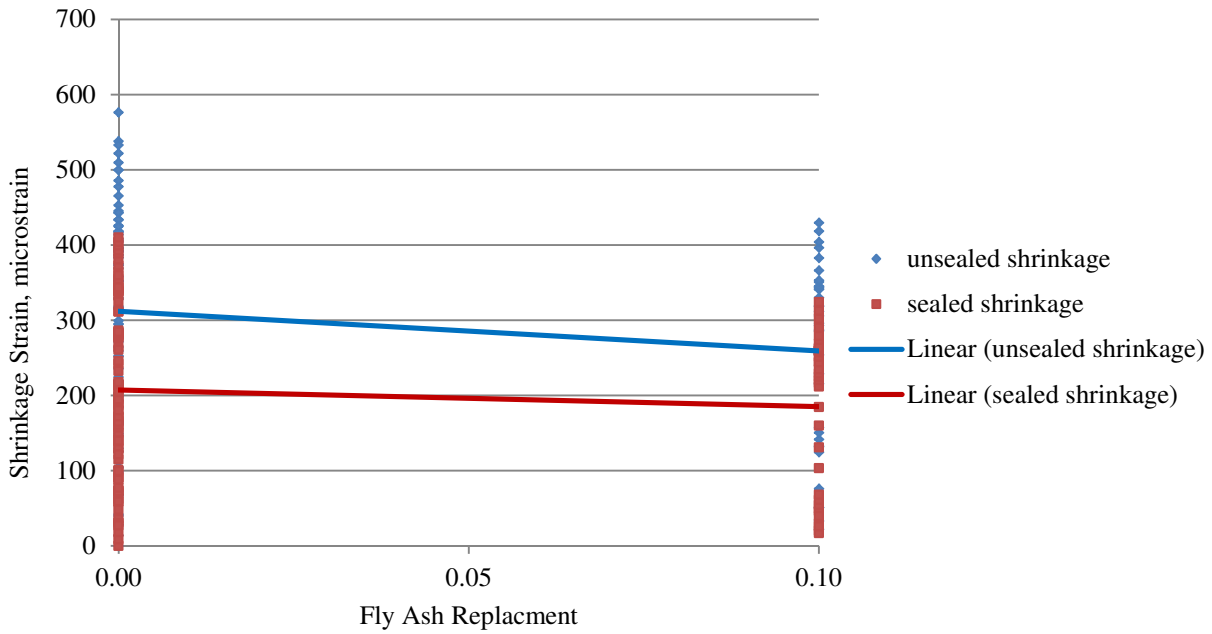

Figure 5.10. Relation between shrinkage and fly ash replacement

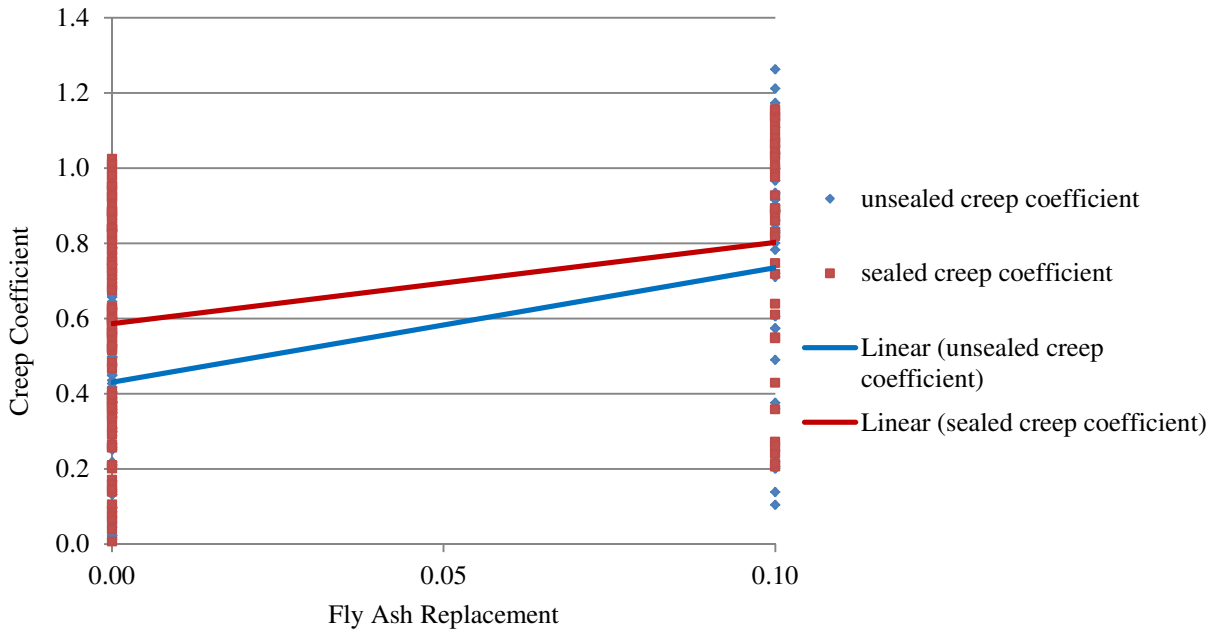

Figure 5.11. Relation between creep coefficient and fly ash replacement

5.4.3 Comparison of HPC and NC

The comparison of average unsealed and sealed creep coefficient and shrinkage for HPC and NC at the same period during one year are shown from Figure 5.12 to Figure 5.15. The difference of shrinkage and creep coefficient between HPC and NC is summarized in Table 5.6 (difference in percent = $\frac{\text{HPC value}-\text{NC value}}{\text{NC value}}$ *100%). The following are the observations:

- Average unsealed shrinkage strain for HPC is higher than that for NC, and the average value is 15%. The difference of average unsealed shrinkage strain for HPC and NC becomes smaller with time;
- Average sealed shrinkage strain for HPC is higher than that for NC during 6-month, and is lower than that for NC between 6-month to 1-year, and the average difference is 5%;
- Average unsealed creep coefficient for HPC is higher than that for NC, and the average value is 88%. The difference decreases with time from 381% at 1-day to 22% at 1-year;
- Average sealed creep coefficient for HPC is higher than that for NC, and the average value is 79%. The difference decreases with time from 398% at 1-day to 24% at 1-year.

From the observation above, it is observed that HPC has higher shrinkage and creep coefficient for both unsealed and sealed specimens than NC at the early age after loading especially during the first month of loading, and after that the difference becomes smaller.

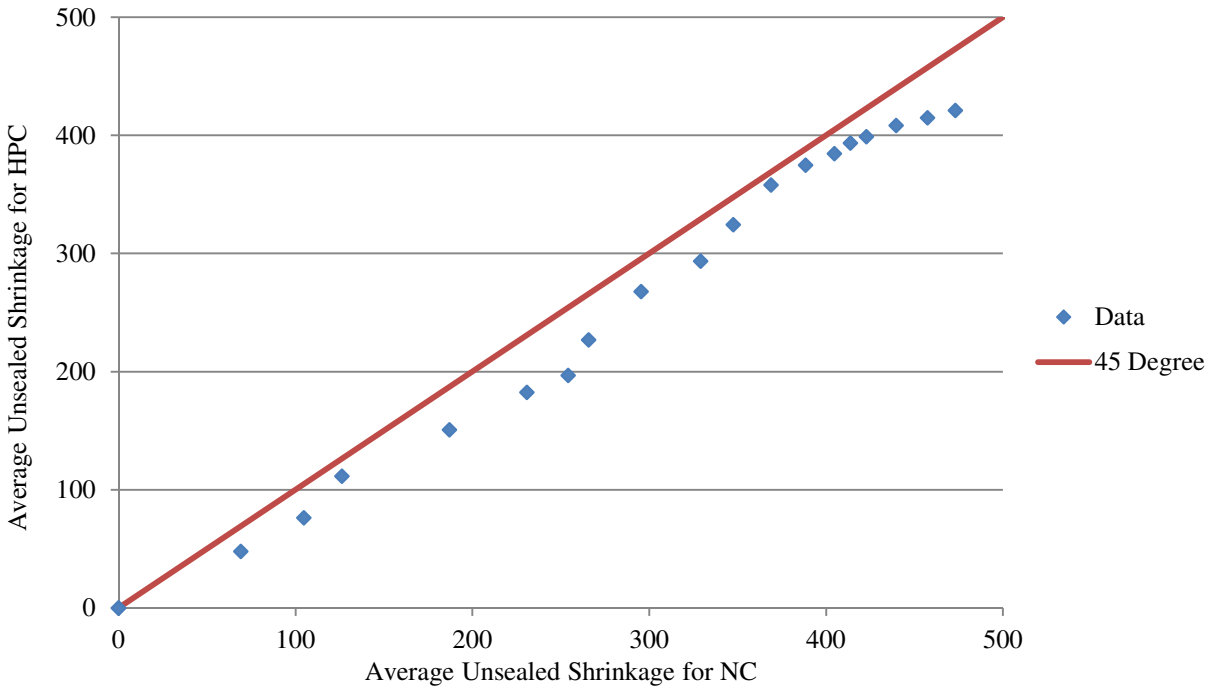

Figure 5.12. Comparison of average unsealed shrinkage for HPC and NC

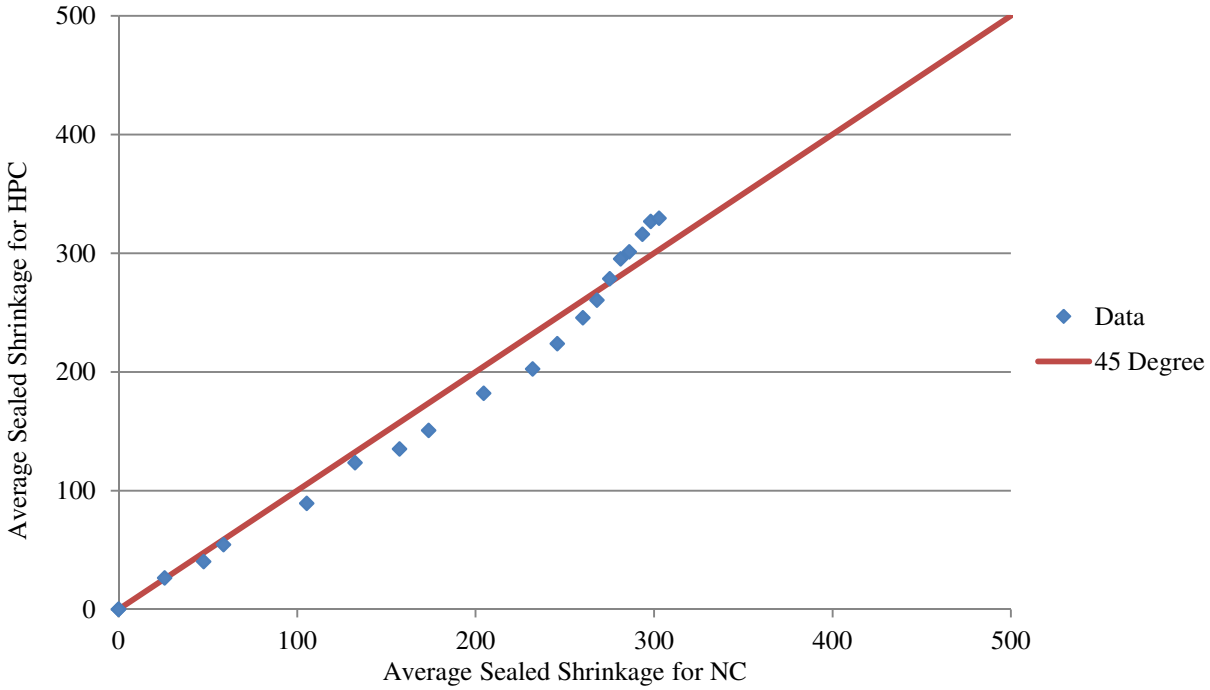

Figure 5.13. Comparison of average sealed shrinkage for HPC and NC

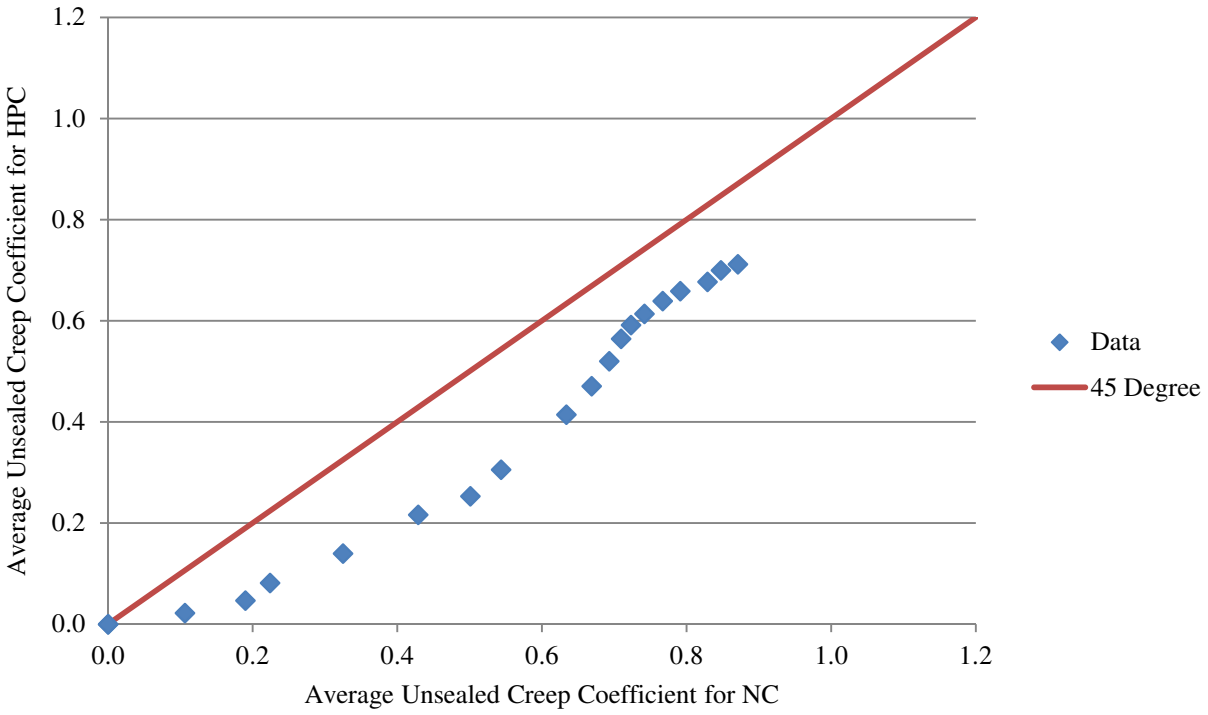

Figure 5.14. Comparison of average unsealed creep coefficient for HPC and NC

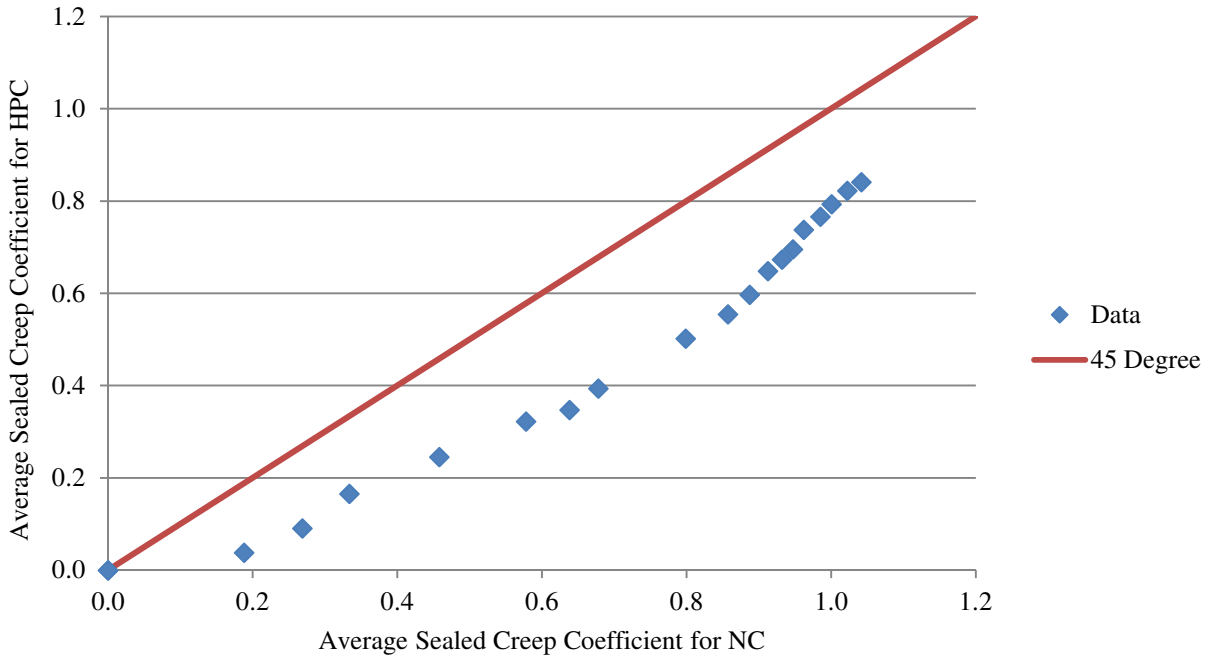

Figure 5.15. Comparison of average sealed creep coefficient for HPC and NC

Table 5.6. Comparison of HPC and NC by using difference in percent

Time after Loading, days	Unsealed Shrinkage	Sealed Shrinkage	Unsealed Creep Coefficient	Sealed Creep Coefficient
0	0	0	0	0
0	0	0	0	0
1	44	-2	381	398
2	37	19	308	197
3	13	8	175	102
7	24	18	133	87
14	26	7	98	79
21	29	16	98	84
28	17	15	78	72
60	10	12	53	59
90	12	15	42	55
120	7	10	33	49
150	3	6	26	41
180	4	3	22	38
210	5	-1	21	36
240	5	-5	20	30
270	6	-5	20	29
300	8	-7	23	26
330	10	-9	21	24
360	12	-8	22	24
Average	15	5	88	79

5.5 Comparison of Measured Data of Creep and Shrinkage Tests and Five Models

Comparison of measured creep and shrinkage data and five models in one year are shown in Table 5.5 and Table 5.6, where unsealed creep coefficient, sealed creep coefficient, unsealed shrinkage and sealed shrinkage are considered (difference in percent = $\frac{\text{Model} - \text{Measured}}{\text{measured}} * 100\%$).

It is found that AASHTO LRFD 2010 model has the best prediction for both HPC and NC. It is also indicated that B3 model has the largest errors for both HPC and NC. Comparisons of measured and predicted results of creep and shrinkage in one year are shown in Appendix B.

Table 5.7. Average difference in percent between creep coefficient and shrinkage of 4 HPC mixes and five models in one year

Models	Unsealed Creep Coefficient	Sealed Creep Coefficient	Unsealed Shrinkage	Sealed Shrinkage	Average Difference in Percent	Rank
AASHTO LRFD 2010	95	-32	-1	-44	4	1
ACI 209R-92	233	-30	-23	\	60	3
ACI 209R-Modified by Huo	203	-37	-21	\	48	2
CEB-FIP 90	264	-14	47	\	99	4
Bazant B3	335	94	57	-62	106	5

Table 5.8. Average difference in percent between creep coefficient and shrinkage of 3 NC mixes and five models in one year

Models	Unsealed Creep Coefficient	Sealed Creep Coefficient	Unsealed Shrinkage	Sealed Shrinkage	Average Difference in Percent	Rank
AASHTO LRFD 2010	119	-6	0	-49	16	1
ACI 209R-92	292	31	-1	\	107	3
ACI 209R-Modified by Huo	396	21	0	\	139	4
CEB-FIP 90	128	95	31	\	85	2
Bazant B3	291	322	91	-60	161	5

5.6 Comparison of Shrinkage Behavior of 4-ft Beam Section and Laboratory Specimens

Figure 5.2 shows the comparison of shrinkage between 4-ft beam section and unsealed and sealed specimens stored in the environmentally controlled chamber. It is found that the 4-ft beam section has a similar shrinkage behavior with sealed specimens, which means the sealed specimens could represent the shrinkage behavior of beam very well. This observation is consistent with previous studies, including Hansen (1966) and Bryant (1987).

In Figure 5.2 shrinkage of the unsealed specimen is adjusted by using volume to surface (*v/s* ratio) according to Eq. 2-65 (ACI 209R 1990). It is observed that average shrinkage of the beam section is similar with that of sealed specimens. It is also found that bottom flange has higher shrinkage strain than top flange and web, which possibly results from the incomplete debonding between strands and concrete, and temperature gradient due to sunshine. After consideration of those two effects, the difference of shrinkage strain between bottom flange and top flange would be smaller. Extent of debonding between strand and concrete and temperature gradient has a smaller effect on the web of beam section, and it is observed that shrinkage of web of is lower than that of sealed specimens.

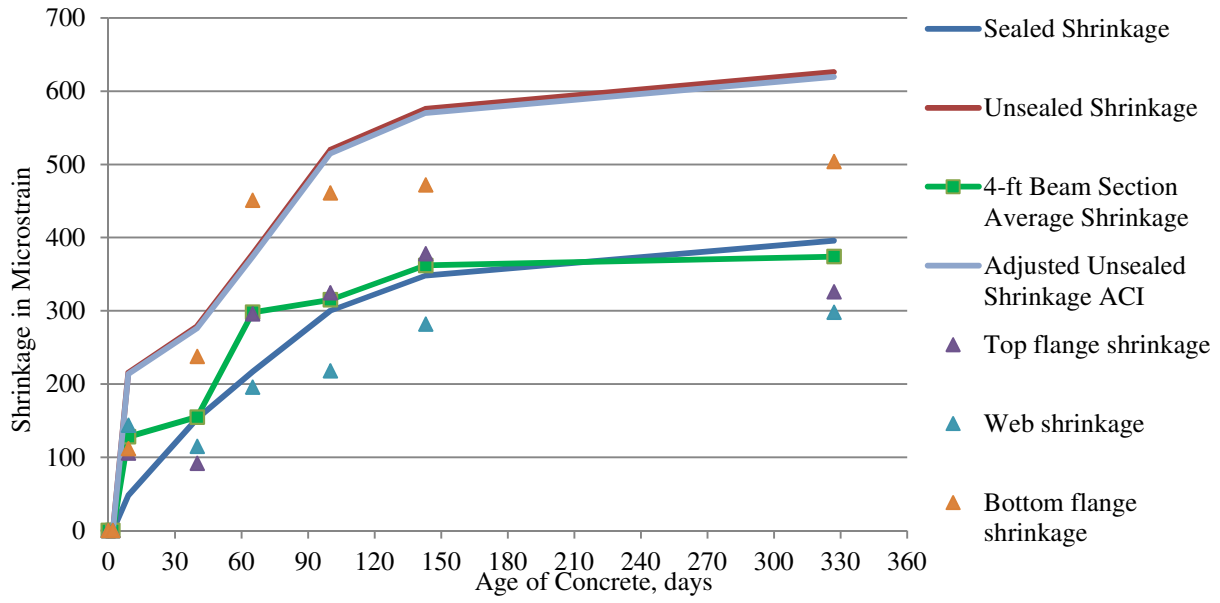

Figure 5.16. Comparison of shrinkage between 4-ft. beam section and laboratory specimens

5.7 Proposed Equations for Creep and Shrinkage of HPC

Measured average creep coefficient and shrinkage strain from sealed specimens of four HPC mixes are used to predict long-term camber of prestressed bridge girders within one year. Table 5.7 and Table 5.8 summarize the measured sealed creep coefficient and shrinkage strain and corresponding average values for four HPC mixes. If a prestressed bridge girder is stored in the yard of a precast plant more than one year, equations to present average sealed creep coefficient and sealed shrinkage strain are proposed according to one year's measured data for the tested four HPC mixes, which have the similar loading age and storage conditions. The format of AASHTO LRFD 2010 model of creep and shrinkage equations is followed. Least square method is used to obtain the appropriate parameters in the equations shown below.

Table 5.9. Measured sealed creep coefficient and average values for four HPC mixes

Time after Loading, days	HPC 1	HPC 2	HPC 3	HPC 4	Average	Sta. Dev.
0	0.00000	0.00000	0.00000	0.00000	0.00000	0.00000
0	0.00000	0.00000	0.00000	0.00000	0.00000	0.00000
1	0.17186	0.20649	0.15996	0.21487	0.18830	0.01149
2	0.20138	0.27289	0.36042	0.24085	0.26888	0.02930
3	0.25699	0.42961	0.38626	0.26184	0.33367	0.03792
7	0.38265	0.55016	0.54134	0.35891	0.45827	0.04397
14	0.48378	0.71894	0.56266	0.54802	0.57835	0.04321
21	0.52042	0.82920	0.59250	0.61062	0.63819	0.05766
28	0.55707	0.88609	0.63087	0.63966	0.67842	0.06206
60	0.76635	0.99837	0.68287	0.74767	0.79882	0.05965
90	0.84151	1.03454	0.73522	0.81871	0.85750	0.05480
120	0.88788	1.05018	0.75161	0.86035	0.88751	0.05343
150	0.92430	1.06514	0.78198	0.87970	0.91278	0.05096
180	0.94038	1.08155	0.81697	0.88930	0.93205	0.04841
210	0.95341	1.10117	0.84013	0.89390	0.94715	0.04877
240	0.95564	1.12276	0.84229	0.92817	0.96221	0.05084
270	0.95299	1.13770	0.87278	0.97726	0.98518	0.04808
300	0.98059	1.13435	0.88203	1.00658	1.00089	0.04499
330	1.00290	1.15021	0.90544	1.03095	1.02238	0.04364
360	1.02522	1.15647	0.92176	1.06521	1.04217	0.04212

Table 5.10. Measured sealed shrinkage strain and average values for four HPC mixes (10^-6 in/in)

Time after Loading, days	HPC 1	HPC 2	HPC 3	HPC 4	Average	Sta. Dev.
0	0	0	0	0	0	0
0	0	0	0	0	0	0
1	31	20	36	17	26	4
2	62	30	73	26	48	10
3	59	46	90	40	59	10
7	74	50	195	103	105	28
14	101	54	214	160	132	30
21	115	61	242	212	157	36
28	129	68	277	220	174	40
60	151	131	311	225	205	35
90	171	185	344	229	232	34
120	180	216	352	235	246	32
150	187	245	365	244	260	32
180	188	260	373	251	268	33
210	192	269	381	259	275	34
240	197	279	389	260	281	35
270	205	290	392	257	286	34
300	213	302	399	259	293	34
330	214	313	404	262	298	35
360	214	324	410	263	303	37

Proposed equation of average creep coefficient for sealed specimens of four HPC mixes is expressed as:

$$\varphi(t) = \frac{1.9t^{0.48}}{8+ t^{0.54}} \qquad \text{(Eq 5-1)}$$

where t = duration after loading for creep or duration after exposure to the air for shrinkage (days)

Proposed equation of average shrinkage strain in microstrain for sealed specimens of four HPC mixes is expressed as:

$$\varepsilon(t) = \frac{480t^{0.60}}{12+ t^{0.62}} \qquad \text{(Eq 5-2)}$$

Figure 5.59 and Figure 5.60 show the comparison of predicted values from proposed equations and measured values. It is found that the standard deviation between predicted sealed

creep coefficient and the measured values is 0.00342. It is also indicated that the standard deviation between predicted sealed shrinkage strain and the measured values is 4.03215 microstrain. Vertical bars represent the standard deviation of measured values for four HPC mixes. According to the Eq 5-1 the ultimate sealed creep coefficient is 1.06.

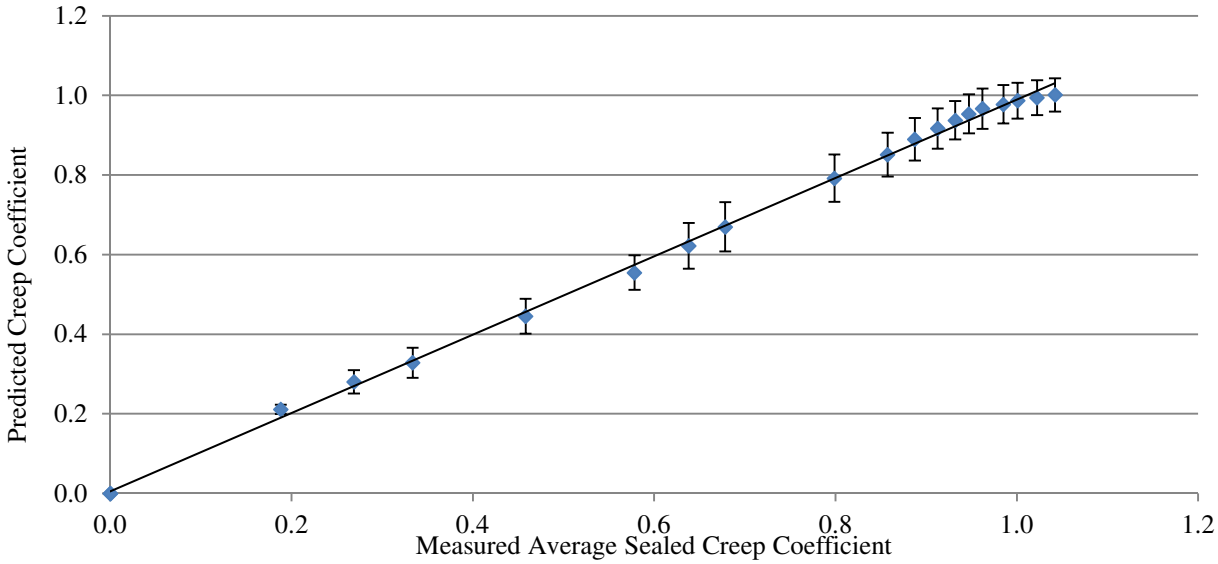

Figure 5.17. Comparison of predicted sealed creep coefficient and measured average values

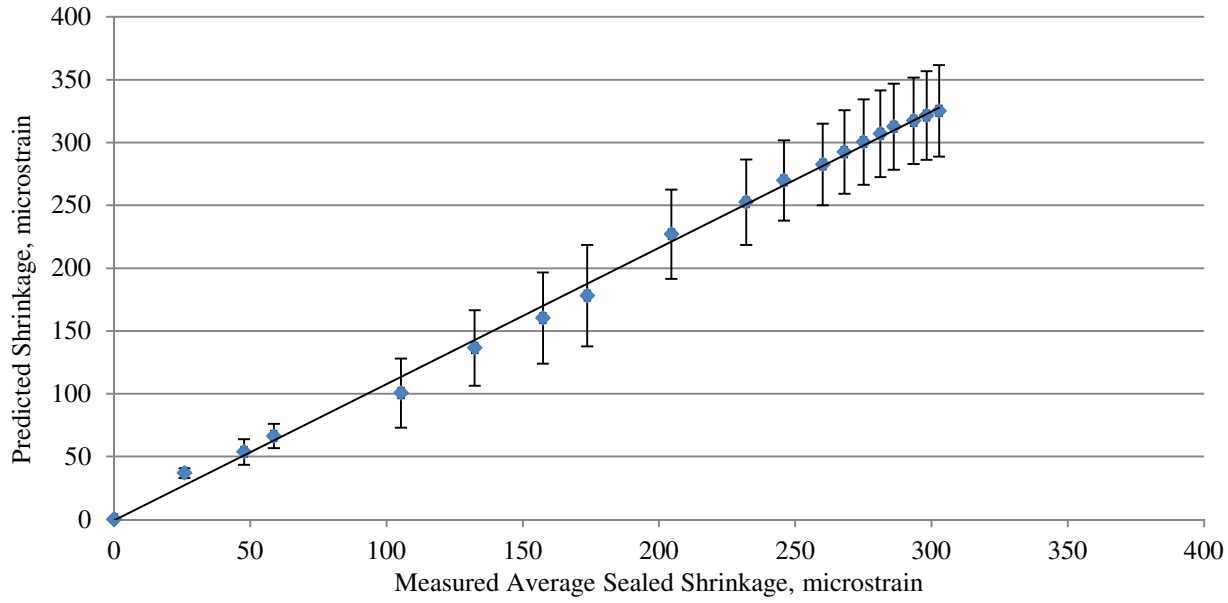

Figure 5.18. Comparison of predicted sealed shrinkage and measured values

5.8 Prediction of the Long-term Camber of Prestressed Bridge Girders

Tadros's Method (2011), Naaman's Method (2004) and incremental method are used to predict long-term camber of a prestressed bridge girder. Average sealed creep coefficient and average sealed shrinkage values are applied. Transformed section properties are used to conduct related calculations. Twenty-six girders are analyzed, including three BTC 120 girders produced by plant A, nine BTE 110 girders and six BTE 145 girders cast by plant B, and eight BTD 135 girders made by plant C, and the analyzed results of camber are compared with measured values. It is observed that Naaman's Method and incremental method have the best prediction of camber of girders, and the results of those two methods are similar.

5.8.1 Tadros's Method

Tadros's Method is highly dependent on the release camber, creep coefficient of HPC and prestress losses. Figure 5.5 and Figure 5.6 show the comparison of predicted camber and measured camber with and without overhang respectively. The release camber calculated by using incremental method is used for the prediction of long-term camber of girders. It is found that the average difference in percent between predicted camber by using Tadros's Method and the measured value is 12% for girders with overhang and 15% for girders without overhang, which means that Tadros's Method typically overestimates long-term camber.

5.8.2 Naaman's Method

Naaman's Method is dependent on time-dependent prestress forces, time-dependent modulus of elasticity and creep. Figure 5.7 and Figure 5.8 show the comparison of predicted camber and measured camber with and without overhang respectively. It is observed that almost all data points are located within ±25% lines. It is also found that the average difference in percent between predicted camber by using Naaman's Method and the measured value is -1% for girders with overhang and 0% for girders without overhang. Naaman's Method is a good method to predict long-term camber.

5.8.3 Incremental Method

Incremental method is affected by the same factors with Naaman's method. Figure 5.9 and Figure 5.10 show the comparison of predicted camber and measured camber with and without overhang respectively. It is found that almost all data points are located within ±25% lines. It is also observed that the average difference in percent between predicted camber using incremental method and the measured value is -1% for girders with overhang and 0% for girders without overhang. Incremental method is also a good method to predict long-term camber.

5.8.4 Comparison of gross section and transformed section on camber of girders

The comparison of predicted camber of girders by using three methods for gross section and transformed section is performed in Appendix C and Appendix D. It is found that predicted cambers of girders using gross section properties are always larger than those using transformed section properties, and the average value for all 26 girders is 13%.

5.8.5 Comparison of average creep and shrinkage and specified creep and shrinkage on the camber of girders

For the analysis above, the results of average sealed creep coefficient and average sealed shrinkage are used to predict long-term camber of girders. Predictions of cambers of girders by using average sealed creep and shrinkage data for four HPC mixes are summarized in Appendix C. Predictions of cambers of girders by using specified sealed creep and shrinkage data are shown in Appendix D, where due to the absence of specified mix of BTE 110 of plant B, the average sealed creep coefficient and sealed shrinkage of HPC 2 and HPC 4 of plant B are applied. It is found that the average difference of cambers of girders for those two types of creep and shrinkage data is on average within ±2%. Therefore, it is acceptable to use the average values of sealed creep coefficient and sealed shrinkage for four HPC mixes to predict long-term camber of girders within one year. If the prestressed bridge girder is stored in the yard of a precast plant more than one year, the proposed equations of sealed creep coefficient and sealed shrinkage can be utilized to predict long-term camber.

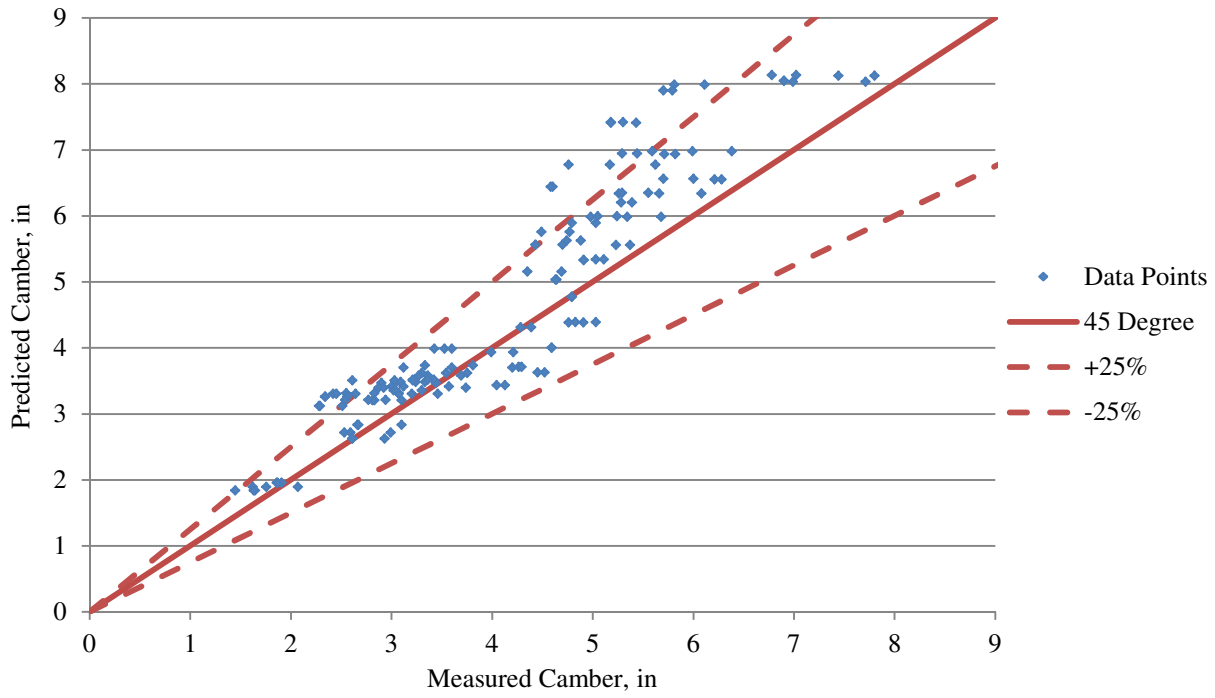

Figure 5.19. Comparison of predicted camber and measured camber with overhang by using Tadros's Method

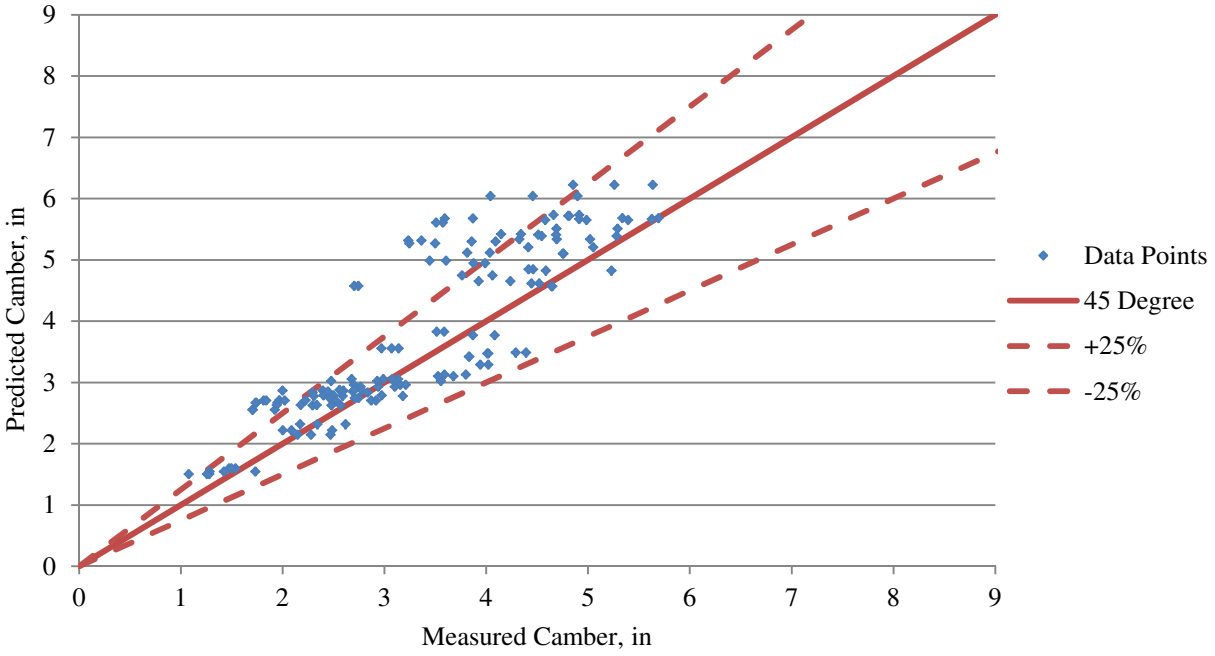

Figure 5.20. Comparison of predicted camber and measured camber without overhang by using Tadros's Method

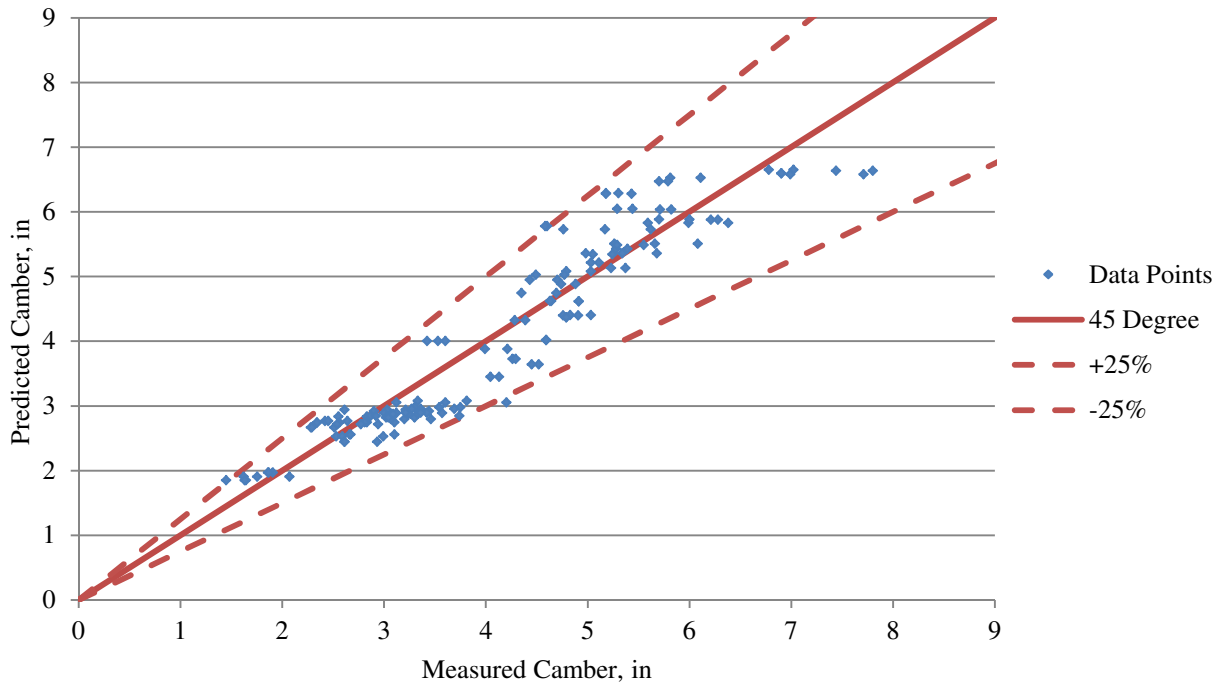

Figure 5.21. Comparison of predicted camber and measured camber with overhang by using Naaman's Method

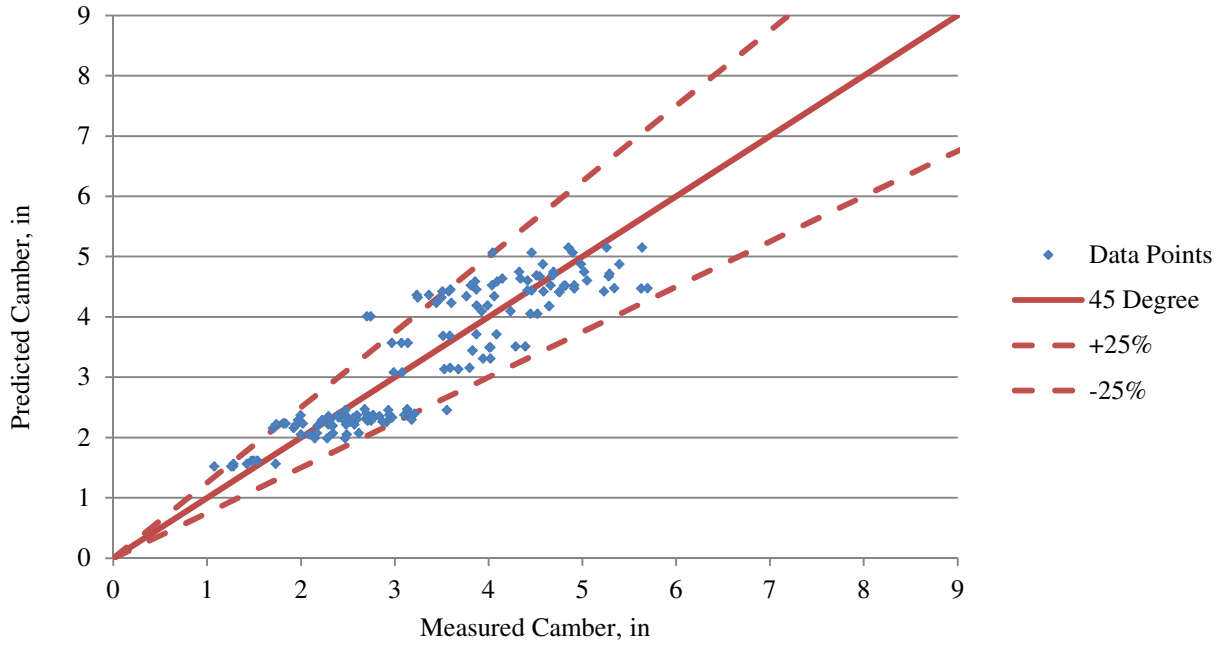

Figure 5.22. Comparison of predicted camber and measured camber without overhang by using Naaman's Method

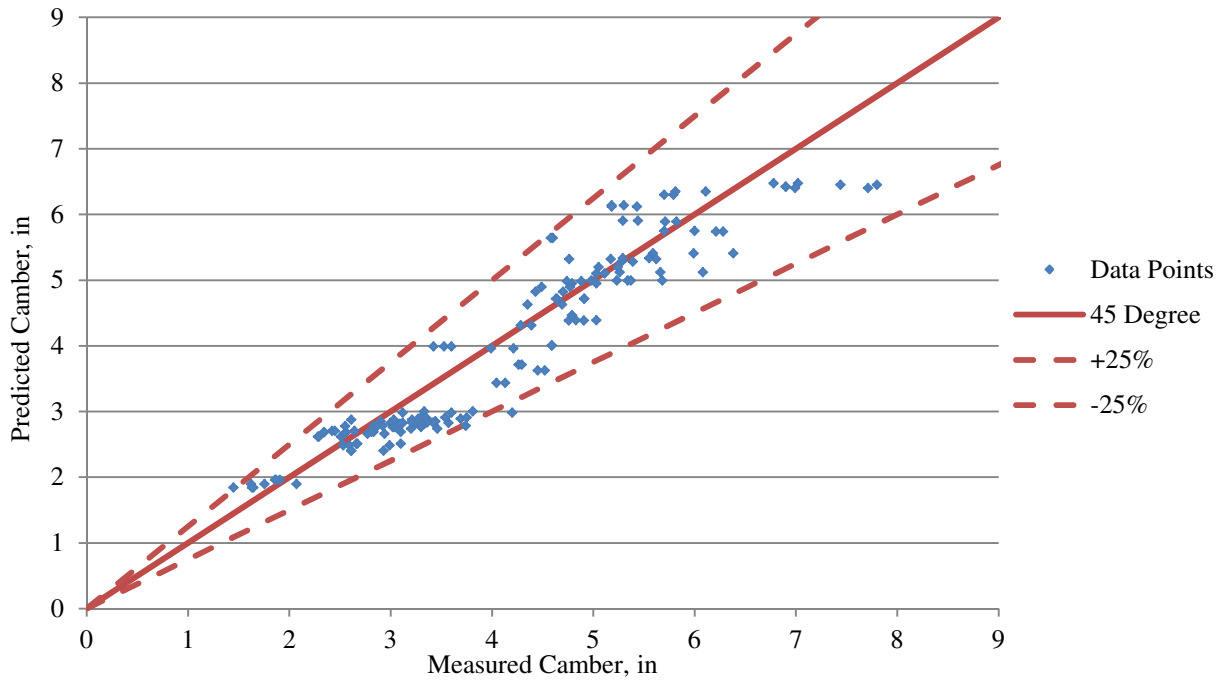

Figure 5.23. Comparison of predicted camber and measured camber with overhang by using Incremental method

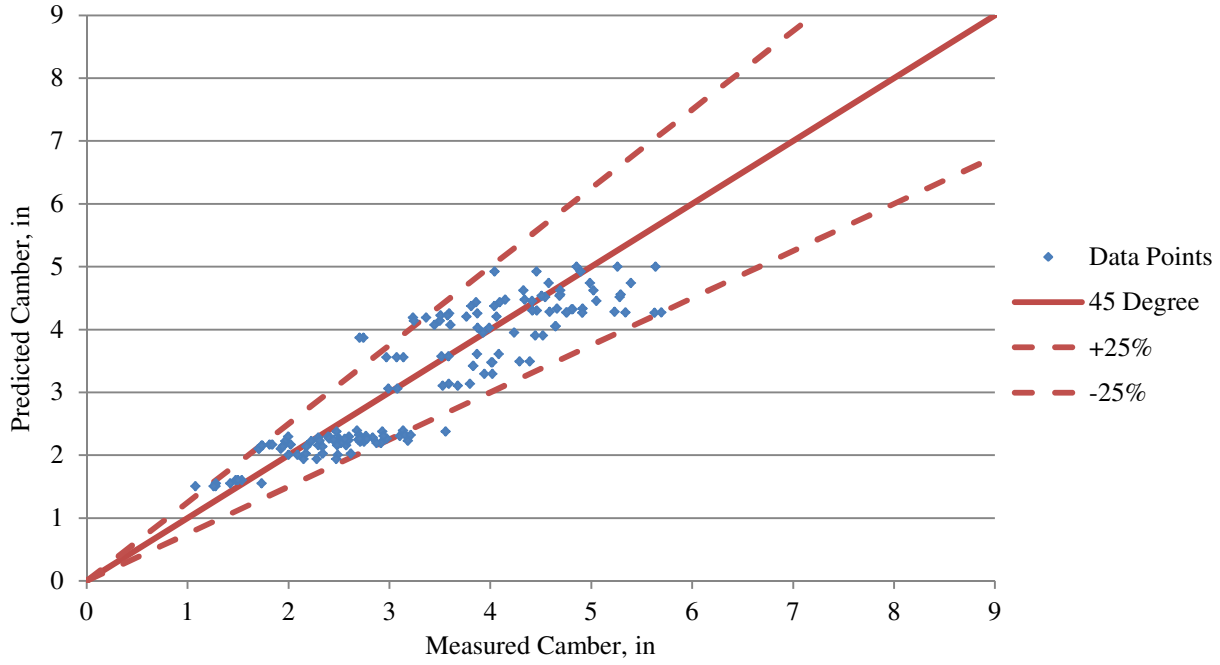

Figure 5.24. Comparison of predicted camber and measured camber without overhang by using Incremental method

5.8.6 Comparison of AASHTO creep and shrinkage model and measured creep and shrinkage on the camber of girders

AASHTO unsealed creep and shrinkage values and gross section properties are typically used to calculate the long-term camber of prestressed bridge girders. If average AASHTO unsealed creep and shrinkage and gross section properties are used to calculate the long-term camber of girders during one year, it is found that the camber from AASHTO is higher on average 22% than the camber calculated by using measured sealed creep and shrinkage values and transformed section properties. That's one of reasons that the predicted camber at erection is typically higher than actual values for long-span bulb tee girders.

5.8.7 Calculated prestress losses and camber growth at 3-month and 1-year

Table 5.11 and Table 5.12 show the short-term and long-term prestress losses in percent and camber growth in percent at 3-month and 1-year. Transformed section properties are used to calculate the short-term and long-term losses. The camber calculated by using Naaman's Method is used to compute camber growth (camber growth in percent= $\frac{\Delta_{\text{long-term}}-\Delta_{\text{release}}}{\Delta_{\text{release}}}*100\%$). It is observed that for 26 girders average short-term prestress losses due to anchorage set, relaxation and elastic shortening is 7%, and average long-term prestress losses due to creep, shrinkage and relaxation is 10% at 3-month, and 12% at 1-year. It is also found that average camber growth for 26 girders is 42% at 3-month, and 50% at 1-year.

Table 5.11. Summary of prestress losses and camber growth at 3-month

Girder Type	Plant	Girder I.D.	Prestress losses due to anchorage set, relaxation and elastic shortening	Prestress Losses due to creep, shrinkage and relaxation after 3-month	Camber Growth at 3-month
BTC 120	A	103-09, 103-10, 103-11	6%	10%	44%
BTE 110	B	144-270, 144-272, 144-268	6%	10%	45%
		144-274, 144-275, 144-278	6%	10%	44%
		144-284, 144-283, 144-280	6%	10%	45%
BTE 145	B	144-311, 144-334	7%	10%	40%
		144-316, 144-317	7%	11%	40%
		144-366, 144-367	7%	10%	40%
BTD 135	C	13501, 13502	7%	10%	42%
		13503, 13504	7%	10%	42%
		13507, 13508	7%	10%	42%
		13511, 13512	7%	10%	42%
		Average	7%	10%	42%

Table 5.12. Summary of prestress losses and camber growth at 1-year

Girder Type	Plant	Girder I.D.	Prestress losses due to anchorage set, relaxation and elastic shortening	Prestress Losses due to creep, shrinkage and relaxation after 1-year	Camber Growth at 1-year
BTC 120	A	103-09, 103-10, 103-11	6%	12%	52%
BTE 110	B	144-270, 144-272, 144-268	6%	12%	53%
		144-274, 144-275, 144-278	6%	12%	53%
		144-284, 144-283, 144-280	6%	12%	53%
BTE 145	B	144-311, 144-334	7%	12%	44%
		144-316, 144-317	7%	12%	43%
		144-366, 144-367	7%	12%	47%
BTD 135	C	13501, 13502	7%	12%	49%
		13503, 13504	7%	12%	50%
		13507, 13508	7%	12%	50%
		13511, 13512	7%	12%	49%
		Average	7%	12%	50%

5.8.8 Effect of errors of three factors on the prediction of camber of prestressed bridge girders

Errors of three factors are considered, including modulus of elasticity, creep and shrinkage, and prestress forces. Table 5.9 shows the average effect of errors on the camber of prestressed bridge girders within one year when those factors are analyzed independently. It is found that ±20% error of modulus can cause 13% error of the camber of girders, and ±20% error of creep and shrinkage values can lead to 8% error of camber, and ±5% error of prestress forces can result in 11% error of camber. (±20% is the error of elastic modulus of concrete discussed in Section 5.3, ±20% is the typically error of creep and shrinkage tests observed from current and previous research projects, and ±5% is the tolerance of error of prestress force approved by IA DOT.)

It is also found that the camber of a girder is very sensitive to the change of prestress forces, which means the inaccuracy of record of prestress forces by precast plants can lead to more error of camber. The error of modulus of elasticity of concrete has the moderate effect on the camber of girders. The error of creep and shrinkage of concrete has the least influence on the camber of a girder.

Table 5.13. Average effect of errors of three factors on camber of prestressed bridge girders within one year

Sources of Errors	Error	BTC 120	BTE 110	BTE 145	BTD 135	Average
Modulus of Elasticity of Concrete	±20%	±13%	±13%	±12%	±12%	±13%
Creep and Shrinkage	±20%	±7%	±8%	±8%	±8%	±8%
Prestress Forces	±5%	±10%	±10%	±11%	±11%	±11%

5.8.9 Comparison of camber at erection between conspan and Naaman's Method

Table 5.14 and Table 5.15 summarize the comparison of camber at erection between Conspan and Naaman's Method for 26 prestressed bridge girders. The release camber is calculated by using Naaman's Method and transformed section properties in Table 5.14 and gross section properties in Table 5.15 respectively. Prestressed bridge girders are typically erected at the construction site at three month after transfer. Conspan uses multipliers to obtain the camber at erection, including 1.80 for camber due to prestress forces, and 1.85 for camber due to self-weight of the girder. Camber at erection by Naaman's Method utilizes transformed or gross section properties, average creep and shrinkage values at 3-month after transfer. In this section the overhang effect is not taken into account, and all corresponding cambers are calculated based on zero overhang. It is found that the camber at erection by Naaman's Method is on average 81% of camber by Consapn with transformed section properties, and 69% of camber by Conspan with gross section properties. It is also observed that the difference between the camber at erection by Naaman's Method and 80% of camber by Conspan with transformed section properties is within 3%, and the erection camber by Naaaman's Method and 70% of camber by Conspan with gross section propreties is within 5%.

Figure 5.25 and Figure 5.26 show the comparison of adjusted measured camber without overhang in a range of 75 days to 100 days after transfer and the camber at erection by Conspan for 12 prestressed bridge girders for transformed section and gross section respectively. It is found that the camber by Conspan for transformed section is on average higher 14% than the adjusted measured camber about 3-month, and the camber by Conspan for gross section is on average higher 30% than the adjusted measured camber at erection. That's another reason why the prediction of camber at erection is typically higher than the actual value for long-span bulb tee girders.

Table 5.14. Comparison of camber at erection between Conspan (Itr) and Naaman's Method

Plant	Girder Type	Girder I.D.	Release Camber Itr, in	Camber at Erection by Conspan Itr, in	Camber at erection by Naaman's Method Itr, in	80% of Camber at Erection from Conspan Itr, in
A	BTC 120	103-09, 103-10, 103-11	3.569	6.265	5.147	5.012
B	BTE 110	144-270,144-272, 144-268	1.561	2.737	2.256	2.190
B	BTE 110	144-274,144-275, 144-278	1.613	2.828	2.329	2.262
B	BTE 110	144-284,144-283, 144-280	1.517	2.660	2.193	2.128
B	BTE 145	144-311, 144-334	3.154	5.491	4.421	4.393
B	BTE 145	144-316, 144-317	3.129	5.442	4.375	4.354
B	BTE 145	144-366, 144-367	3.018	5.252	4.227	4.201
C	BTD 135	13501, 13502	3.438	6.002	4.880	4.802
C	BTD 135	13503, 13504	3.507	6.126	4.988	4.901
C	BTD 135	13507, 13508	3.492	6.100	4.968	4.880
C	BTD 135	13511, 13512	3.308	5.777	4.694	4.621

Table 5.15. Comparison of camber at erection between Conspan (Ig) and Naaman's Method

Plant	Girder Type	Girder I.D.	Release Camber Ig, in	Camber at Erection from Conspan Ig, in	Camber at erection from Naaman' Method Itr, in	70% of Camber at Erection from Conspan Ig, in
A	BTC 120	103-09, 103-10, 103-11	4.15	7.300	5.147	5.110
B	BTE 110	144-270,144-272, 144-268	1.76	3.091	2.256	2.163
B	BTE 110	144-274,144-275, 144-278	1.83	3.214	2.329	2.249
B	BTE 110	144-284,144-283, 144-280	1.7	2.986	2.193	2.090
B	BTE 145	144-311, 144-334	3.76	6.568	4.421	4.597
B	BTE 145	144-316, 144-317	3.75	6.546	4.375	4.582
B	BTE 145	144-366, 144-367	3.58	6.251	4.227	4.375
C	BTD 135	13501, 13502	4.11	7.198	4.880	5.039
C	BTD 135	13503, 13504	4.19	7.342	4.988	5.139
C	BTD 135	13507, 13508	4.16	7.289	4.968	5.102
C	BTD 135	13511, 13512	3.91	6.848	4.694	4.794

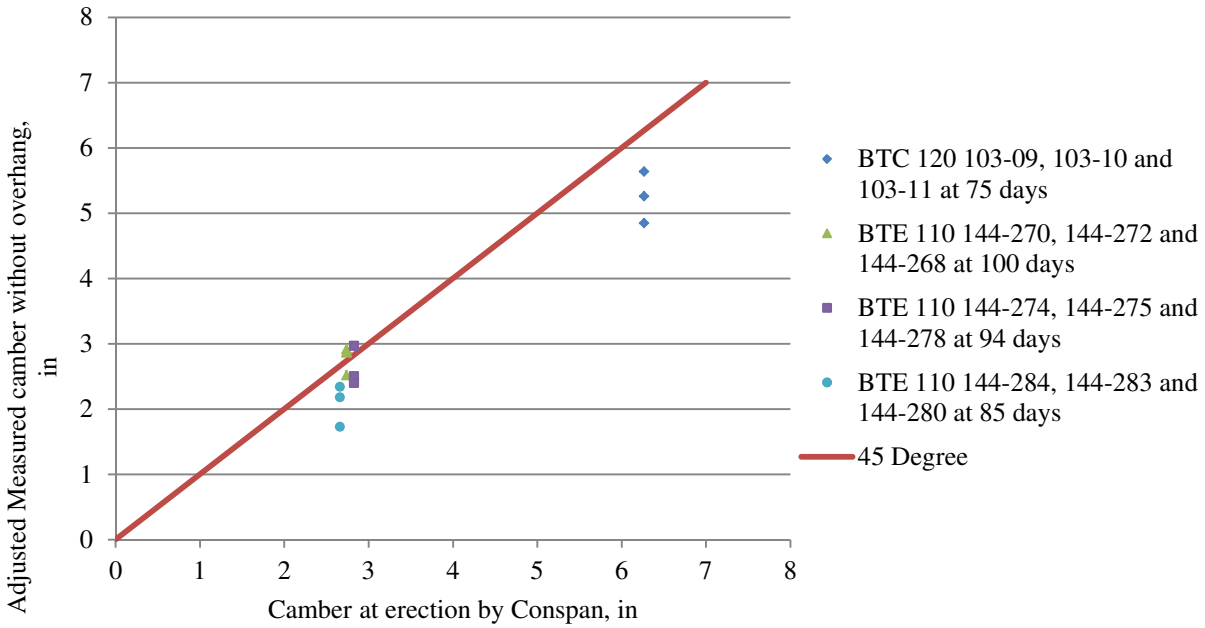

Figure 5.25. Comparison of adjusted measured camber without overhang at erection with camber at erection by Conspan with Itr

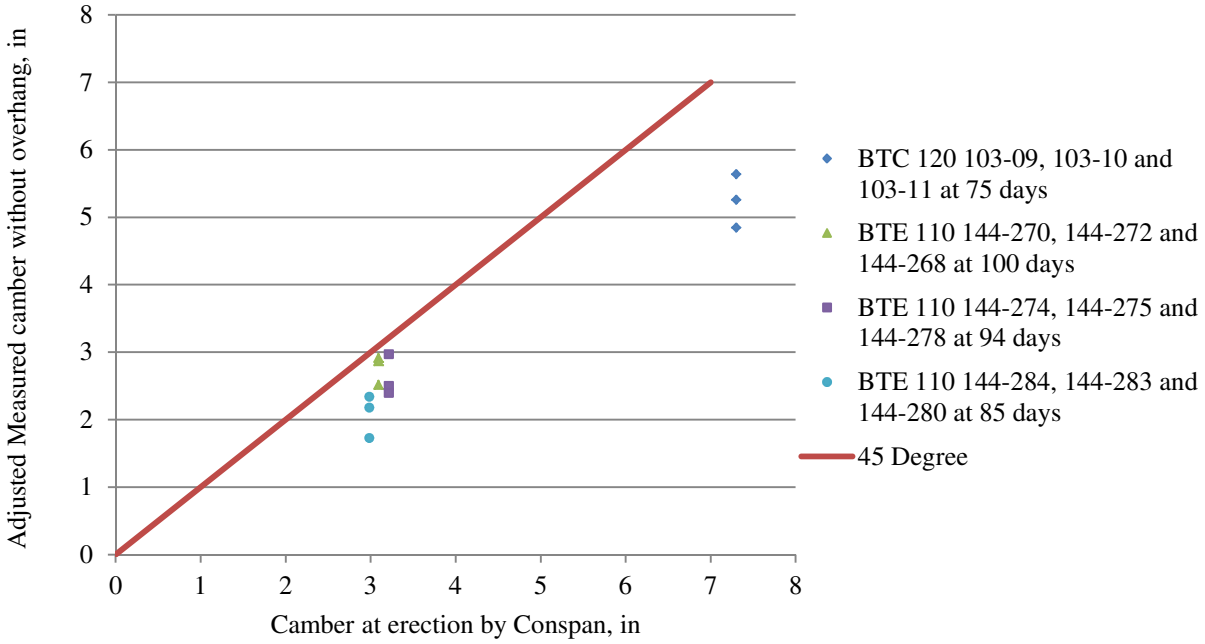

Figure 5.26. Comparison of adjusted measured camber without overhang at erection with camber at erection by Conspan with Ig

5.8.10 Comparison of current study with three previous studies

It was observed that refined method of prestress losses from AASHTO LRFD 2010 had good prediction, which was consistent with four studies. Comparing with three previous studies discussed in Section 2.4.3, more things had been done and found beyond previous studies. In the current study, creep and shrinkage tests of four HPC mixes and three NC mixes during one year from three precast plants were taken, and decent data were collected. It was found that the HPC crept and shrink more than NC due to the use of slag and fly ash and the early age of loading application. Creep and shrinkage behavior between laboratory specimens and the full scale girder was correlated, and it was found that the sealed laboratory specimens could represent the creep and shrinkage behavior of the full scale girder. Additionally, a simplified time-dependent method (Naaman's Method) was recommended to predict long-term camber of a girder due to the uncertainty of erection time after production of a girder, which had the higher accuracy than the simply multipliers.

CHAPTER 6 CONCLUSIONS AND RECOMMENDATIONS

In this chapter, conclusions of this study are presented in Section 6.1, and recommendations of creep and shrinkage tests and prediction of long-term camber of prestressed bridge girders are discussed in Section 6.2.

6.1 Conclusions

In this study, objectives have been completed. It was found that the creep and shrinkage behavior between the measured and five models have large discrepancies. This is one source of error of camber prediction at erection. It was also observed that sealed specimens could represent the behavior of the full scale girders more effectively than unsealed specimens. It was observed that camber of 26 girders investigated in this study calculated by using AASHTO creep and shrinkage model is higher on average 22% than the camber computed by using measured creep and shrinkage values in the sealed specimens.

The IA DOT's current camber prediction method of simple multipliers for camber at release results in large differences with the actual camber at erection due to the uncertainty of time of erection after production, neglect of time-dependent material properties and environmental conditions, and the use of gross rather than transformed section properties. With this current method, camber of long span bulb tee girders is ofent over-predicted by more than 30%. Naaman's Method, which is relatively simple yet accounts for the factors listed above, yields a more accurate camber prediction with ±25% errors with measured camber of girders.

In this study the following conclusions can also be made:

- The errors of modulus of elasticity of concrete are ±20% between the predicted values by using AASHTO model and the measured values;
- AASHTO LRFD 2010 model is the most appropriate model to predict creep and shrinkage of seven groups of concretes for both HPC and NC relative to the rest of four

models investigated, including ACI 209R-90 model, ACI 209R-Modified by Huo model, CEB-FIP 90 model and the B3 model (Bazant). Although AASHTO LRFD 2010 model is better than the rest of four models, large errors exist between measured values and predicted values by using AASHTO model, i.e. under-prediction of sealed creep coefficient and sealed shrinkage on average by 32% and 44% respectively during one year;

- Sealed specimens of concrete represent the behavior of creep and shrinkage of the full scale presressed bridge girder much better than unsealed specimens;
- Results of creep and shrinkage tests from sealed specimens have less standard deviation between four HPC mixes than unsealed specimens, which means the errors of results of creep and shrinkage of sealed specimens are smaller than those of unsealed specimens;
- The camber of 26 girders by gross section properties is on average 13% higher than the camber computed using transformed section properties during one year;
- Average error of the results of camber of girder is within 2% during one year between average creep coefficient and average shrinkage strain and specified sealed creep coefficient and specified shrinkage strain;
- For the prediction of long-term camber of prestressed bridge girders, Naaman's Method is recommended. Both Naaman's Method and the incremental method have the similar results, and the errors between the predicted and the measured values are within ±25%. It is also easier for the calculations to use Naaman's Method than the the incremental method, and both of them yield the better predictions than Tadros's Method;
- The calculated average short-term prestress loss for 26 girders is 7%, and the average long-term prestress loss is 10% at 3-months and 12% at 1-year. Average camber growth for 26 girders is 42% at 3-months and 50% at 1-year;
- Camber of the prestressed girder is more sensitive to the error of prestress forces than modulus of elasticity and creep and shrinkage;
- Conspan typically overestimates camber at erection comparing with results by Naaman's Method. The difference between the camber at erection by Naaman's Method and 70% of camber by Conspan for gross section is within 5%.

6.2 Recommendations

Inaccuracy of prediction of creep and shrinkage by the current approach with no consideration of time-effects results in 31% average errors of camber at erection. This over-estimation of camber of the girder could lead to the increase of cost due to field modification of concrete haunches between the bridge girder and deck. In order to improve the accuracy of the prediction of the long-term camber of prestressed bridge girders, the following recommendations are provided:

- It is acceptable to use AASHTO model to predict modulus of elasticity of concrete according to the corresponding compressive strength and density of concrete;
- In order to obtain more accurate results, creep and shrinkage tests results of concrete using local materials in Iowa should be used;
- Sealed specimens should be used to obtain the similar behavior of creep and shrinkage of the full scale prestressed bridge girder;
- It is acceptable to use average sealed creep coefficient and average sealed shrinkage of four HPC mixes to predict the long-term camber of prestressed bridge girders within one year, and the proposed equations of sealed creep coefficient and sealed shrinkage can be applied to predict the long-term camber after one year;
- For the prediction of the long-term camber of 26 prestressed bridge girders, Naaman's Method is the recommended method comparing with Tadros's Method and the incremental method, and the errors of the prediction of camber are within ±25%;
- Transformed section properties should be utilized for the calculation of the camber of prestressed bridge girders;
- The measurement of prestress forces should be improved by precast plants due to the sensitivity of the camber of the girder to the error of prestress forces. Elongation of each strand should be recorded carefully before and after jacking;
- 70% of camber at erection (typically 3-month after transfer) by Conspan for gross section can be used to estimate the camber of 26 girders at erection.

REFERENCES

AASHTO. (2010). *LRFD Bridge Design Specifications, 5th Edition.* Washington D. C.: American Association of State Highway and Transportation Officials.

ACI 209R. (1992). Prediction of Creep, Shrinkage and Temperature Effects in Concrete Structures.

ACI 209R. (2008). Guide for Modeling and Calculating Shrinkage and Creep in Hardened Concrete.

ACI 232.2R. (1996). Use of fly ash in concrete., (pp. 1-35).

ACI 233R. (2003). Slag Cement in Concrete and Mortar., (pp. 1-19).

ACI 234R. (2006). Guide for the use of silica fume in concrete., (pp. 1-63).

ACI 363R. (1992). State-of-the-Art Report on High-Strength Concrete., (pp. 1-55).

ACI 517. (1963). Low pressure steam curing. *ACI Journal, Proc. 60*, 953-986.

Alexander, M. G. (1996). Aggregates and the Deformation Properties of Concrete. *ACI Materials Journal, Vol. 93*(No. 6), 569-577.

Alfes, C. (1992). Modulus of elasticity and drying shrinkage of high-strength concete containing silica fume. *ACI Proceedings Fourth International Conference: Fly Ash, Silica Fume, Slag, and Natural Pozzolans in Concrete*, *Vol. 2*, pp. 1651-1671. Istanbul, Turkey.

Al-Omaishi, N., & Tadros, M. K. (2009). Elasticity modulus, shrinkage, and creep of high-strength concrete as adopted by AASHTO. *PCI Journal*, 44-63.

ASTM C39. (2004). *Standard test method for compressive strength of cylindrical concrete specimens.* West Conshohocken, PA: American Society of Testing and Materials.

ASTM C512. (2002). *Standard test method for creep of concrete in compression.* West Conshohocken, PA: American Society of Testing and Materials.

ASTM C617. (2009). *Standard practice for capping cylindrical concrete specimens.* West Conshohocken, PA: American Society of Testing and Materials.

Baalbaki, M., Sarker, S. L., & Aitcin, P. C. (1992). Properties and microstructure of high-performance concretes containing silica fume, slag and fly ash. *Fly ash, Silica Fume, Slag, and Natural Pozzolans in Concrete Proceedings Fourth International Conference*, *Vol. 2*, pp. 921-942. Istanbul, Turkey.

Bazant, Z. P. (2000). Creep and shrinkage prediction model for analysis and design of concrete structures: Model B3. *Adam Neville Symposium: Creep and Shrinkage - Structural Design Effects ACI SP-194*, (pp. 1-83). Farmington, Michigan.

Bennett, E. W. (1970, June). Shrinkage and creep of concrete as affected by the fineness of Portland cement. *Mag. Concr. Res., 22*(No. 71).

Bissonnette, B. P. (1999, October). Influence of key parameters on drying shrinkage of cementitious materials. *Cement and Concrete Research, Vol. 29*(No. 10), 1655-1662.

Brooks, J. J. (1989). Influence of mix proportions, plasticizers and superplasticizerson creep and drying shrinkage of concrete. *Magazine of Concrete Research, 41*(No. 148), 14-153.

Brooks, J. J. (1992). Influence of slag type and replacement level on strength, elasticity, shrinkage, and creep of concrete. *ACI Proceedings Fourth International Conference: Fly Ash, Silica Fume, Slag, and Natural Pozzolans in Concrete*, *Vol. 2*, pp. 1325-1341. Istanbul, Turkey.

Brooks, J. J., Wainwright, P. J. and Al-Kaisi, A. F. (1991, March). Compressive and tensile creep of heat-cured ordinary Portland and slag cement concretes. *Magazine of Concrete Research, 43*(No. 154), 1-12.

Bryant, A. H. (1987). Creep, shrinkage-size, and age at loading effects. *ACI Materials Journal, Vol. 84*(No. 2), 117-123.

Buil, M. a. (1985). Creep of Silica Fume Concrete. *Cement and Concrete Research, V. 15*(No. 3), 463-466.

Carlson, R. W. (1937). Drying shrinkage of large concrete members. *ACI Journal, Proceedings, Vol. 33*(No. 3), 327-336.

CEB-FIP Model Code. (1990). Evaluation of the Time Dependent Behavior of Concrete.

Chern, J. C. (1989, July-August). Deformations of concretes made with blast furnace slag cement and ordinary Portland cement. *ACI Materials Journal, 86*(No. 4), 372-382.

Cole, H. A. (2000, Feb.). Direct solution for elastic prestress loss in pretensioned concrte girders. *Practorcal Periodical on Structural Design and Construction*, pp. 27-31.

Davis, R. E. (1931). Flow of concrete under the action of sustained loads. *ACI Journal, Proc. 27*, 410-417.

Davis, R. E. (1934). Plastic flow of concrete under sustained stress. *ASTM, Proc. 34*(Part 2), 354-386.

Ghosh, R. S. (1981, Sept.-Oct.). Creep of Fly Ash Concrete. *ACI Journal, Proceedings V. 78*(No. 5), 351-357.

Glanville, W. H. (1933). Creep of concrete under load. *The Structural Engineer, 11*(No. 2), 54-73.

Glanville, W. H. (1939). *Studies in reinforced concrete-IV: Further investigations on creep or flow of concrete under load.* London: Building Research Techincal.

Glucklich, J. (1968). The effect of microcracking on time-dependent deformations and the long-term strength of concrete. *Intern. Conf. on the Structure of Concrete* (pp. 176-189). London: Cement and Concrete Association.

Gvozdev, A. A. (1966). *Creep of Concrete.* Moscow: Mekhanika Tverdogo Tela.

Hannant, D. J. (1967). Strain behavior of cocnrete up to 95°C under compressive stresses. *Conf. on Prestressed Concrete Pressure Vessels. Paper 17*, pp. 57-71. Institution of Civil Engineers.

Hansen, T. C. (1965). Influence of aggregate properties on concrete shrinkage. *ACI Journal, Proc. 62*, 783-794.

Hansen, T. C. and Mattock A. H. (1966). Influence of size and shape of member on the shrinkage and creep of concrete. *ACI Materials Journal, Proc. 63*(No. 2), 267-290.

Hanson, J. A. (1964). Prestress loss as affected by type of curing. *PCI Journal, No. 9*, 69-93.

Haranki, B. (2009). *Strength, modulus of elasticity, creep and shrinkage of concrete used in Florida.*

Hirsch, T. J. (1962). Modulus of elasticity of concrete affected by elastic moduli of cement paste matrix and aggregate. *ACI Journal, Proc. 59*, 427-451.

Hobbs, D. W. (1974). Influence of aggregate restraint on the shrinkage of concrete. *J. ACI, 71*(No. 9), 445-450.

Hummel, A. V. (1959). des Wasserzementverhaltnisses und des Belastungsalters auf das Kriechen von Beton. *Zement-Kalk-Gips, 12*, 181-187.

Huo, X. S.-O. (2001, December). Creep, shrinkage, and modulus of elasticity of high-performance concrete. *ACI Materials Journal, Vol. 98*(No. 6), 440-449.

Iowa DOT. (2012, 7 23). Retrieved from http://www.iowadot.gov/bridge/standards/english/EnglishBeams.pdf.

Jones, R. S., and Richart, F. E. (1936). The effect of testing speed on strength and elastic properties of concrete. *ASTM, Proc. 36*(Part 2), 380-391.

Keene, P. W. (1960, Jan.). The effect of air-entrainment on the shrinkage of concrete stored in laboratory air. *Cement Concr. Assoc. Tech. Report TRA/331*.

Keeton, J. R. (1960). Time-dependent deformations of plain concrete. *Highway Research Board, Proc. 39*, 310-335.

Khan, A. A., & Cook, W. D. (1997). Creep, shrinkage, and thermal strains in normal, medium and high-strength concretes during hydration. *ACI Materials Journal, Vol. 94*(No. 2), 156-163.

Khatri, R. P., and Sirivivatnanon. (1995). Efeect of Different Supplimentary Cementitious Materials on Mechanical Properties of High Performance Concrete. *Cement and Concrete Research, V. 25*(No. 1), 209-220.

Khayat, K. H. (2009). *Self-consolidating concrete for precast, prestressed concrete bridge elements.* Transportation Research Board of the National Academies.

Kordina, K. (1960). Experiments on the influence of the mineralogical character of aggregates on the creep of concrete. *RILEM Bulletin, No. 6*, 7-22.

Kosmatka, S. H. (2008). *Design and control of concrete mixtures.* Skokie, Illinois.

L' Hermite, R. G. (1960). Volume changes of concrete. *Int. Symp. on the Chemistry of Cement*, *Proc. 4*, pp. 659-94. Washington D. C.

L' Hermite, R. G. (1968). Further results of shrinkage and creep tests. *Intern. Conf. on the Structure of Concrete* (pp. 423-433). London: Cement and Concrete Association.

Lane, R. O. (1982, July). Properties and Use of Fly Ash in Portland Cement Concrete. *Concrete International: Design & Construction, V. 4*(No. 7), 81-92.

Lim, S. N. (2000). Autogenous shrinkage of ground-granulated blast furnace slag concrete. *ACI Materials Journal, Vol. 97*(No. 5), 587-593.

Lorman, W. R. (1940). The theory of of concrete creep. *ASTM, Proc. 40*, 1082-1102.

Malhotra, V. M., H., Z. M., & Read, P. H. (2000). Long-term mechanical properties and durability characteristics of high-strength/high-performance cocnrete incorporating supplementary cementing materials under ourdoor exposure conditions. *ACI Materials Journal, Vol. 97*(No. 5), 518-525.

Martinez, S. N. (1982). *Spirally-Reinforced High-strength Concrete Columns.* Cornell University, Department of Structural Engineering, Ithaca.

Mazloom, M. R. (2004). Effect of silica fume on mechanical properties of high-strength concrete. *Cement & Concrete Composites, 26*, 347-357.

Muller, H. S. and Pristl, M. (1993). Creep and shrinkage of concrete at variable ambient conditions, in creep and shrinkage of concrete. *Proceedings of the Fifth International RILEM Symposium, Z. P. Bazant and I. Carol, eds.* London: E&FN Spon.

Naaman, A. E. (2004). *Prestressed Concrete Analysis and Design: Fundamentals* (2nd Edition ed.). Ann Arbor, Michigan: Techno Press 3000.

Nagataki, S. a. (1978). Studies of the volume of changes of high strength concretes with superplasticizer. *Journal, V. 20*, 26-33.

Naik, T. R. (2007). Shrinkage of cocnrete with and without fly ash. *ACI International Conference on Fly Ash, Silica Fume, Slag, and Natural Pozzolans in Concrete.* Poland.

Nasser, K. W. and Neville, A. M. (1965). Creep of concrete at elevated temperatures. *ACI Journal, Proc. 62*, 1567-1579.

Neville, A. M. (1958). The effect of warm storage conditions on the strength of concrete made with high-alumina cement. *Proc. ICE, No. 10*, 185-192.

Neville, A. M. (1963). A study of deterioration of structural concrete made with high-alumina cement. *Proc. ICE, No. 25*, 287-324.

Neville, A. M. (1970). *Creep of Concrete: Plain, Reinforced, and Prestressed.* New York City: North-Holland Publishing Company-Amsterdam American Elsevier Publishing Company.

Neville, A. M. (1975). Time-dependent behavior of Cemsave concrete. *Concrete, 9*(No. 3), 36-39.

Neville, A. M. (1981). *Properties of Concrete.* London: Pitman Publishing Limited.

Neville, A. M. (1997). Aggregate bond and modulus of elasticity of concrete. *ACI Materials Journal, Vol. 94*(No. 1), 71-74.

Ngataki, S. a. (1978). Studies of the volume changes of high strength concretes with superplasticizer. *Journal, Vol. 20*, 26-33.

Nishiyama, M. (2009, June). Mechanical properties of concrete and reinforcement - State-of-the-art Report on HSC and HSS in Japan. *Journal of Advanced Concrete Technology, Vol. 7*(No. 2), 152-182.

ODman, S. T. (1968). Effects of variations in volume, surface area exposed to drying, and composition of concrete on shrinkage. *RILEM/CEMBUREAU Int. Colloquium on the Shrinkage of Hydraulic Concretes*, *1*, p. 20. Madrid.

O'Neill, Cullen; French, Catherine E. (2012). *Validation of Prestressed Concrete I-Beam Camber and Camber Estimates.* University of Minnesota, Department of Civil Engineering.

Persson, B. (1998). Experimental studies on shrinkage of high-performance concrete. *Cement and Concrete Research, Vol. 28*(No. 7), 1023-1036.

Pickett, G. (1956). Effect of aggregate on shrinkage of concrete and hypothesis concerning shirnkage. *ACI Journal, No. 52*, 581-90.

Polivka, M. P. (1964). Studies of creep in mass concrete. *Paper 12, Symp. on Mass Concrete, ACI Special Publication, No.6*, 30.

Rizkalla, Sami; Zia, Paul; Storm, Tyler. (2011). *Predicting Camber, Camber, and Prestress Losses in Prestressed Concrete Members.* North Corolina State University.

Rosa, Michael A.; Stanton, Jonh F.; Eberhard, Marc O. (2007). *Improving Predictions for Camber in Precast, Prestressed Concrete Bridge Girders.* University of Washington, Washington State Transportation Center (TRAC).

Roy, R. l. (1993). Creep and shrinkage of high-strength concrete. *Proceedings of the Fifth International RILEM Symposium* (pp. 500-508). Barcelona: E&FN Spon, London.

Sakai, K. W. (1992). Properties of granulated blast-furnace slag cement concrete. *ACI Proceedings Fourth International Conference: Fly Ash, Silica Fume, Slag, and Natural Pozzolans in Concrete*, *Vol. 2*, pp. 1367-1383. Istanbul, Turkey.

Saric-Coric, M. a. (2003). Influence of curing conditions on shrinkage of blended cements containing various amounts of slag. *ACI Materials Journal, Vol. 100*(No. 6), 477-484.

Saucier, K. (1984). High-strength Concrete for Peacekeeper Facilities. *Miscellaneous Paper SL-84-3*, 60. Vicksburg, Miss.: U.S. Army Engineer Waterways Experiment Station.

Schindler, A. K. (2007). Properties of self-consolidating concrete for prestressed members. *ACI Materials Journal, Vol. 104*(No. 1), 53-61.

Soroka, I. (1979). Portland Cement Paste and Concrete Macmillan Press Ltd.

Swamy, R. N. (1986). *Cement Replacement Materials.* London: Surrey University Press.

Swayze, M. A. (1960). Discussion on: Volume changes of concrete. *Proc. 4th Int. Symp. on the Chemistry of Cement*, (pp. 700-2). Washington D. C.

Tadros, M. K. (2011). Precast, prestressed girder camber variability. *PCI Journal*, 135-154.

Tadros, M. K. and Al-Omaishi, N. (2003). *Prestressed losses in pretensioned high-strength concrete bridge girders.* Washington D. C.: Transportation Research Board.

Tazawa, E. A. (1989). Drying shrinkage and creep of concrete containing granulated blast furnace slag. *Proceedings Third International Conference: Fly Ash, Silica Fume, Slag, and Natural Pozzolans in Concrete*, *Vol. 2*, pp. 1325-1343. Trondheim, Norway.

Tazawa, E. and Miyazawa, S. (1993). Autogenous shrinkage of concrete and its importance in concrete technology. *Proceedings of Fifth International RILEM Symposium* (pp. 159-168). Barcelona: E&FN Spon, London.

Tazawa, E. and Miyazawa, S. (1997). Study on the prediciton of autogenous shrinkage. *Proceedings of JSCE, 571/V-36*, 211-219.

Townsend, B. D. (2003). *Creep and shrinkage of a high strength concrete mixture.* Blacksburg, VA.

Troxell, G. E. (1958). Long-time creep and shrinkage tests of plain and reinforced concrete. *ASTM, Proc. 58*, 1101-1120.

U.S. Army Engineer Waterways Experiment Station. (1958, Jan.). Investigation of creep in concrete; creep of mass concrete. *Corps of Engineers, Paper No. 6-132, Report No. 3*. Vicksburg, Miss., United States.

Wainwright, P. J. (2000). The influence of ground granulated blast furnace slag (GGBS) additions and time delay on the bleeding of concrete. *Cement and Concrete Composites, Vol. 22*(No. 4), 253-257.

Wang, K. J., Schlorholtz, S. M., Sritharan, S., Seneviratne, H., Wang, X. Hou, Q. Z. (2013). *Investigation into shrinkage of high performance concrete used for Iowa bridge decks and overlays.*

Yashin, A. V. (1959). Creep of young concrete. In A. A. Gvozdev, *Investigation of properties of concrete and reinforced concrete construction* (pp. 18-73). Moscow: Gosudarstviennoye Izdatielstvo Literaturi po Stroitielstvu.

Yildirim, H. a. (2011). Modulus of elasticity of substandard and normal concretes. *Construction and Building Materials, Vol. 25*, 1645-1652.

Yuan, R. L, and Cook, J. E. (1983). Study of Class C Fly Ash Concrete. *Fly Ash, Silica Fume, Slag and Other Mineral By-Products in Concrete, SP-79*, pp. 307-319.

APPENDIX A

Photographs

Figure A.1. Sulfur-capped sealed and unsealed specimens

Figure A.2. Compressive strength test of a cylindrical specimen

Figure A.3. Loaded specimens for creep tests in the environmentally controlled chamber

Figure A.4. Unloaded specimens for shrinkage tests in the environmentally controlled chamber

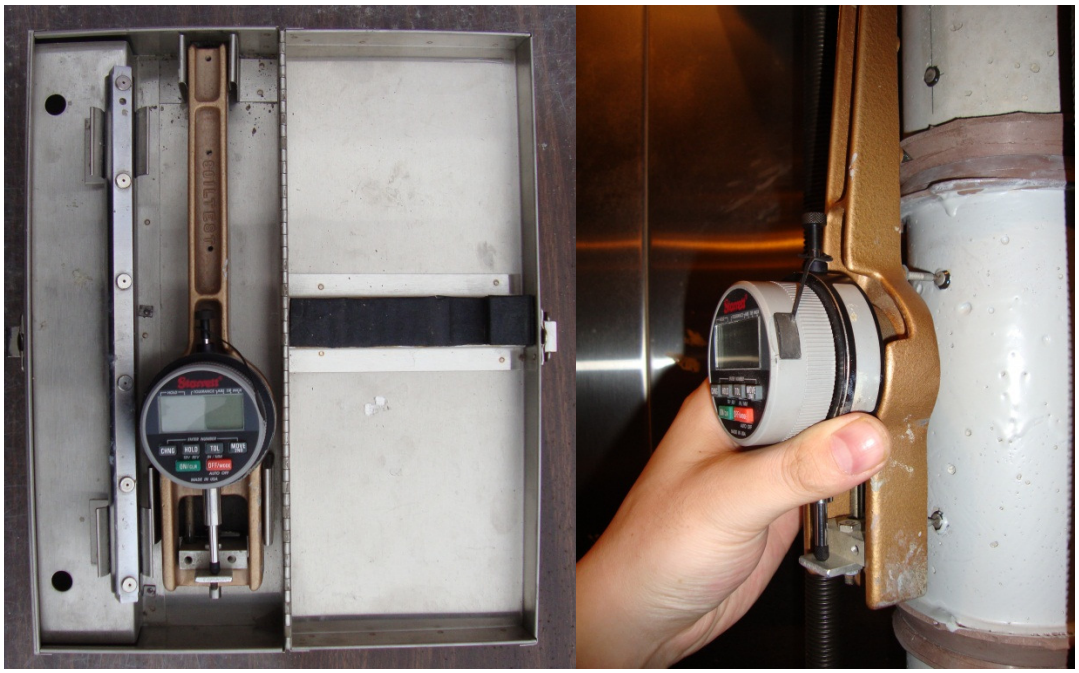

Figure A.5. Device and Measurement of strain by using the DEMEC gage

Figure A.6. Debonded 4-ft BTB Beam section stored in precast plant A

Figure A.7. A Type D 60 prestressed bridge girder stored in precast plant C

Figure A.8. Support of a Type D 60 prestressed bridge girder stored in precast plant C

APPENDIX B

Comparison of Measured Results of Creep and Shrinkage Tests and Five Models

Table B.1. Comparison of measured unsealed creep coefficient with five models for HPC 1

Time after Loading, days	Measured Creep Coefficient	AASHTO LRFD 2010	ACI 209R-1990	ACI 209R-Modified by Huo	CEB-FIP 90	Bazant B3
0	0.00000	0.00000	0.00000	0.00000	0.00000	0.00000
0	0.00000	0.00000	0.00000	0.00000	0.00000	0.00000
1	0.04613	0.05241	0.31131	0.31216	0.80745	1.07852
2	0.09829	0.10190	0.45072	0.44646	0.83970	1.11907
3	0.13338	0.14870	0.55475	0.54455	0.86912	1.15609
7	0.21138	0.31300	0.83292	0.79838	0.96702	1.27985
14	0.29875	0.53445	1.12176	1.04960	1.09369	1.44298
21	0.35857	0.69938	1.31231	1.20889	1.18953	1.57035
28	0.41839	0.82700	1.45454	1.32460	1.26720	1.67688
60	0.60306	1.16798	1.84379	1.62816	1.50709	2.02647
90	0.62695	1.32764	2.04791	1.78011	1.64940	2.24439
120	0.64573	1.42504	2.18729	1.88116	1.75302	2.40274
150	0.66325	1.49066	2.29101	1.95498	1.83326	2.52214
180	0.68093	1.53787	2.37237	2.01208	1.89783	2.61470
210	0.70615	1.57346	2.43855	2.05802	1.95122	2.68818
240	0.72343	1.60125	2.49383	2.09605	1.99627	2.74774
270	0.74416	1.62356	2.54094	2.12821	2.03488	2.79696
300	0.78917	1.64186	2.58174	2.15589	2.06841	2.83834
330	0.78859	1.65714	2.61754	2.18003	2.09783	2.87366
360	0.78800	1.67009	2.64929	2.20134	2.12388	2.90425

Table B.2. Comparison of measured sealed creep coefficient with five models for HPC 1

Time after Loading, days	Measured Creep Coefficient	AASHTO LRFD 2010	ACI 209R-1990	ACI 209R-Modified by Huo	CEB-FIP 90	Bazant B3
0	0.00000	0.00000	0.00000	0.00000	0.00000	0.00000
0	0.00000	0.00000	0.00000	0.00000	0.00000	0.00000
1	0.17186	0.02601	0.09485	0.09511	0.27535	0.85135
2	0.20138	0.05058	0.13733	0.13603	0.28654	0.87873
3	0.25699	0.07380	0.16902	0.16591	0.29679	0.90322
7	0.38265	0.15535	0.25377	0.24325	0.33114	0.98144
14	0.48378	0.26527	0.34178	0.31979	0.37630	1.07570
21	0.52042	0.34713	0.39984	0.36832	0.41119	1.14258
28	0.55707	0.41047	0.44317	0.40358	0.44003	1.19446
60	0.76635	0.57972	0.56176	0.49607	0.53359	1.34541
90	0.84151	0.65897	0.62396	0.54236	0.59368	1.43143
120	0.88788	0.70731	0.66642	0.57315	0.64056	1.49408
150	0.92430	0.73988	0.69802	0.59564	0.67921	1.54338
180	0.94038	0.76331	0.72281	0.61304	0.71216	1.58403
210	0.95341	0.78098	0.74298	0.62704	0.74091	1.61862
240	0.95564	0.79477	0.75982	0.63862	0.76639	1.64872
270	0.95299	0.80584	0.77417	0.64842	0.78926	1.67537
300	0.98059	0.81492	0.78660	0.65685	0.81000	1.69927
330	1.00290	0.82251	0.79751	0.66421	0.82894	1.72095
360	1.02522	0.82894	0.80718	0.67070	0.84636	1.74077

Table B.3. Comparison of measured unsealed shrinkage with five models for HPC 1

Time after Loading, days	Measured Shrinkage	AASHTO LRFD 2010	ACI 209R-1990	ACI 209R-Modified by Huo	CEB-FIP 90	Bazant B3
0	0	0	0	0	0	0
0	0	0	0	0	0	0
1	98	15	8	15	147	152
2	163	30	17	29	156	162
3	166	43	24	41	165	172
7	219	91	53	84	194	207
14	276	155	96	136	232	255
21	285	203	131	171	262	292
28	295	239	159	197	285	322
60	319	338	247	260	353	414
90	353	384	293	287	390	462
120	373	413	324	302	414	493
150	392	432	346	312	431	513
180	414	445	362	319	444	528
210	433	456	374	325	455	538
240	443	464	384	329	463	546
270	453	470	393	332	469	551
300	500	475	399	335	475	556
330	538	480	405	337	480	559
360	576	484	410	339	484	562

Table B.4. Comparison of measured sealed shrinkage with five models for HPC 1

Time after Loading, days	Measured Shrinkage	AASHTO LRFD 2010	ACI 209R-1990	ACI 209R-Modified by Huo	CEB-FIP 90	Bazant B3
0	0	0	\	\	\	0
0	0	0	\	\	\	0
1	31	5	\	\	\	23
2	62	10	\	\	\	24
3	59	15	\	\	\	26
7	74	32	\	\	\	31
14	101	54	\	\	\	38
21	115	71	\	\	\	43
28	129	84	\	\	\	47
60	151	118	\	\	\	59
90	171	134	\	\	\	65
120	180	144	\	\	\	68
150	187	151	\	\	\	70
180	188	156	\	\	\	72
210	192	159	\	\	\	73
240	197	162	\	\	\	73
270	205	164	\	\	\	74
300	213	166	\	\	\	74
330	214	168	\	\	\	75
360	214	169	\	\	\	75

Table B.5. Comparison of measured unsealed creep coefficient with five models for HPC 2

Time after Loading, days	Measured Creep Coefficient	AASHTO LRFD 2010	ACI 209R-1990	ACI 209R-Modified by Huo	CEB-FIP 90	Bazant B3
0	0.00000	0.00000	0.00000	0.00000	0.00000	0.00000
0	0.00000	0.00000	0.00000	0.00000	0.00000	0.00000
1	0.10519	0.05303	0.31131	0.31199	0.84775	0.86016
2	0.13924	0.10326	0.45072	0.44734	0.88160	0.89415
3	0.20651	0.15092	0.55475	0.54664	0.91249	0.92510
7	0.36018	0.31940	0.83292	0.80532	1.01528	1.02785
14	0.57533	0.54939	1.12176	1.06382	1.14826	1.16162
21	0.72104	0.72291	1.31231	1.22901	1.24889	1.26481
28	0.80130	0.85847	1.45454	1.34965	1.33043	1.35035
60	0.86230	1.22646	1.84379	1.66871	1.58230	1.62743
90	0.88825	1.40171	2.04791	1.82982	1.73171	1.79863
120	0.93161	1.50957	2.18729	1.93750	1.84050	1.92306
150	0.96715	1.58263	2.29101	2.01642	1.92474	2.01727
180	0.99976	1.63540	2.37237	2.07764	1.99253	2.09076
210	1.03922	1.67530	2.43855	2.12698	2.04859	2.14953
240	1.07995	1.70652	2.49383	2.16789	2.09588	2.19757
270	1.10826	1.73163	2.54094	2.20254	2.13643	2.23759
300	1.17376	1.75225	2.58174	2.23239	2.17163	2.27152
330	1.21172	1.76949	2.61754	2.25846	2.20252	2.30073
360	1.26346	1.78411	2.64929	2.28149	2.22986	2.32622

Table B.6. Comparison of measured sealed creep coefficient with five models for HPC 2

Time after Loading, days	Measured Creep Coefficient	AASHTO LRFD 2010	ACI 209R-1990	ACI 209R-Modified by Huo	CEB-FIP 90	Bazant B3
0	0.00000	0.00000	0.00000	0.00000	0.00000	0.00000
0	0.00000	0.00000	0.00000	0.00000	0.00000	0.00000
1	0.20649	0.02632	0.09485	0.09506	0.28909	0.69856
2	0.27289	0.05125	0.13733	0.13629	0.30084	0.72319
3	0.42961	0.07491	0.16902	0.16655	0.31160	0.74522
7	0.55016	0.15853	0.25377	0.24536	0.34767	0.81558
14	0.71894	0.27269	0.34178	0.32412	0.39508	0.90036
21	0.82920	0.35881	0.39984	0.37446	0.43171	0.96052
28	0.88609	0.42610	0.44317	0.41121	0.46198	1.00718
60	0.99837	0.60875	0.56176	0.50842	0.56022	1.14296
90	1.03454	0.69573	0.62396	0.55751	0.62331	1.22033
120	1.05018	0.74926	0.66642	0.59032	0.67252	1.27668
150	1.06514	0.78553	0.69802	0.61436	0.71310	1.32102
180	1.08155	0.81172	0.72281	0.63301	0.74770	1.35759
210	1.10117	0.83152	0.74298	0.64805	0.77788	1.38870
240	1.12276	0.84702	0.75982	0.66051	0.80463	1.41578
270	1.13770	0.85948	0.77417	0.67107	0.82865	1.43974
300	1.13435	0.86971	0.78660	0.68016	0.85042	1.46125
330	1.15021	0.87827	0.79751	0.68811	0.87030	1.48074
360	1.15647	0.88553	0.80718	0.69512	0.88859	1.49857

Table B.7. Comparison of measured unsealed shrinkage with five models for HPC 2

Time after Loading, days	Measured Shrinkage	AASHTO LRFD 2010	ACI 209R-1990	ACI 209R-Modified by Huo	CEB-FIP 90	Bazant B3
0	0	0	0	0	0	0
0	0	0	0	0	0	0
1	51	15	10	17	163	162
2	76	30	19	32	174	174
3	125	44	28	47	183	185
7	132	92	61	95	216	222
14	142	159	110	156	259	273
21	150	209	150	199	291	312
28	157	249	183	230	317	345
60	216	355	284	308	393	442
90	254	406	338	341	434	494
120	287	437	373	361	461	527
150	319	458	398	374	480	549
180	344	474	417	383	494	564
210	366	485	431	390	506	576
240	383	494	442	395	515	584
270	396	501	452	400	522	590
300	404	507	460	403	529	594
330	418	512	466	406	534	598
360	429	517	472	408	539	601

Table B.8. Comparison of measured sealed shrinkage with five models for HPC 2

Time after Loading, days	Measured Shrinkage	AASHTO LRFD 2010	ACI 209R-1990	ACI 209R-Modified by Huo	CEB-FIP 90	Bazant B3
0	0	0	\	\	\	0
0	0	0	\	\	\	0
1	20	5	\	\	\	24
2	30	10	\	\	\	26
3	46	15	\	\	\	28
7	50	32	\	\	\	33
14	54	56	\	\	\	40
21	61	73	\	\	\	46
28	68	87	\	\	\	50
60	131	124	\	\	\	63
90	185	142	\	\	\	69
120	216	153	\	\	\	73
150	245	160	\	\	\	75
180	260	166	\	\	\	77
210	269	170	\	\	\	78
240	279	173	\	\	\	79
270	290	175	\	\	\	79
300	302	177	\	\	\	79
330	313	179	\	\	\	80
360	324	181	\	\	\	80

Table B.9. Comparison of measured unsealed creep coefficient with five models for HPC 3

Time after Loading, days	Measured Creep Coefficient	AASHTO LRFD 2010	ACI 209R-1990	ACI 209R-Modified by Huo	CEB-FIP 90	Bazant B3
0	0.00000	0.00000	0.00000	0.00000	0.00000	0.00000
0	0.00000	0.00000	0.00000	0.00000	0.00000	0.00000
1	0.07272	0.05495	0.31131	0.31177	0.91166	0.99677
2	0.30072	0.10725	0.45072	0.44839	0.94807	1.03315
3	0.30802	0.15708	0.55475	0.54915	0.98128	1.06643
7	0.35181	0.33487	0.83292	0.81376	1.09182	1.17809
14	0.35113	0.58183	1.12176	1.08130	1.23483	1.32623
21	0.35019	0.77148	1.31231	1.25393	1.34305	1.44255
28	0.34897	0.92170	1.45454	1.38082	1.43074	1.54016
60	0.35959	1.33880	1.84379	1.71983	1.70159	1.86109
90	0.37776	1.54238	2.04791	1.89293	1.86226	2.06017
120	0.37773	1.66929	2.18729	2.00934	1.97926	2.20363
150	0.37764	1.75599	2.29101	2.09504	2.06985	2.31088
180	0.37749	1.81897	2.37237	2.16172	2.14275	2.39337
210	0.38106	1.86679	2.43855	2.21561	2.20304	2.45840
240	0.40511	1.90434	2.49383	2.26038	2.25390	2.51080
270	0.42800	1.93461	2.54094	2.29837	2.29750	2.55388
300	0.45176	1.95953	2.58174	2.33115	2.33535	2.58995
330	0.47493	1.98039	2.61754	2.35981	2.36857	2.62064
360	0.49840	1.99813	2.64929	2.38516	2.39798	2.64715

Table B.10. Comparison of measured sealed creep coefficient with five models for HPC 3

Time after Loading, days	Measured Creep Coefficient	AASHTO LRFD 2010	ACI 209R-1990	ACI 209R-Modified by Huo	CEB-FIP 90	Bazant B3
0	0.00000	0.00000	0.00000	0.00000	0.00000	0.00000
0	0.00000	0.00000	0.00000	0.00000	0.00000	0.00000
1	0.15996	0.02728	0.09485	0.09499	0.31088	0.77902
2	0.36042	0.05323	0.13733	0.13662	0.32352	0.80268
3	0.38626	0.07796	0.16902	0.16732	0.33509	0.82385
7	0.54134	0.16621	0.25377	0.24794	0.37388	0.89146
14	0.56266	0.28879	0.34178	0.32945	0.42487	0.97292
21	0.59250	0.38292	0.39984	0.38205	0.46425	1.03072
28	0.63087	0.45748	0.44317	0.42071	0.49681	1.07556
60	0.68287	0.66451	0.56176	0.52400	0.60245	1.20603
90	0.73522	0.76555	0.62396	0.57674	0.67030	1.28037
120	0.75161	0.82854	0.66642	0.61221	0.72322	1.33451
150	0.78198	0.87157	0.69802	0.63831	0.76686	1.37712
180	0.81697	0.90283	0.72281	0.65863	0.80407	1.41225
210	0.84013	0.92657	0.74298	0.67505	0.83652	1.44215
240	0.84229	0.94521	0.75982	0.68869	0.86530	1.46817
270	0.87278	0.96023	0.77417	0.70027	0.89112	1.49120
300	0.88203	0.97260	0.78660	0.71025	0.91453	1.51186
330	0.90544	0.98295	0.79751	0.71899	0.93592	1.53059
360	0.92176	0.99176	0.80718	0.72671	0.95558	1.54772

Table B.11. Comparison of measured unsealed shrinkage with five models for HPC 3

Time after Loading, days	Measured Shrinkage	AASHTO LRFD 2010	ACI 209R-1990	ACI 209R-Modified by Huo	CEB-FIP 90	Bazant B3
0	0	0	0	0	0	0
0	0	0	0	0	0	0
1	105	16	8	14	185	172
2	147	31	17	27	197	184
3	164	45	24	39	208	195
7	265	97	53	81	245	234
14	277	168	96	135	293	288
21	295	223	130	174	330	329
28	317	267	159	202	360	363
60	351	388	246	276	446	464
90	404	447	293	308	492	517
120	418	483	323	328	522	550
150	445	508	345	341	544	572
180	465	527	361	350	561	587
210	478	541	373	357	574	598
240	486	551	383	362	584	606
270	500	560	392	366	592	612
300	509	567	398	369	600	617
330	522	573	404	372	606	620
360	533	579	409	375	611	623

Table B.12. Comparison of measured sealed shrinkage with five models for HPC 3

Time after Loading, days	Measured Shrinkage	AASHTO LRFD 2010	ACI 209R-1990	ACI 209R-Modified by Huo	CEB-FIP 90	Bazant B3
0	0	0	\	\	\	0
0	0	0	\	\	\	0
1	36	6	\	\	\	26
2	73	11	\	\	\	28
3	90	16	\	\	\	29
7	195	34	\	\	\	35
14	214	59	\	\	\	43
21	242	78	\	\	\	48
28	277	93	\	\	\	53
60	311	136	\	\	\	66
90	344	156	\	\	\	72
120	352	169	\	\	\	76
150	365	178	\	\	\	78
180	373	184	\	\	\	80
210	381	189	\	\	\	81
240	389	193	\	\	\	81
270	392	196	\	\	\	82
300	399	198	\	\	\	82
330	404	201	\	\	\	83
360	410	202	\	\	\	83

Table B.13. Comparison of measured unsealed creep coefficient with five models for HPC 4

Time after Loading, days	Measured Creep Coefficient	AASHTO LRFD 2010	ACI 209R-1990	ACI 209R-Modified by Huo	CEB-FIP 90	Bazant B3
0	0.00000	0.00000	0.00000	0.00000	0.00000	0.00000
0	0.00019	0.00000	0.00000	0.00000	0.00000	0.00000
1	0.20137	0.05253	0.31131	0.31209	0.82307	1.05867
2	0.22125	0.10218	0.45072	0.44682	0.85594	1.09912
3	0.24892	0.14917	0.55475	0.54542	0.88593	1.13611
7	0.37690	0.31446	0.83292	0.80125	0.98573	1.26014
14	0.49110	0.53804	1.12176	1.05547	1.11485	1.42453
21	0.57438	0.70516	1.31231	1.21718	1.21254	1.55357
28	0.60676	0.83481	1.45454	1.33491	1.29171	1.66190
60	0.71138	1.18274	1.84379	1.64479	1.53625	2.01925
90	0.78334	1.34641	2.04791	1.80047	1.68131	2.24267
120	0.81742	1.44649	2.18729	1.90421	1.78694	2.40491
150	0.83024	1.51401	2.29101	1.98009	1.86872	2.52697
180	0.83552	1.56264	2.37237	2.03885	1.93455	2.62131
210	0.84156	1.59934	2.43855	2.08617	1.98897	2.69594
240	0.86018	1.62801	2.49383	2.12536	2.03489	2.75622
270	0.88508	1.65103	2.54094	2.15853	2.07425	2.80584
300	0.90160	1.66992	2.58174	2.18708	2.10843	2.84741
330	0.91603	1.68570	2.61754	2.21200	2.13842	2.88277
360	0.93464	1.69908	2.64929	2.23400	2.16497	2.91329

Table B.14. Comparison of measured sealed creep coefficient with five models for HPC 4

Time after Loading, days	Measured Creep Coefficient	AASHTO LRFD 2010	ACI 209R-1990	ACI 209R-Modified by Huo	CEB-FIP 90	Bazant B3
0	0.00000	0.00000	0.00000	0.00000	0.00000	0.00000
0	0.00038	0.00000	0.00000	0.00000	0.00000	0.00000
1	0.21487	0.02607	0.09485	0.09509	0.28067	0.81653
2	0.24085	0.05071	0.13733	0.13614	0.29209	0.84295
3	0.26184	0.07404	0.16902	0.16618	0.30253	0.86658
7	0.35891	0.15608	0.25377	0.24412	0.33755	0.94203
14	0.54802	0.26705	0.34178	0.32158	0.38358	1.03297
21	0.61062	0.35000	0.39984	0.37085	0.41914	1.09748
28	0.63966	0.41435	0.44317	0.40672	0.44854	1.14752
60	0.74767	0.58704	0.56176	0.50113	0.54391	1.29315
90	0.81871	0.66828	0.62396	0.54856	0.60517	1.37613
120	0.86035	0.71795	0.66642	0.58017	0.65295	1.43656
150	0.87970	0.75147	0.69802	0.60329	0.69235	1.48412
180	0.88930	0.77561	0.72281	0.62120	0.72594	1.52333
210	0.89390	0.79382	0.74298	0.63561	0.75524	1.55670
240	0.92817	0.80805	0.75982	0.64755	0.78122	1.58574
270	0.97726	0.81948	0.77417	0.65766	0.80453	1.61145
300	1.00658	0.82885	0.78660	0.66636	0.82567	1.63451
330	1.03095	0.83669	0.79751	0.67395	0.84498	1.65542
360	1.06521	0.84333	0.80718	0.68065	0.86273	1.67454

Table B.15. Comparison of measured unsealed shrinkage with five models for HPC 4

Time after Loading, days	Measured Shrinkage	AASHTO LRFD 2010	ACI 209R-1990	ACI 209R-Modified by Huo	CEB-FIP 90	Bazant B3
0	0	0	0	0	0	0
0	0	0	0	0	0	0
1	22	15	10	17	153	152
2	33	30	19	32	163	162
3	51	43	28	46	172	172
7	133	91	60	94	203	207
14	229	156	108	153	243	255
21	286	204	147	194	274	292
28	293	242	180	223	298	322
60	296	342	278	296	369	413
90	306	390	330	327	407	461
120	312	419	365	346	433	492
150	319	438	389	357	451	512
180	330	452	408	366	465	526
210	341	463	422	372	475	537
240	344	471	433	377	484	544
270	342	478	442	381	491	550
300	345	484	450	384	497	554
330	351	488	456	386	502	558
360	353	492	462	389	506	560

Table B.16. Comparison of measured sealed shrinkage with five models for HPC 4

Time after Loading, days	Measured Shrinkage	AASHTO LRFD 2010	ACI 209R-1990	ACI 209R-Modified by Huo	CEB-FIP 90	Bazant B3
0	0	0	\	\	\	0
0	0	0	\	\	\	0
1	17	5	\	\	\	23
2	26	10	\	\	\	24
3	40	15	\	\	\	26
7	103	32	\	\	\	31
14	160	54	\	\	\	38
21	212	71	\	\	\	43
28	220	85	\	\	\	47
60	225	120	\	\	\	59
90	229	136	\	\	\	65
120	235	146	\	\	\	68
150	244	153	\	\	\	70
180	251	158	\	\	\	72
210	259	162	\	\	\	73
240	260	165	\	\	\	73
270	257	167	\	\	\	74
300	259	169	\	\	\	74
330	262	171	\	\	\	74
360	263	172	\	\	\	75

Table B.17. Comparison of measured unsealed creep coefficient with five models for NC 1

Time after Loading, days	Measured Creep Coefficient	AASHTO LRFD 2010	ACI 209R-1990	ACI 209R-Modified by Huo	CEB-FIP 90	Bazant B3
0	0.00000	0.00000	0.00000	0.00000	0.00000	0.00000
0	0.00000	0.00000	0.00000	0.00000	0.00000	0.00000
1	0.06025	0.05442	0.34279	0.31492	0.80745	1.18566
2	0.09649	0.10487	0.49631	0.45039	0.83970	1.23657
3	0.13272	0.15177	0.61086	0.54935	0.86912	1.28289
7	0.21936	0.31040	0.91717	0.80542	0.96702	1.43652
14	0.25714	0.51049	1.23522	1.05886	1.09369	1.63600
21	0.28914	0.65019	1.44505	1.21955	1.18953	1.78938
28	0.30834	0.75326	1.60166	1.33628	1.26720	1.91609
60	0.49544	1.00925	2.03028	1.64252	1.50709	2.32313
90	0.59498	1.12029	2.25505	1.79580	1.64940	2.57133
120	0.69625	1.18551	2.40853	1.89775	1.75302	2.74997
150	0.77192	1.22842	2.52273	1.97221	1.83326	2.88433
180	0.80871	1.25879	2.61232	2.02982	1.89783	2.98874
210	0.83287	1.28142	2.68520	2.07617	1.95122	3.07211
240	0.83909	1.29893	2.74607	2.11453	1.99627	3.14028
270	0.83635	1.31289	2.79794	2.14698	2.03488	3.19717
300	0.84556	1.32428	2.84287	2.17490	2.06841	3.24554
330	0.85776	1.33374	2.88229	2.19926	2.09783	3.28731
360	0.86399	1.34173	2.91726	2.22075	2.12388	3.32391

Table B.18. Comparison of measured sealed creep coefficient with five models for NC 1

Time after Loading, days	Measured Creep Coefficient	AASHTO LRFD 2010	ACI 209R-1990	ACI 209R-Modified by Huo	CEB-FIP 90	Bazant B3
0	0.00000	0.00000	0.00000	0.00000	0.00000	0.00000
0	0.00000	0.00000	0.00000	0.00000	0.00000	0.00000
1	0.03997	0.02701	0.10444	0.09595	0.27535	0.95653
2	0.08978	0.05205	0.15122	0.13723	0.28654	0.99401
3	0.13959	0.07533	0.18612	0.16738	0.29679	1.02755
7	0.26657	0.15407	0.27944	0.24539	0.33114	1.13463
14	0.33955	0.25338	0.37635	0.32261	0.37630	1.26367
21	0.36494	0.32272	0.44028	0.37157	0.41119	1.35523
28	0.38016	0.37388	0.48799	0.40714	0.44003	1.42625
60	0.51619	0.50093	0.61858	0.50044	0.53359	1.63291
90	0.55266	0.55605	0.68707	0.54714	0.59368	1.75067
120	0.56393	0.58842	0.73383	0.57820	0.64056	1.83643
150	0.56711	0.60972	0.76862	0.60089	0.67921	1.90392
180	0.57925	0.62479	0.79592	0.61845	0.71216	1.95957
210	0.59197	0.63602	0.81812	0.63257	0.74091	2.00693
240	0.59922	0.64472	0.83667	0.64425	0.76639	2.04814
270	0.60374	0.65164	0.85248	0.65414	0.78926	2.08462
300	0.61190	0.65729	0.86616	0.66265	0.81000	2.11735
330	0.62097	0.66199	0.87818	0.67007	0.82894	2.14702
360	0.62822	0.66596	0.88883	0.67662	0.84636	2.17416

Table B.19. Comparison of measured unsealed shrinkage with five models for NC 1

Time after Loading, days	Measured Shrinkage	AASHTO LRFD 2010	ACI 209R-1990	ACI 209R-Modified by Huo	CEB-FIP 90	Bazant B3
0	0	0	0	0	0	0
0	0	0	0	0	0	0
1	0	16	8	14	117	156
2	40	30	17	26	124	167
3	68	44	25	38	131	178
7	150	90	53	76	154	213
14	185	148	96	123	185	262
21	193	188	131	155	208	300
28	199	218	160	179	227	330
60	253	292	247	236	281	421
90	287	324	294	260	310	468
120	328	343	325	274	330	498
150	369	356	347	283	343	518
180	391	364	363	289	354	531
210	397	371	375	294	362	541
240	406	376	385	298	369	548
270	417	380	394	301	374	553
300	426	383	400	303	378	557
330	434	386	406	305	382	560
360	443	389	411	307	386	562

Table B.20. Comparison of measured sealed shrinkage with five models for NC 1

Time after Loading, days	Measured Shrinkage	AASHTO LRFD 2010	ACI 209R-1990	ACI 209R-Modified by Huo	CEB-FIP 90	Bazant B3
0	0	0	\	\	\	0
0	0	0	\	\	\	0
1	0	6	\	\	\	24
2	30	11	\	\	\	25
3	59	15	\	\	\	27
7	130	31	\	\	\	32
14	161	52	\	\	\	39
21	167	66	\	\	\	44
28	171	76	\	\	\	48
60	216	102	\	\	\	60
90	246	113	\	\	\	65
120	278	120	\	\	\	69
150	312	124	\	\	\	71
180	333	127	\	\	\	72
210	338	130	\	\	\	73
240	339	132	\	\	\	74
270	338	133	\	\	\	74
300	340	134	\	\	\	74
330	343	135	\	\	\	75
360	344	136	\	\	\	75

Table B.21. Comparison of measured unsealed creep coefficient with five models for NC 2

Time after Loading, days	Measured Creep Coefficient	AASHTO LRFD 2010	ACI 209R-1990	ACI 209R-Modified by Huo	CEB-FIP 90	Bazant B3
0	0.00000	0.00000	0.00000	0.00000	0.00000	0.00000
0	0.00000	0.00000	0.00000	0.00000	0.00000	0.00000
1	-0.00768	0.05262	0.31131	0.31190	0.86954	1.25687
2	0.02393	0.10239	0.45072	0.44774	0.90427	1.30066
3	0.08715	0.14952	0.55475	0.54759	0.93595	1.34061
7	0.14514	0.31551	0.83292	0.80850	1.04139	1.47389
14	0.25188	0.54052	1.12176	1.07038	1.17779	1.64892
21	0.30063	0.70909	1.31231	1.23835	1.28100	1.78505
28	0.33857	0.84009	1.45454	1.36130	1.36464	1.89854
60	0.43608	1.19262	1.84379	1.68773	1.62298	2.26868
90	0.47820	1.35893	2.04791	1.85326	1.77623	2.49773
120	0.49850	1.46079	2.18729	1.96414	1.88782	2.66347
150	0.53189	1.52958	2.29101	2.04553	1.97423	2.78818
180	0.56235	1.57916	2.37237	2.10874	2.04377	2.88480
210	0.60038	1.61659	2.43855	2.15975	2.10126	2.96154
240	0.62798	1.64584	2.49383	2.20206	2.14978	3.02385
270	0.65742	1.66934	2.54094	2.23793	2.19136	3.07544
300	0.68564	1.68862	2.58174	2.26885	2.22747	3.11893
330	0.71447	1.70474	2.61754	2.29586	2.25915	3.15618
360	0.73004	1.71840	2.64929	2.31973	2.28720	3.18853

Table B.22. Comparison of measured sealed creep coefficient with five models for NC 2

Time after Loading, days	Measured Creep Coefficient	AASHTO LRFD 2010	ACI 209R-1990	ACI 209R-Modified by Huo	CEB-FIP 90	Bazant B3
0	0.00000	0.00000	0.00000	0.00000	0.00000	0.00000
0	0.00000	0.00000	0.00000	0.00000	0.00000	0.00000
1	0.00779	0.02612	0.09485	0.09503	0.29652	1.02440
2	0.07495	0.05082	0.13733	0.13642	0.30858	1.05466
3	0.20926	0.07421	0.16902	0.16684	0.31961	1.08173
7	0.25892	0.15660	0.25377	0.24633	0.35661	1.16817
14	0.33585	0.26828	0.34178	0.32612	0.40524	1.27233
21	0.36312	0.35195	0.39984	0.37730	0.44281	1.34624
28	0.40630	0.41697	0.44317	0.41476	0.47386	1.40357
60	0.52148	0.59195	0.56176	0.51422	0.57462	1.57038
90	0.58374	0.67450	0.62396	0.56465	0.63933	1.66544
120	0.62707	0.72505	0.66642	0.59843	0.68981	1.73467
150	0.70029	0.75920	0.69802	0.62323	0.73143	1.78915
180	0.71463	0.78381	0.72281	0.64249	0.76693	1.83407
210	0.75244	0.80238	0.74298	0.65803	0.79788	1.87229
240	0.78744	0.81690	0.75982	0.67092	0.82532	1.90556
270	0.80916	0.82856	0.77417	0.68185	0.84996	1.93501
300	0.83973	0.83814	0.78660	0.69127	0.87228	1.96143
330	0.86587	0.84613	0.79751	0.69950	0.89268	1.98538
360	0.88432	0.85292	0.80718	0.70677	0.91144	2.00729

Table B.23. Comparison of measured unsealed shrinkage with five models for NC 2

Time after Loading, days	Measured Shrinkage	AASHTO LRFD 2010	ACI 209R-1990	ACI 209R-Modified by Huo	CEB-FIP 90	Bazant B3
0	0	0	0	0	0	0
0	0	0	0	0	0	0
1	130	21	13	21	171	177
2	161	40	25	41	182	190
3	225	58	36	59	192	202
7	236	118	79	122	226	242
14	259	194	142	201	271	298
21	271	247	193	257	305	341
28	279	286	236	298	333	376
60	299	383	365	401	412	481
90	315	426	435	446	455	536
120	330	450	480	473	483	571
150	352	467	512	491	503	595
180	358	478	536	503	519	611
210	373	487	555	512	531	623
240	387	493	570	519	540	631
270	396	499	582	525	548	638
300	408	503	592	530	555	642
330	419	507	600	534	560	646
360	425	510	607	537	565	649

Table B.24. Comparison of measured sealed shrinkage with five models for NC 2

Time after Loading, days	Measured Shrinkage	AASHTO LRFD 2010	ACI 209R-1990	ACI 209R-Modified by Huo	CEB-FIP 90	Bazant B3
0	0	0	\	\	\	0
0	0	0	\	\	\	0
1	70	7	\	\	\	27
2	73	14	\	\	\	29
3	77	20	\	\	\	30
7	91	41	\	\	\	36
14	122	68	\	\	\	44
21	139	86	\	\	\	50
28	141	100	\	\	\	55
60	150	134	\	\	\	69
90	157	149	\	\	\	75
120	161	157	\	\	\	79
150	165	163	\	\	\	81
180	172	167	\	\	\	83
210	218	170	\	\	\	84
240	265	173	\	\	\	85
270	286	174	\	\	\	85
300	325	176	\	\	\	86
330	354	177	\	\	\	86
360	360	178	\	\	\	86

Table B.25. Comparison of measured unsealed creep coefficient with five models for NC 3

Time after Loading, days	Measured Creep Coefficient	AASHTO LRFD 2010	ACI 209R-1990	ACI 209R-Modified by Huo	CEB-FIP 90	Bazant B3
0	0.00000	0.00000	0.00000	0.00000	0.00000	0.00000
0	0.00000	0.00000	0.00000	0.00000	0.00000	0.00000
1	0.01379	0.05752	0.31131	0.36248	0.71950	1.44676
2	0.01916	0.11025	0.45072	0.51591	0.74823	1.49629
3	0.02452	0.15877	0.55475	0.62705	0.77445	1.54133
7	0.05440	0.31936	0.83292	0.91101	0.86169	1.69059
14	0.14018	0.51452	1.12176	1.18706	0.97455	1.88401
21	0.16816	0.64614	1.31231	1.35956	1.05996	2.03233
28	0.26889	0.74091	1.45454	1.48366	1.12917	2.15455
60	0.31187	0.96809	1.84379	1.80453	1.34293	2.54453
90	0.33835	1.06317	2.04791	1.96262	1.46974	2.77988
120	0.36531	1.11808	2.18729	2.06685	1.56207	2.94803
150	0.38972	1.15383	2.29101	2.14252	1.63356	3.07392
180	0.40353	1.17896	2.37237	2.20081	1.69110	3.17153
210	0.40667	1.19759	2.43855	2.24753	1.73868	3.24942
240	0.44864	1.21196	2.49383	2.28610	1.77882	3.31317
270	0.48179	1.22337	2.54094	2.31864	1.81323	3.36647
300	0.49901	1.23266	2.58174	2.34658	1.84310	3.41190
330	0.52618	1.24037	2.61754	2.37092	1.86932	3.45126
360	0.54098	1.24686	2.64929	2.39236	1.89253	3.48586

Table B.26. Comparison of measured sealed creep coefficient with five models for NC 3

Time after Loading, days	Measured Creep Coefficient	AASHTO LRFD 2010	ACI 209R-1990	ACI 209R-Modified by Huo	CEB-FIP 90	Bazant B3
0	0.00000	0.00000	0.00000	0.00000	0.00000	0.00000
0	0.00000	0.00000	0.00000	0.00000	0.00000	0.00000
1	0.06562	0.02855	0.09485	0.11044	0.24535	1.23318
2	0.10648	0.05472	0.13733	0.15719	0.25533	1.27008
3	0.14733	0.07880	0.16902	0.19105	0.26446	1.30309
7	0.21115	0.15851	0.25377	0.27757	0.29507	1.40852
14	0.29153	0.25538	0.34178	0.36167	0.33531	1.53556
21	0.31410	0.32071	0.39984	0.41423	0.36640	1.62569
28	0.39536	0.36775	0.44317	0.45204	0.39210	1.69561
60	0.46723	0.48050	0.56176	0.54980	0.47547	1.89906
90	0.52824	0.52770	0.62396	0.59797	0.52901	2.01500
120	0.60072	0.55495	0.66642	0.62973	0.57078	2.09943
150	0.67654	0.57269	0.69802	0.65278	0.60522	2.16588
180	0.72637	0.58517	0.72281	0.67054	0.63459	2.22066
210	0.74236	0.59442	0.74298	0.68478	0.66020	2.26728
240	0.82635	0.60155	0.75982	0.69653	0.68291	2.30786
270	0.88451	0.60721	0.77417	0.70644	0.70329	2.34377
300	0.92715	0.61182	0.78660	0.71495	0.72177	2.37599
330	0.97949	0.61565	0.79751	0.72237	0.73864	2.40520
360	1.01115	0.61887	0.80718	0.72890	0.75416	2.43192

Table B.27. Comparison of measured unsealed shrinkage with five models for NC 3

Time after Loading, days	Measured Shrinkage	AASHTO LRFD 2010	ACI 209R-1990	ACI 209R-Modified by Huo	CEB-FIP 90	Bazant B3
0	0	0	0	0	0	0
0	0	0	0	0	0	0
1	14	17	10	17	100	166
2	28	32	20	32	107	177
3	42	46	29	47	113	188
7	67	92	64	96	133	226
14	104	149	116	158	159	277
21	126	187	157	202	179	316
28	204	215	192	235	195	348
60	252	280	297	317	242	442
90	278	308	353	352	267	490
120	315	324	390	373	283	520
150	353	334	417	387	295	539
180	375	341	436	397	304	552
210	383	347	451	404	311	562
240	387	351	463	410	317	568
270	383	354	473	414	321	573
300	391	357	481	418	325	577
330	392	359	488	421	329	580
360	395	361	494	424	331	582

Table B.28. Comparison of measured sealed shrinkage with five models for NC 3

Time after Loading, days	Measured Shrinkage	AASHTO LRFD 2010	ACI 209R-1990	ACI 209R-Modified by Huo	CEB-FIP 90	Bazant B3
0	0	0	\	\	\	0
0	0	0	\	\	\	0
1	9	6	\	\	\	25
2	18	11	\	\	\	27
3	27	16	\	\	\	28
7	48	32	\	\	\	34
14	88	52	\	\	\	41
21	99	65	\	\	\	46
28	140	75	\	\	\	51
60	180	98	\	\	\	63
90	204	108	\	\	\	68
120	233	113	\	\	\	71
150	261	117	\	\	\	73
180	277	119	\	\	\	75
210	281	121	\	\	\	76
240	282	123	\	\	\	76
270	280	124	\	\	\	77
300	283	125	\	\	\	77
330	283	126	\	\	\	77
360	285	126	\	\	\	77

APPENDIX C

Comparison of Cambers for Different Types of Girders by Using Three Methods, and Gross Section Properties and Transformed Section Properties, and Average Sealed Creep Coefficient and Sealed Shrinkage Data

Table C.1. Camber prediction of 3 BTC 120 prestressed girders with overhang by using three methods and two types of section properties at plant A

Time after Transfer, days	Ig & Incremental method	Ig &Naaman's Method	Ig &Tadros's Method	Itr &Incrementa l method	Itr & Naaman's Method	Itr &Tadros's Method
0	4.562	4.614	4.562	3.991	4.003	3.991
0	4.430	4.476	4.444	3.701	3.949	3.885
1	5.065	5.128	5.232	4.245	4.540	4.579
2	5.276	5.347	5.563	4.433	4.745	4.870
3	5.441	5.518	5.833	4.581	4.906	5.107
7	5.662	5.751	6.336	4.792	5.137	5.550
14	5.874	5.975	6.833	4.993	5.359	5.987
21	5.953	6.060	7.073	5.072	5.447	6.198
28	6.007	6.118	7.235	5.125	5.506	6.341
60	6.222	6.347	7.730	5.324	5.730	6.777
90	6.319	6.451	7.964	5.411	5.831	6.982
120	6.365	6.502	8.083	5.454	5.881	7.088
150	6.405	6.545	8.182	5.489	5.922	7.175
180	6.438	6.581	8.260	5.519	5.957	7.243
210	6.464	6.608	8.320	5.542	5.984	7.296
240	6.491	6.638	8.380	5.566	6.012	7.349
270	6.542	6.692	8.475	5.610	6.062	7.433
300	6.571	6.723	8.538	5.635	6.092	7.488
330	6.618	6.773	8.627	5.676	6.139	7.566
360	6.660	6.819	8.709	5.713	6.181	7.638

Table C.2. Camber prediction of 3 BTC 120 prestressed girders without overhang by using three methods and two types of section properties at plant A

Time after Transfer, days	Ig & Incremental method	Ig &Naaman's Method	Ig &Tadros's Method	Itr &Incrementa l method	Itr & Naaman's Method	Itr &Tadros's Method
0	4.103	4.153	4.103	3.558	3.569	3.558
0	3.967	4.012	3.995	3.434	3.512	3.463
1	4.529	4.589	4.706	3.937	4.033	4.082
2	4.713	4.782	5.004	4.110	4.212	4.342
3	4.858	4.932	5.247	4.246	4.353	4.554
7	5.046	5.132	5.700	4.438	4.553	4.950
14	5.227	5.324	6.147	4.623	4.745	5.340
21	5.292	5.395	6.363	4.693	4.820	5.528
28	5.337	5.444	6.509	4.741	4.870	5.655
60	5.519	5.640	6.955	4.922	5.062	6.045
90	5.599	5.726	7.166	5.000	5.147	6.228
120	5.637	5.768	7.273	5.038	5.188	6.322
150	5.668	5.803	7.363	5.069	5.222	6.400
180	5.696	5.833	7.432	5.096	5.251	6.461
210	5.717	5.856	7.486	5.116	5.273	6.508
240	5.740	5.881	7.541	5.138	5.297	6.556
270	5.783	5.927	7.627	5.177	5.340	6.630
300	5.806	5.953	7.683	5.200	5.365	6.679
330	5.846	5.995	7.763	5.237	5.405	6.749
360	5.882	6.034	7.837	5.270	5.441	6.813

Table C.3. Camber prediction of 3 BTE 110 prestressed girders with overhang by using three methods and two types of section properties at plant B, including 144-270, 144-272 and 144-268

Time after Transfer, days	Ig & Incremental method	Ig &Naaman's Method	Ig &Tadros's Method	Itr &Incrementa l method	Itr & Naaman's Method	Itr &Tadros's Method
0	2.105	2.126	2.105	1.896	1.906	1.896
0	2.048	2.067	2.042	1.843	1.869	1.838
1	2.350	2.376	2.407	2.122	2.154	2.168
2	2.452	2.482	2.560	2.219	2.254	2.306
3	2.532	2.564	2.684	2.295	2.333	2.419
7	2.642	2.680	2.916	2.406	2.448	2.629
14	2.748	2.791	3.146	2.512	2.558	2.837
21	2.789	2.834	3.256	2.554	2.603	2.937
28	2.818	2.865	3.331	2.584	2.633	3.004
60	2.927	2.980	3.559	2.691	2.746	3.211
90	2.977	3.033	3.667	2.740	2.799	3.308
120	3.002	3.060	3.722	2.765	2.824	3.358
150	3.023	3.082	3.767	2.785	2.846	3.399
180	3.040	3.101	3.803	2.802	2.864	3.431
210	3.054	3.115	3.830	2.815	2.878	3.456
240	3.068	3.130	3.858	2.829	2.892	3.482
270	3.094	3.157	3.902	2.853	2.918	3.521
300	3.109	3.173	3.931	2.867	2.933	3.547
330	3.133	3.198	3.972	2.890	2.957	3.585
360	3.154	3.221	4.010	2.911	2.979	3.619

Table C.4. Camber prediction of 3 BTE 110 prestressed girders without overhang by using three methods and two types of section properties at plant B, including 144-270, 144-272 and 144-268

Time after Transfer, days	Ig & Incremental method	Ig &Naaman's Method	Ig &Tadros's Method	Itr &Incrementa l method	Itr & Naaman's Method	Itr &Tadros's Method
0	1.739	1.761	1.739	1.551	1.561	1.551
0	1.680	1.699	1.687	1.496	1.521	1.503
1	1.923	1.949	1.989	1.718	1.751	1.774
2	2.004	2.033	2.115	1.795	1.830	1.887
3	2.067	2.099	2.219	1.855	1.893	1.979
7	2.152	2.189	2.411	1.940	1.983	2.151
14	2.233	2.276	2.600	2.022	2.071	2.321
21	2.263	2.308	2.692	2.054	2.105	2.403
28	2.284	2.331	2.754	2.076	2.128	2.459
60	2.367	2.420	2.943	2.157	2.216	2.628
90	2.404	2.460	3.032	2.193	2.256	2.708
120	2.422	2.479	3.078	2.211	2.275	2.749
150	2.437	2.496	3.115	2.226	2.291	2.783
180	2.450	2.510	3.145	2.238	2.304	2.809
210	2.460	2.520	3.168	2.247	2.315	2.830
240	2.470	2.532	3.191	2.258	2.326	2.850
270	2.490	2.553	3.227	2.276	2.346	2.883
300	2.501	2.565	3.251	2.286	2.357	2.904
330	2.519	2.584	3.285	2.303	2.375	2.935
360	2.535	2.602	3.316	2.319	2.392	2.963

Table C.5. Camber prediction of 3 BTE 110 prestressed girders with overhang by using three methods and two types of section properties at plant B, including 144-274, 144-275 and 144-278

Time after Transfer, days	Ig & Incremental method	Ig &Naaman's Method	Ig &Tadros's Method	Itr &Incrementa l method	Itr & Naaman's Method	Itr &Tadros's Method
0	2.187	2.209	2.187	1.960	1.971	1.960
0	2.128	2.149	2.122	1.906	1.934	1.901
1	2.440	2.469	2.500	2.193	2.229	2.241
2	2.546	2.578	2.658	2.293	2.332	2.384
3	2.628	2.664	2.788	2.372	2.413	2.501
7	2.742	2.783	3.028	2.486	2.531	2.717
14	2.851	2.897	3.265	2.595	2.645	2.931
21	2.893	2.942	3.380	2.639	2.691	3.034
28	2.922	2.973	3.457	2.669	2.723	3.104
60	3.034	3.091	3.694	2.779	2.839	3.317
90	3.085	3.146	3.805	2.830	2.892	3.418
120	3.111	3.173	3.862	2.854	2.919	3.469
150	3.132	3.196	3.909	2.875	2.941	3.511
180	3.150	3.215	3.946	2.893	2.960	3.545
210	3.164	3.230	3.975	2.906	2.974	3.571
240	3.178	3.246	4.004	2.920	2.989	3.597
270	3.205	3.273	4.049	2.945	3.015	3.638
300	3.220	3.290	4.079	2.959	3.031	3.664
330	3.244	3.316	4.122	2.983	3.055	3.703
360	3.267	3.339	4.161	3.004	3.078	3.738

Table C.6. Camber prediction of 3 BTE 110 prestressed girders without overhang by using three methods and two types of section properties at plant B, including 144-274, 144-275 and 144-278

Time after Transfer, days	Ig & Incremental method	Ig &Naaman's Method	Ig &Tadros's Method	Itr &Incrementa l method	Itr & Naaman's Method	Itr &Tadros's Method
0	1.806	1.829	1.806	1.602	1.613	1.602
0	1.745	1.766	1.752	1.546	1.573	1.553
1	1.996	2.025	2.065	1.775	1.810	1.832
2	2.080	2.112	2.196	1.853	1.892	1.948
3	2.145	2.180	2.303	1.915	1.957	2.044
7	2.232	2.272	2.502	2.003	2.050	2.221
14	2.315	2.361	2.698	2.087	2.139	2.397
21	2.346	2.395	2.793	2.119	2.175	2.481
28	2.367	2.418	2.857	2.142	2.199	2.538
60	2.452	2.509	3.053	2.225	2.289	2.713
90	2.490	2.550	3.146	2.262	2.329	2.795
120	2.508	2.570	3.193	2.280	2.349	2.837
150	2.523	2.587	3.232	2.295	2.366	2.872
180	2.536	2.601	3.262	2.308	2.379	2.899
210	2.546	2.612	3.286	2.317	2.390	2.920
240	2.557	2.624	3.310	2.328	2.401	2.942
270	2.577	2.645	3.348	2.346	2.422	2.975
300	2.588	2.657	3.372	2.357	2.433	2.997
330	2.607	2.677	3.408	2.374	2.452	3.029
360	2.623	2.696	3.440	2.390	2.469	3.058

Table C.7. Camber prediction of 3 BTE 110 prestressed girders with overhang by using three methods and two types of section properties at plant B, including 144-284, 144-283 and 144-280

Time after Transfer, days	Ig & Incremental method	Ig &Naaman's Method	Ig &Tadros's Method	Itr &Incrementa l method	Itr & Naaman's Method	Itr &Tadros's Method
0	2.037	2.056	2.037	1.842	1.851	1.842
0	1.981	1.999	1.975	1.790	1.814	1.785
1	2.274	2.298	2.329	2.061	2.091	2.106
2	2.373	2.401	2.477	2.156	2.189	2.241
3	2.451	2.481	2.598	2.230	2.265	2.351
7	2.559	2.594	2.823	2.338	2.377	2.555
14	2.662	2.702	3.045	2.441	2.484	2.757
21	2.702	2.744	3.152	2.483	2.528	2.854
28	2.730	2.774	3.224	2.511	2.558	2.920
60	2.837	2.886	3.446	2.617	2.668	3.121
90	2.886	2.938	3.550	2.665	2.719	3.216
120	2.910	2.964	3.604	2.688	2.744	3.264
150	2.931	2.986	3.648	2.708	2.765	3.304
180	2.948	3.004	3.682	2.725	2.783	3.336
210	2.961	3.018	3.709	2.738	2.797	3.360
240	2.975	3.033	3.736	2.751	2.811	3.384
270	3.000	3.059	3.779	2.775	2.836	3.423
300	3.015	3.075	3.807	2.789	2.851	3.448
330	3.038	3.100	3.846	2.811	2.874	3.485
360	3.060	3.122	3.883	2.831	2.896	3.518

Table C.8. Camber prediction of 3 BTE 110 prestressed girders without overhang by using three methods and two types of section properties at plant B, including 144-284, 144-283 and 144-280

Time after Transfer, days	Ig & Incremental method	Ig &Naaman's Method	Ig &Tadros's Method	Itr &Incrementa l method	Itr & Naaman's Method	Itr &Tadros's Method
0	1.683	1.703	1.683	1.507	1.517	1.507
0	1.625	1.643	1.632	1.454	1.477	1.461
1	1.861	1.886	1.925	1.671	1.701	1.724
2	1.940	1.968	2.048	1.745	1.778	1.834
3	2.002	2.032	2.148	1.804	1.840	1.925
7	2.085	2.119	2.334	1.887	1.927	2.092
14	2.164	2.204	2.518	1.967	2.012	2.258
21	2.194	2.236	2.607	1.998	2.046	2.338
28	2.214	2.258	2.667	2.019	2.069	2.391
60	2.296	2.345	2.850	2.100	2.155	2.557
90	2.332	2.384	2.937	2.135	2.193	2.634
120	2.350	2.403	2.981	2.152	2.212	2.674
150	2.364	2.419	3.018	2.167	2.228	2.707
180	2.377	2.433	3.046	2.179	2.241	2.733
210	2.387	2.443	3.068	2.188	2.251	2.753
240	2.397	2.454	3.091	2.198	2.262	2.773
270	2.416	2.475	3.126	2.216	2.281	2.804
300	2.427	2.487	3.149	2.226	2.292	2.825
330	2.445	2.506	3.182	2.243	2.310	2.855
360	2.461	2.523	3.212	2.258	2.327	2.882

Table C.9. Camber prediction of 2 BTE 145 prestressed girders with overhang by using three methods and two types of section properties at plant B, including 144-311 and 144-334

Time after Transfer, days	Ig & Incremental method	Ig &Naaman's Method	Ig &Tadros's Method	Itr &Incrementa l method	Itr & Naaman's Method	Itr &Tadros's Method
0	5.037	5.094	5.037	4.390	4.405	4.390
0	4.893	4.942	4.903	4.258	4.344	4.270
1	5.590	5.658	5.766	4.886	4.992	5.027
2	5.821	5.899	6.127	5.104	5.216	5.344
3	6.001	6.086	6.423	5.274	5.392	5.603
7	6.242	6.340	6.972	5.519	5.644	6.086
14	6.471	6.583	7.515	5.753	5.886	6.562
21	6.556	6.675	7.777	5.844	5.982	6.792
28	6.614	6.739	7.954	5.907	6.047	6.948
60	6.846	6.988	8.495	6.138	6.291	7.423
90	6.951	7.101	8.750	6.241	6.401	7.647
120	7.001	7.156	8.880	6.291	6.455	7.761
150	7.043	7.202	8.988	6.333	6.500	7.856
180	7.079	7.241	9.073	6.368	6.538	7.930
210	7.107	7.271	9.138	6.395	6.567	7.988
240	7.137	7.303	9.204	6.423	6.598	8.046
270	7.191	7.361	9.308	6.475	6.653	8.137
300	7.222	7.395	9.377	6.504	6.685	8.197
330	7.273	7.450	9.474	6.552	6.736	8.283
360	7.319	7.499	9.563	6.595	6.783	8.361

Table C.10. Camber prediction of 2 BTE 145 prestressed girders without overhang by using three methods and two types of section properties at plant B, including 144-311 and 144-334

Time after Transfer, days	Ig & Incremental method	Ig &Naaman's Method	Ig &Tadros's Method	Itr &Incrementa l method	Itr & Naaman's Method	Itr &Tadros's Method
0	3.695	3.760	3.695	3.132	3.154	3.132
0	3.542	3.599	3.595	2.992	3.077	3.045
1	4.055	4.135	4.274	3.443	3.551	3.624
2	4.191	4.278	4.517	3.570	3.685	3.832
3	4.272	4.365	4.687	3.649	3.769	3.977
7	4.435	4.542	5.103	3.815	3.947	4.332
14	4.559	4.681	5.487	3.947	4.090	4.659
21	4.630	4.761	5.716	4.021	4.172	4.855
28	4.678	4.815	5.875	4.071	4.228	4.991
60	4.794	4.949	6.262	4.191	4.362	5.321
90	4.845	5.008	6.435	4.242	4.421	5.469
120	4.875	5.043	6.540	4.272	4.456	5.558
150	4.895	5.066	6.611	4.292	4.479	5.619
180	4.909	5.082	6.662	4.306	4.496	5.662
210	4.919	5.094	6.700	4.316	4.507	5.694
240	4.926	5.103	6.729	4.323	4.516	5.719
270	4.932	5.110	6.752	4.329	4.523	5.739
300	4.936	5.115	6.770	4.333	4.528	5.754
330	4.939	5.119	6.785	4.336	4.532	5.767
360	4.942	5.122	6.797	4.339	4.536	5.777

Table C.11. Camber prediction of 2 BTE 145 prestressed girders with overhang by using three methods and two types of section properties at plant B, including 144-316 and 144-317

Time after Transfer, days	Ig & Incremental method	Ig &Naaman's Method	Ig &Tadros's Method	Itr &Incrementa l method	Itr & Naaman's Method	Itr &Tadros's Method
0	5.050	5.109	5.050	4.386	4.402	4.386
0	4.904	4.955	4.915	4.253	4.341	4.265
1	5.600	5.671	5.779	4.879	4.988	5.021
2	5.830	5.911	6.140	5.095	5.211	5.338
3	6.009	6.098	6.436	5.265	5.387	5.596
7	6.248	6.350	6.986	5.508	5.637	6.078
14	6.475	6.592	7.529	5.740	5.878	6.553
21	6.558	6.683	7.791	5.831	5.973	6.783
28	6.616	6.746	7.968	5.892	6.038	6.937
60	6.846	6.993	8.510	6.121	6.280	7.412
90	6.948	7.105	8.765	6.223	6.389	7.635
120	6.998	7.159	8.895	6.272	6.442	7.749
150	7.039	7.204	9.003	6.313	6.487	7.844
180	7.075	7.243	9.088	6.348	6.524	7.918
210	7.102	7.273	9.154	6.374	6.553	7.975
240	7.132	7.305	9.220	6.403	6.584	8.033
270	7.185	7.363	9.324	6.453	6.638	8.124
300	7.216	7.396	9.392	6.482	6.670	8.184
330	7.266	7.450	9.489	6.529	6.720	8.269
360	7.312	7.499	9.579	6.572	6.767	8.348

Table C.12. Camber prediction of 2 BTE 145 prestressed girders without overhang by using three methods and two types of section properties at plant B, including 144-316 and 144-317

Time after Transfer, days	Ig & Incremental method	Ig &Naaman's Method	Ig &Tadros's Method	Itr &Incrementa l method	Itr & Naaman's Method	Itr &Tadros's Method
0	3.682	3.750	3.682	3.106	3.130	3.106
0	3.526	3.586	3.582	2.965	3.052	3.019
1	4.035	4.117	4.258	3.409	3.521	3.593
2	4.168	4.259	4.500	3.534	3.653	3.799
3	4.248	4.345	4.669	3.611	3.736	3.942
7	4.407	4.519	5.083	3.774	3.911	4.294
14	4.528	4.655	5.465	3.903	4.051	4.618
21	4.596	4.733	5.693	3.975	4.132	4.812
28	4.643	4.786	5.851	4.024	4.187	4.947
60	4.755	4.916	6.236	4.139	4.318	5.274
90	4.804	4.973	6.408	4.189	4.375	5.420
120	4.833	5.007	6.513	4.218	4.409	5.509
150	4.852	5.029	6.583	4.237	4.432	5.569
180	4.865	5.045	6.633	4.250	4.447	5.612
210	4.874	5.056	6.671	4.259	4.459	5.644
240	4.881	5.065	6.700	4.266	4.467	5.668
270	4.886	5.071	6.723	4.272	4.474	5.687
300	4.890	5.076	6.741	4.276	4.479	5.703
330	4.893	5.080	6.756	4.279	4.483	5.715
360	4.896	5.083	6.768	4.281	4.486	5.726

Table C.13. Camber prediction of 2 BTE 145 prestressed girders with overhang by using three methods and two types of section properties at plant B, including 144-366 and 144-367

Time after Transfer, days	Ig & Incremental method	Ig &Naaman's Method	Ig &Tadros's Method	Itr &Incrementa l method	Itr & Naaman's Method	Itr &Tadros's Method
0	4.948	5.004	4.948	4.313	4.328	4.313
0	4.803	4.852	4.815	4.180	4.265	4.193
1	5.487	5.555	5.662	4.797	4.901	4.937
2	5.714	5.791	6.017	5.010	5.121	5.248
3	5.890	5.974	6.307	5.177	5.294	5.503
7	6.126	6.223	6.847	5.417	5.541	5.977
14	6.350	6.462	7.380	5.646	5.778	6.445
21	6.433	6.552	7.637	5.735	5.872	6.671
28	6.490	6.614	7.811	5.796	5.936	6.823
60	6.718	6.858	8.343	6.023	6.175	7.290
90	6.819	6.968	8.593	6.123	6.282	7.510
120	6.868	7.022	8.721	6.172	6.335	7.623
150	6.910	7.067	8.827	6.213	6.379	7.716
180	6.945	7.106	8.910	6.247	6.416	7.789
210	6.972	7.135	8.974	6.273	6.444	7.845
240	7.001	7.166	9.039	6.301	6.475	7.902
270	7.054	7.223	9.142	6.351	6.528	7.992
300	7.084	7.256	9.209	6.380	6.560	8.051
330	7.134	7.310	9.304	6.427	6.610	8.134
360	7.179	7.358	9.392	6.469	6.656	8.211

Table C.14. Camber prediction of 2 BTE 145 prestressed girders without overhang by using three methods and two types of section properties at plant B, including 144-366 and 144-367

Time after Transfer, days	Ig & Incremental method	Ig &Naaman's Method	Ig &Tadros's Method	Itr &Incrementa l method	Itr & Naaman's Method	Itr &Tadros's Method
0	3.610	3.674	3.610	3.058	3.081	3.058
0	3.456	3.513	3.511	2.918	3.002	2.972
1	3.926	4.003	4.132	3.331	3.436	3.502
2	4.075	4.161	4.393	3.469	3.583	3.724
3	4.192	4.286	4.605	3.579	3.699	3.905
7	4.332	4.440	5.001	3.724	3.856	4.243
14	4.469	4.592	5.392	3.866	4.010	4.576
21	4.512	4.642	5.581	3.916	4.065	4.737
28	4.542	4.676	5.708	3.949	4.103	4.846
60	4.674	4.826	6.098	4.083	4.252	5.178
90	4.727	4.888	6.281	4.135	4.313	5.335
120	4.751	4.917	6.375	4.160	4.342	5.415
150	4.771	4.940	6.453	4.179	4.365	5.481
180	4.789	4.962	6.514	4.197	4.386	5.533
210	4.803	4.978	6.561	4.210	4.402	5.573
240	4.818	4.995	6.609	4.225	4.419	5.614
270	4.849	5.031	6.683	4.254	4.452	5.678
300	4.865	5.049	6.733	4.268	4.469	5.720
330	4.894	5.081	6.803	4.295	4.499	5.779
360	4.919	5.111	6.867	4.319	4.527	5.834

Table C.15. Camber prediction of 2 BTD 135 prestressed girders with overhang by using three methods and two types of section properties at plant C, including 13501 and 13502

Time after Transfer, days	Ig & Incremental method	Ig &Naaman's Method	Ig &Tadros's Method	Itr &Incrementa l method	Itr & Naaman's Method	Itr &Tadros's Method
0	4.270	4.324	4.270	3.714	3.729	3.714
0	4.121	4.169	4.152	3.578	3.657	3.609
1	4.708	4.774	4.890	4.105	4.202	4.254
2	4.902	4.976	5.200	4.286	4.390	4.525
3	5.053	5.134	5.453	4.429	4.538	4.746
7	5.252	5.344	5.924	4.631	4.747	5.158
14	5.443	5.548	6.388	4.825	4.949	5.565
21	5.512	5.624	6.613	4.900	5.027	5.761
28	5.559	5.675	6.764	4.950	5.081	5.893
60	5.753	5.883	7.228	5.141	5.283	6.299
90	5.837	5.975	7.446	5.224	5.372	6.490
120	5.877	6.020	7.558	5.264	5.416	6.588
150	5.911	6.057	7.650	5.297	5.452	6.669
180	5.941	6.089	7.723	5.325	5.483	6.732
210	5.963	6.113	7.779	5.346	5.506	6.781
240	5.987	6.140	7.835	5.369	5.531	6.831
270	6.032	6.188	7.924	5.412	5.576	6.908
300	6.057	6.216	7.983	5.435	5.602	6.960
330	6.099	6.261	8.066	5.474	5.645	7.032
360	6.138	6.302	8.143	5.510	5.683	7.099

Table C.16. Camber prediction of 2 BTD 135 prestressed girders without overhang by using three methods and two types of section properties at plant C, including 13501 and 13502

Time after Transfer, days	Ig & Incremental method	Ig &Naaman's Method	Ig &Tadros's Method	Itr &Incrementa l method	Itr & Naaman's Method	Itr &Tadros's Method
0	4.043	4.107	4.043	3.422	3.438	3.422
0	3.884	3.940	3.934	3.277	3.369	3.326
1	4.420	4.496	4.631	3.748	3.862	3.920
2	4.592	4.678	4.923	3.907	4.029	4.169
3	4.727	4.821	5.161	4.033	4.162	4.372
7	4.895	5.003	5.605	4.206	4.344	4.750
14	5.058	5.179	6.044	4.373	4.522	5.124
21	5.112	5.241	6.255	4.434	4.588	5.304
28	5.149	5.283	6.398	4.475	4.633	5.426
60	5.309	5.460	6.836	4.634	4.807	5.798
90	5.375	5.535	7.042	4.699	4.880	5.974
120	5.406	5.570	7.147	4.731	4.916	6.064
150	5.431	5.600	7.234	4.755	4.944	6.138
180	5.455	5.626	7.303	4.778	4.969	6.196
210	5.472	5.646	7.356	4.794	4.988	6.242
240	5.491	5.667	7.409	4.812	5.009	6.287
270	5.528	5.709	7.493	4.847	5.047	6.359
300	5.548	5.731	7.548	4.865	5.068	6.406
330	5.583	5.770	7.627	4.897	5.104	6.473
360	5.614	5.805	7.699	4.926	5.136	6.534

Table C.17. Camber prediction of 2 BTD 135 prestressed girders with overhang by using three methods and two types of section properties at plant C, including 13503 and 13504

Time after Transfer, days	Ig & Incremental method	Ig &Naaman's Method	Ig &Tadros's Method	Itr &Incrementa l method	Itr & Naaman's Method	Itr &Tadros's Method
0	4.269	4.333	4.269	3.629	3.645	3.629
0	4.293	4.167	4.155	3.656	3.579	3.529
1	4.895	4.760	4.890	4.188	4.105	4.159
2	5.092	4.954	5.198	4.371	4.284	4.422
3	5.246	5.107	5.450	4.515	4.426	4.638
7	5.444	5.304	5.919	4.717	4.623	5.039
14	5.634	5.496	6.382	4.911	4.815	5.435
21	5.701	5.563	6.605	4.985	4.887	5.627
28	5.746	5.610	6.756	5.035	4.936	5.756
60	5.937	5.803	7.218	5.223	5.125	6.151
90	6.019	5.885	7.435	5.304	5.206	6.337
120	6.058	5.925	7.547	5.342	5.245	6.432
150	6.090	5.958	7.639	5.374	5.277	6.511
180	6.118	5.987	7.711	5.401	5.305	6.573
210	6.140	6.009	7.767	5.422	5.326	6.621
240	6.163	6.033	7.823	5.444	5.348	6.669
270	6.208	6.078	7.912	5.486	5.390	6.745
300	6.232	6.102	7.970	5.508	5.413	6.795
330	6.274	6.144	8.053	5.547	5.452	6.866
360	6.311	6.183	8.129	5.581	5.488	6.931

Table C.18. Camber prediction of 2 BTD 135 prestressed girders without overhang by using three methods and two types of section properties at plant C, including 13503 and 13504

Time after Transfer, days	Ig & Incremental method	Ig &Naaman's Method	Ig &Tadros's Method	Itr &Incrementa l method	Itr & Naaman's Method	Itr &Tadros's Method
0	4.122	4.186	4.122	3.491	3.507	3.491
0	3.963	4.019	4.011	3.347	3.440	3.395
1	4.511	4.588	4.722	3.829	3.944	4.001
2	4.688	4.774	5.020	3.992	4.115	4.255
3	4.826	4.919	5.263	4.121	4.251	4.462
7	4.999	5.106	5.716	4.299	4.438	4.848
14	5.166	5.288	6.163	4.471	4.620	5.229
21	5.222	5.351	6.379	4.533	4.688	5.414
28	5.260	5.395	6.524	4.576	4.734	5.538
60	5.425	5.577	6.970	4.740	4.913	5.918
90	5.494	5.654	7.180	4.808	4.988	6.097
120	5.526	5.691	7.288	4.840	5.025	6.189
150	5.553	5.721	7.377	4.866	5.055	6.265
180	5.577	5.748	7.447	4.889	5.081	6.324
210	5.594	5.769	7.501	4.906	5.100	6.371
240	5.614	5.791	7.555	4.925	5.121	6.417
270	5.653	5.834	7.641	4.961	5.161	6.490
300	5.673	5.857	7.697	4.980	5.183	6.538
330	5.709	5.896	7.777	5.013	5.219	6.606
360	5.742	5.932	7.851	5.042	5.253	6.669

Table C.19. Camber prediction of 2 BTD 135 prestressed girders with overhang by using three methods and two types of section properties at plant C, including 13507 and 13508

Time after Transfer, days	Ig & Incremental method	Ig &Naaman's Method	Ig &Tadros's Method	Itr &Incrementa l method	Itr & Naaman's Method	Itr &Tadros's Method
0	4.663	4.727	4.663	4.005	4.021	4.005
0	4.508	4.565	4.539	3.864	3.957	3.895
1	5.144	5.222	5.341	4.430	4.544	4.589
2	5.353	5.440	5.678	4.625	4.746	4.880
3	5.516	5.611	5.953	4.778	4.905	5.117
7	5.728	5.838	6.464	4.994	5.130	5.560
14	5.932	6.056	6.969	5.202	5.347	5.996
21	6.005	6.136	7.213	5.282	5.431	6.207
28	6.055	6.192	7.378	5.336	5.488	6.350
60	6.260	6.414	7.881	5.539	5.705	6.785
90	6.349	6.512	8.119	5.627	5.800	6.991
120	6.392	6.559	8.240	5.670	5.847	7.096
150	6.428	6.599	8.341	5.704	5.885	7.183
180	6.459	6.633	8.420	5.734	5.918	7.251
210	6.482	6.659	8.481	5.757	5.943	7.304
240	6.508	6.687	8.542	5.781	5.970	7.357
270	6.556	6.739	8.639	5.826	6.018	7.441
300	6.583	6.769	8.703	5.851	6.046	7.496
330	6.627	6.817	8.793	5.892	6.091	7.574
360	6.668	6.861	8.876	5.930	6.132	7.646

Table C.20. Camber prediction of 2 BTD 135 prestressed girders without overhang by using three methods and two types of section properties at plant C, including 13507 and 13508

Time after Transfer, days	Ig & Incremental method	Ig &Naaman's Method	Ig &Tadros's Method	Itr &Incrementa l method	Itr & Naaman's Method	Itr &Tadros's Method
0	4.100	4.163	4.100	3.477	3.493	3.477
0	3.942	3.997	3.990	3.333	3.425	3.381
1	4.487	4.563	4.697	3.813	3.927	3.984
2	4.664	4.748	4.993	3.976	4.097	4.237
3	4.801	4.894	5.235	4.105	4.232	4.444
7	4.974	5.080	5.686	4.281	4.419	4.829
14	5.140	5.261	6.131	4.453	4.601	5.208
21	5.196	5.324	6.346	4.515	4.668	5.392
28	5.235	5.367	6.491	4.558	4.714	5.515
60	5.399	5.549	6.935	4.722	4.893	5.894
90	5.468	5.626	7.144	4.789	4.968	6.073
120	5.500	5.663	7.251	4.821	5.004	6.164
150	5.526	5.693	7.339	4.847	5.034	6.240
180	5.551	5.720	7.409	4.870	5.060	6.299
210	5.568	5.741	7.463	4.888	5.079	6.345
240	5.588	5.763	7.517	4.906	5.101	6.391
270	5.627	5.805	7.602	4.942	5.140	6.464
300	5.647	5.828	7.658	4.961	5.162	6.512
330	5.683	5.868	7.738	4.994	5.198	6.580
360	5.715	5.904	7.811	5.024	5.232	6.642

Table C.21. Camber prediction of 2 BTD 135 prestressed girders with overhang by using three methods and two types of section properties at plant C, including 13511 and 13512

Time after Transfer, days	Ig & Incremental method	Ig &Naaman's Method	Ig &Tadros's Method	Itr &Incrementa l method	Itr & Naaman's Method	Itr &Tadros's Method
0	4.010	4.068	4.010	3.437	3.452	3.437
0	4.029	3.906	3.900	3.458	3.381	3.340
1	4.597	4.465	4.593	3.964	3.879	3.937
2	4.783	4.648	4.883	4.138	4.049	4.188
3	4.929	4.792	5.120	4.274	4.183	4.392
7	5.117	4.979	5.562	4.465	4.370	4.773
14	5.298	5.161	5.998	4.650	4.551	5.149
21	5.362	5.225	6.208	4.720	4.620	5.331
28	5.405	5.270	6.350	4.767	4.666	5.453
60	5.587	5.453	6.785	4.947	4.845	5.828
90	5.665	5.531	6.990	5.023	4.922	6.005
120	5.703	5.569	7.095	5.060	4.959	6.095
150	5.733	5.600	7.182	5.090	4.989	6.170
180	5.761	5.628	7.250	5.117	5.016	6.229
210	5.781	5.649	7.302	5.136	5.036	6.274
240	5.803	5.671	7.356	5.157	5.057	6.320
270	5.846	5.714	7.439	5.197	5.097	6.392
300	5.869	5.738	7.494	5.219	5.119	6.439
330	5.909	5.777	7.572	5.255	5.156	6.507
360	5.945	5.814	7.644	5.288	5.190	6.568

Table C.22. Camber prediction of 2 BTD 135 prestressed girders without overhang by using three methods and two types of section properties at plant C, including 13511 and 13512

Time after Transfer, days	Ig & Incremental method	Ig &Naaman's Method	Ig &Tadros's Method	Itr &Incrementa l method	Itr & Naaman's Method	Itr &Tadros's Method
0	3.856	3.913	3.856	3.292	3.308	3.292
0	3.700	3.751	3.749	3.151	3.235	3.199
1	4.215	4.284	4.416	3.606	3.710	3.772
2	4.381	4.459	4.695	3.760	3.871	4.012
3	4.511	4.596	4.923	3.882	3.999	4.208
7	4.674	4.772	5.348	4.049	4.175	4.573
14	4.833	4.943	5.767	4.211	4.347	4.933
21	4.886	5.003	5.970	4.271	4.411	5.107
28	4.922	5.044	6.106	4.311	4.454	5.224
60	5.079	5.216	6.525	4.466	4.623	5.584
90	5.144	5.289	6.722	4.530	4.694	5.753
120	5.175	5.324	6.823	4.560	4.729	5.839
150	5.200	5.352	6.906	4.585	4.756	5.911
180	5.223	5.378	6.972	4.607	4.781	5.967
210	5.240	5.397	7.022	4.623	4.799	6.011
240	5.258	5.418	7.073	4.641	4.819	6.055
270	5.295	5.459	7.154	4.675	4.857	6.124
300	5.314	5.480	7.206	4.693	4.877	6.169
330	5.348	5.518	7.282	4.724	4.912	6.234
360	5.379	5.552	7.351	4.752	4.944	6.293

APPENDIX D

Comparison of Cambers for Different Types of Girders by Using Three Methods, and Gross Section Properties and Transformed Section Properties, and Specified Sealed Creep Coefficient and Sealed Shrinkage Data

Table D.1. Camber prediction of 3 BTC 120 prestressed girders with overhang by using three methods and two types of section properties at plant A

Time after Transfer, days	Ig & Incremental method	Ig &Naaman's Method	Ig &Tadros's Method	Itr &Incrementa l method	Itr & Naaman's Method	Itr &Tadros's Method
0	4.562	4.614	4.562	3.991	4.003	3.991
0	4.430	4.476	4.444	3.701	3.949	3.885
1	4.998	5.060	5.159	4.189	4.480	4.514
2	5.016	5.079	5.265	4.213	4.505	4.608
3	5.166	5.235	5.505	4.349	4.652	4.819
7	5.438	5.518	6.033	4.602	4.926	5.284
14	5.604	5.694	6.448	4.764	5.103	5.649
21	5.632	5.724	6.596	4.798	5.140	5.779
28	5.685	5.782	6.744	4.850	5.198	5.909
60	6.190	6.311	7.625	5.298	5.696	6.684
90	6.345	6.475	7.934	5.437	5.852	6.956
120	6.443	6.580	8.126	5.524	5.951	7.125
150	6.523	6.665	8.278	5.595	6.031	7.259
180	6.556	6.700	8.345	5.625	6.065	7.318
210	6.581	6.726	8.399	5.647	6.091	7.365
240	6.576	6.721	8.405	5.643	6.087	7.371
270	6.556	6.701	8.389	5.626	6.069	7.357
300	6.616	6.765	8.501	5.678	6.129	7.456
330	6.672	6.824	8.597	5.727	6.184	7.539
360	6.728	6.884	8.692	5.776	6.239	7.623

Table D.2. Camber prediction of 3 BTC 120 prestressed girders without overhang by using three methods and two types of section properties at plant A

Time after Transfer, days	Ig & Incremental method	Ig &Naaman's Method	Ig &Tadros's Method	Itr &Incremental method	Itr & Naaman's Method	Itr &Tadros's Method
0	4.103	4.153	4.103	3.558	3.569	3.558
0	3.967	4.012	3.995	3.434	3.512	3.463
1	4.469	4.528	4.639	3.885	3.979	4.025
2	4.481	4.542	4.735	3.905	3.999	4.108
3	4.614	4.680	4.951	4.031	4.128	4.297
7	4.851	4.928	5.427	4.264	4.369	4.711
14	4.992	5.079	5.800	4.413	4.523	5.037
21	5.014	5.103	5.933	4.443	4.555	5.153
28	5.059	5.151	6.067	4.490	4.604	5.269
60	5.496	5.612	6.860	4.901	5.037	5.961
90	5.628	5.753	7.138	5.027	5.171	6.204
120	5.711	5.843	7.311	5.106	5.256	6.355
150	5.779	5.916	7.447	5.170	5.325	6.474
180	5.808	5.946	7.508	5.197	5.354	6.527
210	5.829	5.968	7.556	5.217	5.376	6.569
240	5.823	5.963	7.562	5.213	5.372	6.574
270	5.804	5.944	7.547	5.197	5.355	6.561
300	5.855	5.999	7.649	5.244	5.406	6.650
330	5.903	6.050	7.735	5.289	5.454	6.724
360	5.952	6.102	7.820	5.333	5.502	6.799

Table D.3. Camber prediction of 3 BTE 110 prestressed girders with overhang by using three methods and two types of section properties at plant B, including 144-270, 144-272 and 144-268

Time after Transfer, days	Ig & Incremental method	Ig &Naaman's Method	Ig &Tadros's Method	Itr &Incrementa l method	Itr & Naaman's Method	Itr &Tadros's Method
0	2.105	2.126	2.105	1.896	1.906	1.896
0	2.048	2.067	2.042	1.843	1.869	1.838
1	2.392	2.420	2.454	2.160	2.194	2.211
2	2.438	2.468	2.542	2.206	2.241	2.291
3	2.558	2.591	2.713	2.319	2.358	2.446
7	2.648	2.685	2.918	2.411	2.453	2.631
14	2.843	2.888	3.263	2.599	2.648	2.943
21	2.918	2.968	3.425	2.674	2.727	3.089
28	2.952	3.004	3.507	2.709	2.763	3.164
60	3.042	3.099	3.715	2.798	2.857	3.352
90	3.083	3.143	3.812	2.839	2.901	3.439
120	3.102	3.164	3.862	2.858	2.922	3.485
150	3.109	3.172	3.890	2.866	2.930	3.511
180	3.116	3.180	3.913	2.873	2.938	3.531
210	3.125	3.189	3.934	2.882	2.947	3.550
240	3.156	3.222	3.987	2.911	2.978	3.598
270	3.193	3.261	4.050	2.946	3.016	3.655
300	3.204	3.273	4.073	2.957	3.027	3.676
330	3.225	3.295	4.111	2.976	3.048	3.710
360	3.246	3.317	4.149	2.996	3.069	3.745

Table D.4. Camber prediction of 3 BTE 110 prestressed girders without overhang by using three methods and two types of section properties at plant B, including 144-270, 144-272 and 144-268

Time after Transfer, days	Ig & Incremental method	Ig &Naaman's Method	Ig &Tadros's Method	Itr &Incrementa l method	Itr & Naaman's Method	Itr &Tadros's Method
0	1.739	1.761	1.739	1.551	1.561	1.551
0	1.680	1.699	1.687	1.496	1.521	1.503
1	1.958	1.985	2.027	1.750	1.783	1.808
2	1.994	2.023	2.101	1.786	1.821	1.874
3	2.090	2.122	2.242	1.876	1.914	2.001
7	2.159	2.196	2.412	1.946	1.990	2.153
14	2.311	2.356	2.698	2.093	2.145	2.408
21	2.368	2.418	2.832	2.150	2.206	2.528
28	2.394	2.446	2.900	2.177	2.235	2.590
60	2.461	2.518	3.072	2.244	2.307	2.744
90	2.490	2.550	3.152	2.273	2.339	2.816
120	2.503	2.564	3.194	2.286	2.354	2.853
150	2.506	2.569	3.217	2.290	2.359	2.874
180	2.511	2.574	3.236	2.295	2.365	2.890
210	2.517	2.581	3.253	2.300	2.371	2.906
240	2.540	2.606	3.298	2.323	2.395	2.946
270	2.569	2.636	3.349	2.350	2.424	2.992
300	2.577	2.645	3.369	2.357	2.432	3.009
330	2.592	2.662	3.400	2.372	2.448	3.037
360	2.608	2.679	3.431	2.387	2.464	3.066

Table D.5. Camber prediction of 3 BTE 110 prestressed girders with overhang by using three methods and two types of section properties at plant B, including 144-274, 144-275 and 144-278

Time after Transfer, days	Ig & Incremental method	Ig &Naaman's Method	Ig &Tadros's Method	Itr &Incrementa l method	Itr & Naaman's Method	Itr &Tadros's Method
0	2.187	2.209	2.187	1.960	1.971	1.960
0	2.128	2.149	2.122	1.906	1.934	1.901
1	2.485	2.514	2.548	2.233	2.270	2.285
2	2.532	2.564	2.640	2.281	2.318	2.368
3	2.656	2.692	2.818	2.397	2.439	2.528
7	2.748	2.789	3.030	2.491	2.537	2.719
14	2.948	2.998	3.387	2.685	2.738	3.041
21	3.026	3.080	3.555	2.762	2.819	3.192
28	3.061	3.117	3.640	2.797	2.856	3.269
60	3.152	3.214	3.855	2.889	2.953	3.462
90	3.194	3.259	3.956	2.930	2.998	3.553
120	3.213	3.281	4.008	2.950	3.019	3.600
150	3.221	3.289	4.037	2.958	3.028	3.626
180	3.228	3.297	4.060	2.966	3.036	3.647
210	3.237	3.307	4.082	2.974	3.046	3.667
240	3.268	3.340	4.138	3.004	3.077	3.717
270	3.306	3.380	4.202	3.040	3.115	3.775
300	3.318	3.393	4.226	3.051	3.127	3.797
330	3.339	3.415	4.265	3.071	3.149	3.832
360	3.361	3.438	4.305	3.092	3.171	3.868

Table D.6. Camber prediction of 3 BTE 110 prestressed girders without overhang by using three methods and two types of section properties at plant B, including 144-274, 144-275 and 144-278

Time after Transfer, days	Ig & Incremental method	Ig &Naaman's Method	Ig &Tadros's Method	Itr &Incrementa l method	Itr & Naaman's Method	Itr &Tadros's Method
0	1.683	1.703	1.683	1.507	1.517	1.507
0	1.625	1.643	1.632	1.454	1.477	1.461
1	1.895	1.921	1.962	1.701	1.733	1.758
2	1.931	1.958	2.033	1.737	1.769	1.822
3	2.024	2.054	2.171	1.824	1.860	1.946
7	2.091	2.126	2.336	1.893	1.933	2.093
14	2.240	2.282	2.612	2.037	2.085	2.342
21	2.296	2.342	2.742	2.092	2.144	2.459
28	2.322	2.370	2.809	2.119	2.172	2.519
60	2.387	2.440	2.975	2.184	2.243	2.669
90	2.416	2.472	3.053	2.213	2.275	2.739
120	2.429	2.486	3.094	2.226	2.289	2.776
150	2.432	2.490	3.116	2.230	2.294	2.796
180	2.437	2.496	3.134	2.234	2.300	2.812
210	2.442	2.502	3.151	2.240	2.306	2.827
240	2.466	2.527	3.194	2.262	2.329	2.866
270	2.494	2.557	3.244	2.288	2.358	2.911
300	2.501	2.565	3.263	2.296	2.366	2.928
330	2.516	2.581	3.293	2.310	2.381	2.955
360	2.532	2.598	3.324	2.325	2.397	2.983

Table D.7. Camber prediction of 3 BTE 110 prestressed girders with overhang by using three methods and two types of section properties at plant B, including 144-284, 144-283 and 144-280

Time after Transfer, days	Ig & Incremental method	Ig &Naaman's Method	Ig &Tadros's Method	Itr &Incrementa l method	Itr & Naaman's Method	Itr &Tadros's Method
0	2.037	2.056	2.037	1.842	1.851	1.842
0	1.981	1.999	1.975	1.790	1.814	1.785
1	2.315	2.341	2.374	2.099	2.130	2.147
2	2.360	2.387	2.460	2.143	2.176	2.225
3	2.477	2.507	2.626	2.254	2.289	2.376
7	2.564	2.599	2.825	2.343	2.382	2.557
14	2.754	2.796	3.159	2.526	2.572	2.860
21	2.828	2.874	3.316	2.600	2.649	3.003
28	2.861	2.910	3.396	2.634	2.685	3.075
60	2.949	3.002	3.597	2.721	2.777	3.258
90	2.989	3.045	3.691	2.761	2.819	3.343
120	3.008	3.066	3.740	2.780	2.839	3.388
150	3.015	3.073	3.767	2.787	2.848	3.413
180	3.022	3.081	3.789	2.795	2.856	3.432
210	3.031	3.091	3.809	2.803	2.865	3.451
240	3.061	3.122	3.861	2.832	2.895	3.498
270	3.097	3.160	3.922	2.866	2.931	3.553
300	3.108	3.172	3.944	2.877	2.943	3.573
330	3.128	3.194	3.981	2.896	2.963	3.607
360	3.149	3.216	4.018	2.916	2.984	3.640

Table D.8. Camber prediction of 3 BTE 110 prestressed girders without overhang by using three methods and two types of section properties at plant B, including 144-284, 144-283 and 144-280

Time after Transfer, days	Ig & Incremental method	Ig &Naaman's Method	Ig &Tadros's Method	Itr &Incrementa l method	Itr & Naaman's Method	Itr &Tadros's Method
0	1.806	1.829	1.806	1.602	1.613	1.602
0	1.745	1.766	1.752	1.546	1.573	1.553
1	2.032	2.062	2.105	1.807	1.843	1.867
2	2.070	2.101	2.181	1.845	1.882	1.935
3	2.168	2.204	2.328	1.936	1.978	2.066
7	2.239	2.279	2.503	2.009	2.056	2.223
14	2.395	2.444	2.799	2.160	2.216	2.486
21	2.454	2.507	2.938	2.218	2.278	2.610
28	2.480	2.536	3.009	2.245	2.308	2.673
60	2.548	2.610	3.187	2.314	2.382	2.832
90	2.578	2.643	3.270	2.343	2.415	2.906
120	2.591	2.658	3.313	2.357	2.430	2.945
150	2.594	2.662	3.337	2.361	2.436	2.966
180	2.599	2.667	3.356	2.366	2.441	2.983
210	2.605	2.674	3.375	2.372	2.448	2.999
240	2.629	2.700	3.421	2.394	2.472	3.040
270	2.658	2.731	3.474	2.422	2.502	3.088
300	2.666	2.740	3.494	2.429	2.511	3.106
330	2.682	2.757	3.526	2.444	2.527	3.135
360	2.698	2.775	3.559	2.459	2.543	3.164

Table D.9. Camber prediction of 2 BTE 145 prestressed girders with overhang by using three methods and two types of section properties at plant B, including 144-311 and 144-334

Time after Transfer, days	Ig & Incremental method	Ig &Naaman's Method	Ig &Tadros's Method	Itr &Incrementa l method	Itr & Naaman's Method	Itr &Tadros's Method
0	5.037	5.094	5.037	4.390	4.405	4.390
0	4.893	4.942	4.903	4.258	4.344	4.270
1	5.708	5.780	5.897	4.991	5.100	5.142
2	5.729	5.803	6.012	5.022	5.131	5.243
3	5.737	5.813	6.100	5.039	5.147	5.320
7	5.878	5.963	6.509	5.193	5.304	5.679
14	6.336	6.445	7.353	5.631	5.760	6.421
21	6.403	6.519	7.609	5.706	5.839	6.645
28	6.434	6.554	7.739	5.744	5.878	6.759
60	6.664	6.798	8.241	5.971	6.116	7.200
90	6.838	6.982	8.570	6.137	6.291	7.489
120	6.935	7.085	8.761	6.230	6.389	7.657
150	6.967	7.120	8.845	6.262	6.424	7.730
180	6.977	7.132	8.885	6.273	6.436	7.765
210	6.974	7.129	8.901	6.272	6.435	7.779
240	7.067	7.228	9.060	6.359	6.527	7.919
270	7.207	7.376	9.292	6.489	6.665	8.123
300	7.284	7.458	9.428	6.561	6.742	8.242
330	7.346	7.524	9.540	6.618	6.804	8.340
360	7.437	7.622	9.700	6.704	6.895	8.480

Table D.10. Camber prediction of 2 BTE 145 prestressed girders without overhang by using three methods and two types of section properties at plant B, including 144-311 and 144-334

Time after Transfer, days	Ig & Incremental method	Ig &Naaman's Method	Ig &Tadros's Method	Itr &Incrementa l method	Itr & Naaman's Method	Itr &Tadros's Method
0	3.695	3.760	3.695	3.132	3.154	3.132
0	3.542	3.599	3.595	2.992	3.077	3.045
1	4.109	4.190	4.327	3.490	3.599	3.669
2	4.120	4.203	4.412	3.509	3.620	3.742
3	4.120	4.205	4.477	3.518	3.629	3.798
7	4.194	4.289	4.779	3.604	3.722	4.055
14	4.483	4.602	5.401	3.878	4.018	4.586
21	4.505	4.632	5.590	3.910	4.056	4.747
28	4.521	4.651	5.685	3.931	4.080	4.828
60	4.668	4.812	6.055	4.076	4.238	5.144
90	4.779	4.934	6.298	4.181	4.353	5.351
120	4.838	5.000	6.438	4.238	4.416	5.471
150	4.855	5.019	6.500	4.255	4.436	5.524
180	4.857	5.024	6.529	4.258	4.441	5.549
210	4.852	5.019	6.541	4.254	4.437	5.559
240	4.912	5.084	6.659	4.309	4.498	5.660
270	5.003	5.184	6.830	4.392	4.589	5.805
300	5.051	5.237	6.930	4.437	4.639	5.891
330	5.089	5.279	7.012	4.471	4.678	5.961
360	5.146	5.343	7.130	4.524	4.737	6.061

Table D.11. Camber prediction of 2 BTE 145 prestressed girders with overhang by using three methods and two types of section properties at plant B, including 144-316 and 144-317

Time after Transfer, days	Ig & Incremental method	Ig &Naaman's Method	Ig &Tadros's Method	Itr &Incrementa l method	Itr & Naaman's Method	Itr &Tadros's Method
0	5.050	5.109	5.050	4.386	4.402	4.386
0	4.904	4.955	4.915	4.253	4.341	4.265
1	5.718	5.792	5.909	4.983	5.096	5.136
2	5.739	5.816	6.025	5.014	5.126	5.237
3	5.746	5.825	6.113	5.031	5.142	5.314
7	5.885	5.974	6.522	5.183	5.298	5.672
14	6.340	6.453	7.367	5.619	5.752	6.411
21	6.405	6.526	7.623	5.692	5.830	6.635
28	6.436	6.560	7.752	5.729	5.869	6.749
60	6.664	6.803	8.255	5.955	6.106	7.189
90	6.837	6.987	8.585	6.120	6.280	7.478
120	6.932	7.089	8.776	6.212	6.377	7.645
150	6.964	7.124	8.860	6.243	6.411	7.718
180	6.974	7.135	8.900	6.254	6.423	7.753
210	6.971	7.132	8.916	6.253	6.422	7.767
240	7.063	7.231	9.076	6.339	6.514	7.907
270	7.202	7.378	9.308	6.468	6.651	8.110
300	7.279	7.460	9.444	6.539	6.728	8.229
330	7.339	7.525	9.555	6.596	6.789	8.327
360	7.430	7.622	9.715	6.681	6.880	8.467

Table D.12. Camber prediction of 2 BTE 145 prestressed girders without overhang by using three methods and two types of section properties at plant B, including 144-316 and 144-317

Time after Transfer, days	Ig & Incremental method	Ig &Naaman's Method	Ig &Tadros's Method	Itr &Incrementa l method	Itr & Naaman's Method	Itr &Tadros's Method
0	3.682	3.750	3.682	3.106	3.130	3.106
0	3.526	3.586	3.582	2.965	3.052	3.019
1	4.088	4.172	4.311	3.455	3.569	3.638
2	4.098	4.185	4.395	3.475	3.589	3.710
3	4.098	4.186	4.460	3.483	3.598	3.765
7	4.169	4.268	4.760	3.567	3.689	4.019
14	4.452	4.576	5.379	3.835	3.980	4.546
21	4.472	4.604	5.566	3.864	4.016	4.705
28	4.487	4.622	5.662	3.885	4.039	4.786
60	4.630	4.781	6.030	4.027	4.195	5.098
90	4.739	4.901	6.271	4.130	4.309	5.304
120	4.797	4.965	6.411	4.185	4.370	5.423
150	4.813	4.984	6.473	4.201	4.389	5.475
180	4.815	4.988	6.502	4.205	4.394	5.500
210	4.809	4.983	6.514	4.200	4.390	5.510
240	4.868	5.047	6.631	4.254	4.450	5.609
270	4.957	5.145	6.801	4.335	4.540	5.753
300	5.004	5.198	6.900	4.378	4.589	5.838
330	5.041	5.239	6.982	4.412	4.627	5.908
360	5.098	5.302	7.100	4.464	4.685	6.007

Table D.13. Camber prediction of 2 BTE 145 prestressed girders with overhang by using three methods and two types of section properties at plant B, including 144-366 and 144-367

Time after Transfer, days	Ig & Incremental method	Ig &Naaman's Method	Ig &Tadros's Method	Itr &Incrementa l method	Itr & Naaman's Method	Itr &Tadros's Method
0	4.948	5.004	4.948	4.313	4.328	4.313
0	4.803	4.852	4.815	4.180	4.265	4.193
1	5.603	5.674	5.791	4.900	5.008	5.050
2	5.624	5.697	5.904	4.930	5.037	5.149
3	5.632	5.707	5.991	4.947	5.053	5.225
7	5.769	5.853	6.392	5.096	5.206	5.577
14	6.218	6.325	7.221	5.526	5.654	6.305
21	6.282	6.397	7.472	5.599	5.731	6.526
28	6.313	6.431	7.599	5.635	5.769	6.638
60	6.539	6.671	8.093	5.859	6.003	7.071
90	6.709	6.852	8.417	6.022	6.175	7.355
120	6.804	6.953	8.604	6.112	6.271	7.520
150	6.835	6.987	8.686	6.144	6.304	7.592
180	6.845	6.998	8.725	6.154	6.316	7.626
210	6.842	6.996	8.741	6.153	6.315	7.640
240	6.933	7.093	8.898	6.238	6.406	7.778
270	7.071	7.239	9.126	6.366	6.541	7.978
300	7.146	7.319	9.259	6.436	6.617	8.095
330	7.206	7.383	9.369	6.493	6.677	8.191
360	7.296	7.479	9.526	6.577	6.767	8.329

Table D.14. Camber prediction of 2 BTE 145 prestressed girders without overhang by using three methods and two types of section properties at plant B, including 144-366 and 144-367

Time after Transfer, days	Ig & Incremental method	Ig &Naaman's Method	Ig &Tadros's Method	Itr &Incrementa l method	Itr & Naaman's Method	Itr &Tadros's Method
0	3.610	3.674	3.610	3.058	3.081	3.058
0	3.456	3.513	3.511	2.918	3.002	2.972
1	4.009	4.089	4.227	3.403	3.511	3.582
2	4.019	4.102	4.310	3.422	3.531	3.653
3	4.019	4.104	4.373	3.430	3.540	3.707
7	4.090	4.184	4.667	3.513	3.630	3.958
14	4.370	4.488	5.275	3.778	3.917	4.477
21	4.390	4.516	5.460	3.807	3.953	4.634
28	4.406	4.535	5.553	3.828	3.976	4.713
60	4.548	4.692	5.914	3.969	4.130	5.022
90	4.656	4.810	6.152	4.071	4.242	5.224
120	4.714	4.874	6.289	4.126	4.303	5.341
150	4.729	4.893	6.349	4.142	4.322	5.393
180	4.732	4.897	6.378	4.146	4.327	5.417
210	4.726	4.892	6.390	4.141	4.323	5.427
240	4.784	4.956	6.505	4.194	4.382	5.525
270	4.873	5.053	6.671	4.275	4.471	5.667
300	4.920	5.105	6.769	4.318	4.520	5.751
330	4.956	5.146	6.850	4.352	4.557	5.819
360	5.012	5.208	6.965	4.403	4.615	5.918

Table D.15. Camber prediction of 2 BTD 135 prestressed girders with overhang by using three methods and two types of section properties at plant C, including 13501 and 13502

Time after Transfer, days	Ig & Incremental method	Ig &Naaman's Method	Ig &Tadros's Method	Itr &Incrementa l method	Itr & Naaman's Method	Itr &Tadros's Method
0	4.270	4.324	4.270	3.714	3.729	3.714
0	4.121	4.169	4.152	3.578	3.657	3.609
1	4.600	4.663	4.771	4.010	4.104	4.150
2	5.184	5.268	5.551	4.535	4.651	4.832
3	5.193	5.280	5.644	4.553	4.669	4.914
7	5.407	5.510	6.202	4.769	4.896	5.401
14	5.309	5.412	6.275	4.704	4.826	5.466
21	5.292	5.397	6.378	4.700	4.822	5.556
28	5.314	5.424	6.510	4.728	4.852	5.671
60	5.328	5.443	6.698	4.755	4.881	5.836
90	5.396	5.517	6.888	4.822	4.953	6.002
120	5.412	5.535	6.949	4.839	4.972	6.055
150	5.462	5.589	7.062	4.887	5.023	6.155
180	5.531	5.663	7.198	4.951	5.093	6.273
210	5.573	5.708	7.286	4.990	5.134	6.350
240	5.565	5.700	7.289	4.983	5.128	6.353
270	5.630	5.770	7.409	5.044	5.192	6.458
300	5.641	5.782	7.442	5.054	5.204	6.487
330	5.689	5.833	7.533	5.098	5.251	6.566
360	5.718	5.864	7.595	5.125	5.281	6.620

Table D.16. Camber prediction of 2 BTD 135 prestressed girders without overhang by using three methods and two types of section properties at plant C, including 13501 and 13502

Time after Transfer, days	Ig & Incremental method	Ig &Naaman's Method	Ig &Tadros's Method	Itr &Incrementa l method	Itr & Naaman's Method	Itr &Tadros's Method
0	4.043	4.107	4.043	3.422	3.438	3.422
0	3.884	3.940	3.934	3.277	3.369	3.326
1	4.319	4.392	4.518	3.661	3.771	3.824
2	4.845	4.943	5.254	4.124	4.260	4.451
3	4.849	4.950	5.342	4.138	4.275	4.526
7	5.018	5.138	5.868	4.311	4.463	4.974
14	4.922	5.041	5.937	4.252	4.398	5.033
21	4.898	5.021	6.034	4.244	4.391	5.116
28	4.910	5.037	6.159	4.261	4.412	5.222
60	4.911	5.044	6.336	4.278	4.432	5.373
90	4.963	5.103	6.515	4.329	4.490	5.526
120	4.974	5.116	6.573	4.342	4.505	5.575
150	5.014	5.161	6.680	4.380	4.547	5.666
180	5.073	5.225	6.808	4.434	4.606	5.775
210	5.107	5.263	6.891	4.465	4.641	5.846
240	5.097	5.253	6.894	4.458	4.634	5.849
270	5.153	5.314	7.007	4.508	4.689	5.945
300	5.160	5.323	7.038	4.516	4.698	5.971
330	5.200	5.367	7.124	4.552	4.738	6.044
360	5.224	5.393	7.182	4.573	4.762	6.094

Table D.17. Camber prediction of 2 BTD 135 prestressed girders with overhang by using three methods and two types of section properties at plant C, including 13503 and 13504

Time after Transfer, days	Ig & Incremental method	Ig &Naaman's Method	Ig &Tadros's Method	Itr &Incrementa l method	Itr & Naaman's Method	Itr &Tadros's Method
0	4.269	4.333	4.269	3.629	3.645	3.629
0	4.293	4.167	4.155	3.656	3.579	3.529
1	4.784	4.650	4.771	4.092	4.008	4.057
2	5.379	5.237	5.548	4.620	4.532	4.722
3	5.387	5.246	5.641	4.638	4.548	4.801
7	5.596	5.455	6.197	4.850	4.756	5.277
14	5.492	5.354	6.270	4.785	4.688	5.340
21	5.472	5.335	6.372	4.780	4.682	5.427
28	5.491	5.355	6.504	4.806	4.707	5.540
60	5.501	5.367	6.691	4.831	4.731	5.700
90	5.566	5.433	6.881	4.896	4.796	5.863
120	5.581	5.448	6.941	4.912	4.813	5.914
150	5.630	5.497	7.054	4.959	4.859	6.011
180	5.699	5.567	7.189	5.022	4.923	6.127
210	5.740	5.608	7.277	5.060	4.962	6.202
240	5.731	5.599	7.281	5.053	4.954	6.205
270	5.796	5.664	7.400	5.113	5.015	6.307
300	5.806	5.675	7.433	5.123	5.025	6.335
330	5.853	5.722	7.523	5.166	5.068	6.413
360	5.882	5.751	7.585	5.192	5.095	6.465

Table D.18. Camber prediction of 2 BTD 135 prestressed girders without overhang by using three methods and two types of section properties at plant C, including 13503 and 13504

Time after Transfer, days	Ig & Incremental method	Ig &Naaman's Method	Ig &Tadros's Method	Itr &Incrementa l method	Itr & Naaman's Method	Itr &Tadros's Method
0	4.122	4.186	4.122	3.491	3.507	3.491
0	3.963	4.019	4.011	3.347	3.440	3.395
1	4.408	4.482	4.607	3.741	3.851	3.903
2	4.946	5.044	5.357	4.215	4.351	4.543
3	4.951	5.052	5.447	4.229	4.366	4.619
7	5.127	5.247	5.984	4.409	4.561	5.077
14	5.029	5.149	6.055	4.349	4.496	5.137
21	5.006	5.129	6.154	4.341	4.489	5.222
28	5.018	5.146	6.281	4.360	4.511	5.331
60	5.021	5.154	6.462	4.378	4.532	5.485
90	5.075	5.215	6.645	4.431	4.592	5.641
120	5.087	5.229	6.703	4.445	4.608	5.691
150	5.129	5.276	6.813	4.484	4.651	5.784
180	5.189	5.341	6.943	4.540	4.712	5.895
210	5.224	5.380	7.027	4.572	4.748	5.967
240	5.214	5.371	7.031	4.564	4.741	5.970
270	5.272	5.433	7.146	4.617	4.798	6.069
300	5.280	5.443	7.178	4.624	4.807	6.096
330	5.320	5.487	7.265	4.661	4.848	6.170
360	5.345	5.514	7.325	4.684	4.873	6.221

Table D.19. Camber prediction of 2 BTD 135 prestressed girders with overhang by using three methods and two types of section properties at plant C, including 13507 and 13508

Time after Transfer, days	Ig & Incremental method	Ig &Naaman's Method	Ig &Tadros's Method	Itr &Incrementa l method	Itr & Naaman's Method	Itr &Tadros's Method
0	4.663	4.727	4.663	4.005	4.021	4.005
0	4.508	4.565	4.539	3.864	3.957	3.895
1	5.027	5.101	5.212	4.328	4.438	4.477
2	5.657	5.757	6.060	4.891	5.026	5.210
3	5.668	5.770	6.161	4.911	5.046	5.297
7	5.896	6.018	6.767	5.142	5.291	5.822
14	5.789	5.910	6.847	5.074	5.216	5.891
21	5.769	5.893	6.959	5.070	5.212	5.988
28	5.793	5.922	7.103	5.100	5.245	6.112
60	5.806	5.941	7.307	5.129	5.277	6.289
90	5.878	6.021	7.513	5.200	5.354	6.467
120	5.895	6.040	7.579	5.219	5.374	6.525
150	5.949	6.098	7.703	5.270	5.429	6.631
180	6.023	6.177	7.850	5.338	5.503	6.759
210	6.067	6.225	7.946	5.380	5.548	6.841
240	6.058	6.217	7.950	5.372	5.541	6.845
270	6.128	6.292	8.080	5.437	5.610	6.958
300	6.139	6.305	8.116	5.448	5.622	6.988
330	6.190	6.359	8.215	5.494	5.673	7.074
360	6.221	6.393	8.282	5.523	5.704	7.132

Table D.20. Camber prediction of 2 BTD 135 prestressed girders without overhang by using three methods and two types of section properties at plant C, including 13507 and 13508

Time after Transfer, days	Ig & Incremental method	Ig &Naaman's Method	Ig &Tadros's Method	Itr &Incrementa l method	Itr & Naaman's Method	Itr &Tadros's Method
0	4.100	4.163	4.100	3.477	3.493	3.477
0	3.942	3.997	3.990	3.333	3.425	3.381
1	4.385	4.458	4.583	3.725	3.834	3.887
2	4.921	5.018	5.330	4.198	4.333	4.524
3	4.926	5.026	5.419	4.212	4.348	4.600
7	5.101	5.220	5.953	4.392	4.542	5.056
14	5.004	5.122	6.024	4.331	4.477	5.117
21	4.981	5.102	6.122	4.324	4.470	5.201
28	4.994	5.120	6.249	4.343	4.492	5.309
60	4.997	5.128	6.429	4.361	4.513	5.462
90	5.050	5.189	6.611	4.414	4.573	5.618
120	5.062	5.203	6.669	4.428	4.588	5.668
150	5.104	5.250	6.778	4.467	4.632	5.761
180	5.164	5.315	6.907	4.522	4.693	5.871
210	5.199	5.353	6.991	4.554	4.728	5.943
240	5.190	5.344	6.995	4.547	4.721	5.946
270	5.247	5.406	7.110	4.599	4.778	6.044
300	5.255	5.416	7.141	4.606	4.787	6.071
330	5.295	5.460	7.228	4.644	4.828	6.145
360	5.320	5.487	7.288	4.666	4.853	6.196

Table D.21. Camber prediction of 2 BTD 135 prestressed girders with overhang by using three methods and two types of section properties at plant C, including 13511 and 13512

Time after Transfer, days	Ig & Incremental method	Ig &Naaman's Method	Ig &Tadros's Method	Itr &Incrementa l method	Itr & Naaman's Method	Itr &Tadros's Method
0	4.010	4.068	4.010	3.437	3.452	3.437
0	4.029	3.906	3.900	3.458	3.381	3.340
1	4.492	4.361	4.480	3.872	3.787	3.841
2	5.054	4.915	5.213	4.375	4.284	4.472
3	5.062	4.924	5.300	4.391	4.299	4.547
7	5.260	5.120	5.823	4.592	4.495	4.998
14	5.163	5.026	5.892	4.529	4.430	5.058
21	5.143	5.008	5.988	4.524	4.424	5.141
28	5.162	5.027	6.112	4.548	4.447	5.248
60	5.171	5.038	6.288	4.571	4.469	5.400
90	5.233	5.100	6.467	4.632	4.530	5.554
120	5.248	5.115	6.524	4.648	4.546	5.603
150	5.295	5.161	6.630	4.692	4.590	5.695
180	5.360	5.227	6.757	4.753	4.651	5.804
210	5.399	5.266	6.840	4.789	4.688	5.875
240	5.390	5.257	6.843	4.782	4.680	5.878
270	5.452	5.320	6.956	4.839	4.738	5.976
300	5.462	5.330	6.987	4.848	4.747	6.002
330	5.507	5.374	7.072	4.889	4.789	6.076
360	5.534	5.402	7.130	4.915	4.814	6.126

Table D.22. Camber prediction of 2 BTD 135 prestressed girders without overhang by using three methods and two types of section properties at plant C, including 13511 and 13512

Time after Transfer, days	Ig & Incremental method	Ig &Naaman's Method	Ig &Tadros's Method	Itr &Incrementa l method	Itr & Naaman's Method	Itr &Tadros's Method
0	3.856	3.913	3.856	3.292	3.308	3.292
0	3.700	3.751	3.749	3.151	3.235	3.199
1	4.118	4.185	4.308	3.522	3.622	3.679
2	4.624	4.713	5.012	3.971	4.094	4.284
3	4.629	4.720	5.096	3.984	4.108	4.356
7	4.794	4.902	5.599	4.152	4.290	4.788
14	4.702	4.810	5.665	4.094	4.227	4.845
21	4.680	4.791	5.758	4.087	4.220	4.925
28	4.692	4.807	5.878	4.104	4.241	5.028
60	4.695	4.815	6.047	4.120	4.260	5.173
90	4.745	4.872	6.218	4.170	4.316	5.321
120	4.757	4.886	6.273	4.183	4.331	5.368
150	4.796	4.929	6.376	4.220	4.372	5.456
180	4.853	4.991	6.498	4.273	4.429	5.561
210	4.886	5.027	6.577	4.303	4.463	5.629
240	4.877	5.019	6.581	4.296	4.456	5.632
270	4.931	5.078	6.689	4.345	4.510	5.725
300	4.939	5.086	6.719	4.353	4.519	5.750
330	4.978	5.129	6.801	4.388	4.557	5.821
360	5.001	5.154	6.856	4.409	4.581	5.869

Appendix E

Properties of Prestressed Bridge Girders, including BTC 120, BTE 110, BTE 145 and BTD 135

Table E.1. Properties of four types of prestressed bridge girders

Girder Type	span length	overall length	no. of straight strand	no. of deflected strand	weight, tons
BTC 120	120'-0"	121'-4"	38	12	43.7
BTE 110	110'-0"	111'-4"	26	4	46.8
BTE 145	145'-0"	146'-4"	42	10	61.5
BTD 135	135'-0"	136'-4"	42	12	53.2

Table E.2. Comparison of properties of gross section and transformed section at release

Girder Type	Plant	Girder I.D.	Ig, in^4	Ag, in^2	y bar for gross, in	Average Itr, in^4	Average Atr, in^2	Average y bar for transformed, in
BTC 120	A	103-09, 103-10, 103-11	178971	691.8	20.74	190884	739.8	20.14
BTE 110	B	144-270, 144-272, 144-268	422790	807.4	28.75	450005	849.6	28.09
		144-274, 144-275, 144-278	422790	807.4	28.75	451355	851.8	28.05
		144-284, 144-283, 144-280	422790	807.4	28.75	448880	847.8	28.11
BTE 145	B	144-311, 144-334	422790	807.4	28.75	454232	864.9	27.77
		144-316, 144-317	422790	807.4	28.75	454968	866.3	27.75
		144-366, 144-367	422790	807.4	28.75	454108	864.6	27.77
BTD 135	C	13501, 13502	285860	748.8	24.64	306922	805.7	23.81
		13503, 13504	285860	748.8	24.64	306926	805.7	23.81
		13507, 13508	285860	748.8	24.64	306776	805.3	23.81
		13511, 13512	285860	748.8	24.64	305695	802.2	23.85

Table E.3. Material properties of concrete at release

Girder Type	Plant	Girder I.D.	Release Concrete Strength, psi	Release Modulus of Elasticity of Concrete, ksi
BTC 120	A	103-09, 103-10, 103-11	8610	5761
BTE 110	B	144-270, 144-272, 144-268	6090	4449
		144-274, 144-275, 144-278	5598	4266
		144-284, 144-283, 144-280	6550	4614
BTE 145	B	144-311, 144-334	8066	5120
		144-316, 144-317	7750	5019
		144-366, 144-367	8121	5138
BTD 135	C	13501, 13502	8121	5306
		13503, 13504	8118	5305
		13507, 13508	8218	5338
		13511, 13512	8992	5583

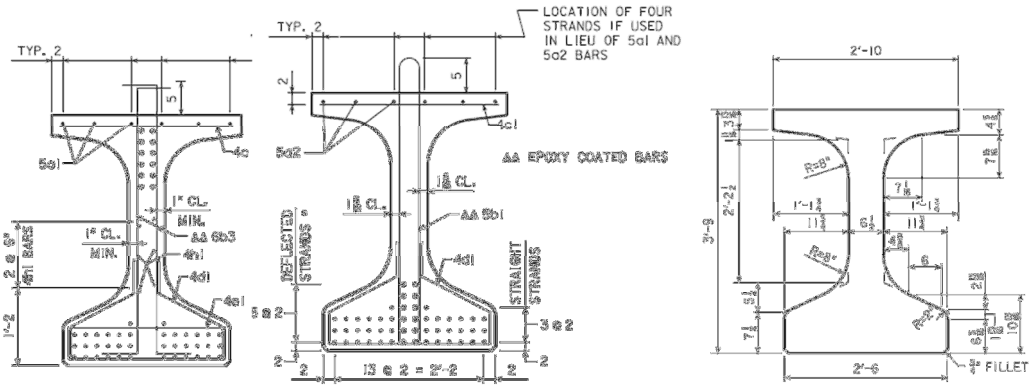

Figure E.1. Cross section of the end span, the mid-span and the gross cross section of BTC 120 girder

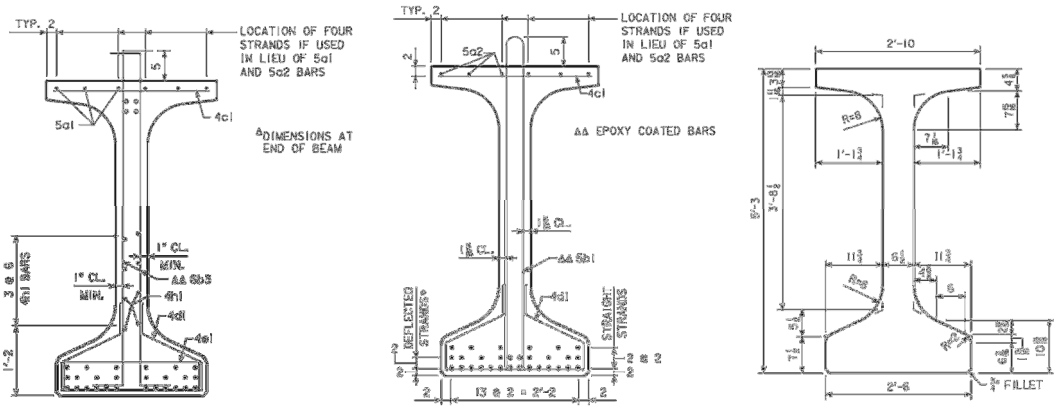

Figure E.2. Cross section of the end span, the mid-span and the gross cross section of BTE 110 girder

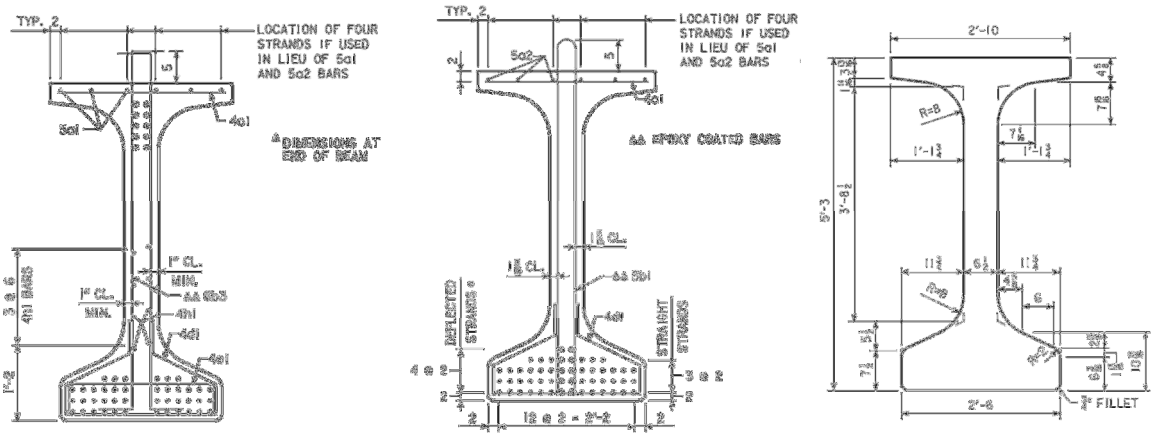

Figure E.3. Cross section of the end span, the mid-span and the gross cross section of BTE 145 girder

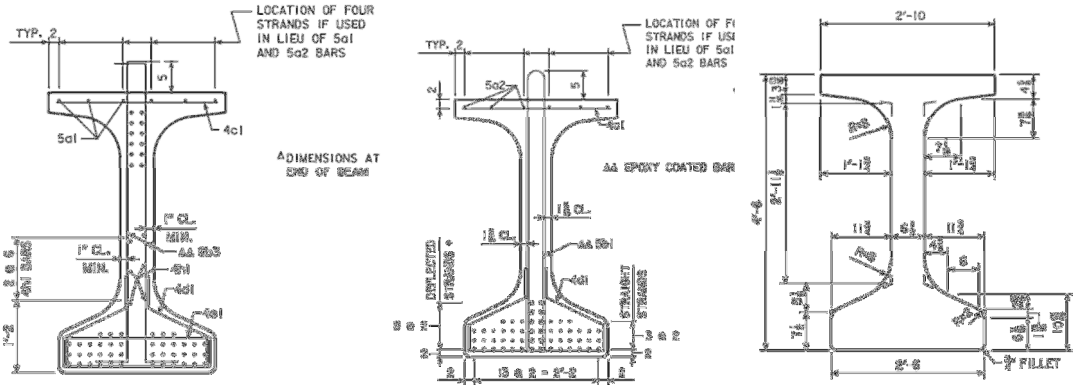

Figure E.4. Cross section of the end span, the mid-span and the gross cross section of BTD 135 girder